The Dissertation Committee for Kally Corissa O'Reilly Certifies that this is the approved version of the following dissertation:

Behavioral and Neuronal Changes Due to 13-*Cis*-Retinoic Acid Treatment

Committee:

Michelle Lane, Supervisor

Francisco Gonzalez-Lima

Andrea Gore

Hitoshi Morikawa

Phillip Tucker

Behavioral and Neuronal Changes Due to 13-*Cis*-Retinoic Acid Treatment

by

Kally Corissa O'Reilly, B.S.

Dissertation

Presented to the Faculty of the Graduate School of

The University of Texas at Austin

in Partial Fulfillment

of the Requirements

for the Degree of

Doctor of Philosophy

The University of Texas at Austin

May, 2008

Dedication

to colm and magnet o’reilly

Acknowledgements

I would like to offer sincere thanks to Dr. Michelle Lane and her previous lab members, Dr. Alice Dillard and Dr. Eun Young Park for their friendship and support throughout this project. I also would like to thank the members of my committee, especially Dr. Gonzalez-Lima and Dr. Gore for hospitality in their respective labs and for taking their time to train me in the histochemical techniques.

I thank my close friend, Mychel Varner, for her time, her presence, her laughter. Thanks to Patrick Killion, who has graciously listened throughout the course of this achievement and chose to care about me as a scientist, a musician, and as a friend.

Many thanks to my mom and dad, Darlene and Duane Bowers, for love and support. My dad has said there are no maps unless we draw them ourselves. Thanks, dad, for understanding that and for supporting my desire to draw them. My sister, Alexia Bowers, I thank you for being a rational, yet fun, human being. Family-in-law, thanks for being supportive and loving, every one of you. Lastly, loving thanks to my husband, Colm O'Reilly, who smiled quietly when I succeeded and quietly held me up when I failed. He is sweet, kind, and generous. It is to him that I owe this doctoral degree.

Behavioral and Neuronal Changes Due to 13-*Cis*-Retinoic Acid Treatment

Publication No._____

Kally Corissa O'Reilly, PhD

The University of Texas at Austin, 2008

Supervisor: Michelle Lane

13-*Cis*-retinoic acid (13-*cis*-RA) is a synthetic retinoid and the active ingredient in the oral acne treatment Accutane. The medical literature has suggested that the use of 13-*cis*-RA for acne treatment can induce depression, but because acne itself can have a negative psychosocial impact on self esteem, whether or not 13-*cis*-RA can cause depression remains controversial. The purpose of this work was to examine whether chronic 13-*cis*-RA administration could induce depression-related behaviors in mice and to determine the impact 13-*cis*-RA has on regions of the brain thought to be associated with mood and depression. We found that chronic treatment of adolescent male mice with 13-*cis*-RA induced depression-related behaviors, as assessed by immobility in the tail suspension and forced swim tests. Although depression is a multifaceted disease in which many brain regions are involved, the regions that seem particularly vulnerable to the effects of 13-*cis*-RA are the serotonergic and hippocampal systems. In serotonergic cells *in vitro*, 13-*cis*-RA treatment increases protein levels of the serotonergic 5-HT_{1A} autoreceptor and the serotonin reuptake transporter (SERT), two inhibitory components

of serotonin (5-HT) signaling. *In vivo*, the median and dorsal raphe nuclei contain the main 5-HT producing cells. 13-*Cis*-RA uncoupled the functional connectivity of dorsal raphe nuclei from the hippocampal regions as measured by interregional correlations of cytochrome oxidase (CO) activity, a metabolic marker of neuronal activity. Decreased hippocampal neurogenesis is thought to occur in depression and is decreased by 13-*cis*-RA. 5-HT is also a known regulator of hippocampal neurogenesis. Uncoupling of the dorsal raphe nuclei from the regions of the hippocampus by 13-*cis*-RA treatment may be the cause of, or a result from, the decreased neurogenesis. Although retinoids are known regulators of apoptosis, the uncoupling of the dorsal raphe nuclei from the hippocampal regions was not due to serotonergic cell loss. Interestingly, 13-*cis*-RA treated animals with the lowest CO activity in the dentate gyrus have the highest immobility in the tail suspension and forced swim tests. Ultimately, the effects of 13-*cis*-RA on the serotonergic and hippocampal systems might be inducing depression-related behaviors.

Table of Contents

List of Tables

List of Figures

Chapter 1: Introduction and Literature Review

GENERAL OVERVIEW OF RETINOIDS

Chemical Classification and Structure

Retinoids are a class of compounds derived from vitamin A (retinol) that are found in the diet as retinyl esters or β-carotene. Retinyl esters are consumed in foods such as whole milk, liver, egg yolks, oily fish, butter and cheese. β-carotene is found in many fruits and vegetables, including red peppers, carrots, broccoli, spinach, some herbs, apricots and mangos. Retinyl esters and β-carotene are converted to retinol (Fig. 1.1A and 1.1B) in the intestinal lumen and mucosa, respectfully, where retinol is then absorbed. Once absorbed by the gut, retinol is converted back to retinyl esters and packaged with other lipids in chylomicrons that are transported to the liver (1).

Retinol binds to retinol binding protein (RBP) and is secreted into the blood to be transported to cells through circulation. Due to its lipophylic properties, retinol can diffuse freely across cell membranes to bind cellular retinol binding protein (CRBP), which can transport retinol throughout the cytosol (Fig. 1.2). Once in a cell, retinol can be converted back to retinyl esters for storage by lecithin retinol acetyltransferase (LRAT) or metabolized to its active form, *all-trans*-retinoic acid (ATRA). Metabolism of ATRA is a two step, enzymatically driven process: 1) the reversible reaction of a conversion of retinol to retinaldehyde by retinol dehydrogenase (ROLDH) or alcohol dehydrogenase (ADH) and 2) conversion of retinaldehyde to ATRA by retinaldehydrogenase (RALDH) (1). ATRA can be degraded to its inactive form, 4-oxo-retinoic acid, by the phase I cytochrome P450 enzyme CYP26A1 (2).

Serum levels of retinol are 0.5 to 2 μM and the physiological level of ATRA is 14 nM, although pharmacological levels of ATRA could be around 10 μM. Increases in dietary vitamin A do not lead to an increase in serum levels of retinol bound to chylomicrons or free retinol, but does lead to an increase in tissues that have the capacity to store retinol as retinyl esters, such as the liver.

ATRA is transported through the blood bound to albumin (3) and pharmacokinetic studies of synthetic analogs of ATRA, such as 13-*cis*-retinoic acid (13-*cis*-RA), indicate that they are absorbed in the same way as ATRA [reviewed in (4)]. It has been shown in rats that most tissues derive 5-30% of the ATRA within that tissue from circulating ATRA (5). However, the brain and the liver derive greater than 80% of their ATRA from the circulating pool (5).

13-*Cis*-Retinoic Acid

13-*Cis*-RA (isotretinoin) is the active ingredient in the acne medication, Accutane. It is administered to humans as a soft-gelatin oral capsule (6). 13-*Cis*-RA is a synthetic retinoid and isomer of ATRA. The drug Accutane was approved for use in 1982 to treat severe nodular acne and it was originally intended to treat cases where acne was resistant to antibiotic or topical retinoid treatment (7).

According to the Roche Accutane insert, side effects of Accutane use include headaches, blurred vision or loss of night vision, dizziness, nausea or vomiting, seizures, diarrhea or rectal bleeding, and decreased bone density (6). Additionally, the insert reports that "Accutane use may cause depression, psychosis, and, rarely, suicidal ideation, suicide attempts, suicide, and aggressive and/or violent behaviors" (6).

In patients aged 12-15 chronically taking 13-*cis*-RA, the maximum plasma concentration of 13-*cis*-RA ranged from 370 ng/mL (1.2 μM) to 1,094 ng/mL (3.6 μM)

with the median concentration being 750 ng/mL (2.5 μM) (6). Adult plasma concentrations were not found to be significantly different (6). The time required to reach this peak plasma concentration ranges from 4 to 8 hours (6, 8), while the half-life of elimination is approximately 21 hours (6). The metabolites of 13-*cis*-RA found in patients are 13-*cis*-4-oxo-retinoic acid, ATRA, and 4-oxo-retinoic acid (6, 8).

Mechanism of Action

The retinoids have varying affects on several biological phenomena including cellular differentiation, embryonic central nervous system and limb development, vision, reproduction, and the immune response. ATRA is the most active naturally occurring retinoid. ATRA binds to cellular retinoic acid binding proteins I and II (CRABP I and II) for transport throughout the cytosol (Fig. 1.2). It is thought that CRABP I promotes catabolism of ATRA by transporting it to CYP261A while CRABP II has been suggested to shuttle ATRA to the nucleus where ATRA is capable of initiating transcription. Once in the nucleus, ATRA binds to the retinoic acid receptors (RAR-α, -β, and -γ) that heterodimerize with retinoid X receptors (RXR-α. –β, and -γ). The RAR/RXR heterodimers bind to recognition sequences in the promoter region of genes known as retinoic acid response elements (RARE). Once ligand bound by ATRA, transcription is activated.

The exact mechanism by which 13-*cis*-RA reduces sebum production and stabilizes keratinization are unknown, but 13-*cis*-RA is thought to affect transcription in cells by one of two ways. First, 13-*cis*-RA can isomerize to ATRA (Fig. 1.3) and then bind to the RAR to initiate transcription (9). Second, 13-*cis*-RA can itself bind to the RAR to initiate transcription (10). The affinity of 13-*cis*-RA for the RAR is much lower

than ATRA, but the activation of the RAR, and therefore subsequent transcription, is very effective (10).

13-*Cis*-RA reduces sebaceous gland size (11) and sebum production (12) in humans and is capable of inducing apoptosis and cell cycle arrest in immortalized sebaceous glands in a non-RAR dependent fashion (13). Additionally, the effects of 13-*cis*-RA on immortalized sebaceous glands are either not seen due to ATRA treatment, or happen much longer after treatment with ATRA (13). Retinoids are also capable of affecting cells via non-transcription mediated methods, such as mRNA stability and protein stability. Although the mechanism is not completely understood, ATRA can reduce TNF-α mRNA stability in a RXR-mediated manner in hepatocytes (14), increase keratin 19 mRNA stability in cultured keratinocytes (15) and increase protein stability in P19 cells (16). Thus, although 13-*cis*-RA is capable of isomerizing to ATRA to act through the RAR, or acting through the RAR itself, the effects of Accutane treatment may be due to 13-*cis*-RA acting in a non-RAR-mediated manner.

RETINOID SIGNALING MACHINERY IN THE ADULT CENTRAL NERVOUS SYSTEM

ATRA has been found in the adult brain, with the highest levels being found in the hippocampus (17). Although retinoids are lipid soluble and thus capable of easily crossing the blood brain barrier, the adult cerebrum, cerebellum, meninges and pia matter have the capability of synthesizing ATRA (18-20). CRBP and CRABP are also expressed in the adult brain (21). Cellular retinoic acid binding protein I is thought to shuttle ATRA to the nucleus where it can then activate gene transcription and is found throughout the adult brain including the cortex, amygdala, hippocampus, thalamus, and substantia nigra with high expression occurring in the hypothalamus (21).

The presence of CRABPI may indicate that ATRA is shuttled to the nucleus so that it can activate gene transcription in the adult brain. RAR expression is distributed throughout hippocampus, cortex (RARα), caudate/putamen, nucleus acumbens and olfactory tubercle (RARβ and γ) (21) and differs between developing and adult brains, implying a physiological role for retinoids in the adult brain (22). The presence of RARs indicates gene transcription by ATRA occurs in the adult brain, regulating gene expression in areas such as the hippocampus and cortex. Additionally, high levels of CYP26A1, which degrades ATRA, are expressed in the adult cerebellum (23). The ability to regulate ATRA levels indicates the adult brain is susceptible to high levels of retinoids. The dopamine receptor 2 (D2R) has been found to contain a functional RARE (24). Other genes known to regulated by ATRA are tyrosine hydroxylase (an enzyme involved in dopamine production) and dopamine β-hydroxylase (25, 26). The presence of enzymes to produce ATRA, the proteins to shuttle ATRA to the nucleus and the proteins to bind ATRA and induce gene transcription along with the presence of RAREs in regulating regions of genes expressed in the adult central nervous system indicates a role for retinoids in regulating gene transcription and cell signaling in the adult brain. The ability of retinoids to exert effects in the adult CNS is further implied in the medical literature by the ability of 13-*cis*-RA to induce depression in humans.

EFFECTS OF RETINOIDS ON THE DOPAMINERGIC AND NOREPINEPHRINERGIC SYSTEMS

Norepinepherine (NE) has been implicated in depression based on much clinical data, for example depressed patients exhibit lower urinary levels of the NE metabolite, 3-methoxy-4-hydroxy-phenylglycol (27). In the transthyretin null mouse retinol transport would theoretically be reduced, and thus the cellular levels of ATRA would also be

decreased. Interestingly, tissue NE levels were increased in limbic forebrain of the transthyretin null mouse (28) suggesting that retinoids may influence norepinephrinergic transmission. However, the effect of retinoids on brain NE levels has not been directly examined.

The mesolimbic DA system is a key element of the brain's motivational and reward system and its dysregulation in depression may underlie symptoms of anhedonia [for reviews see (29, 30)]. Repeated treatment with antidepressants increases dopamine 2 (D2) receptor binding (31). ATRA has been shown to increase D2 receptor expression in the striatum (24, 32) and in cultured cells via activation of a functional RARE in its promoter region (33). RARβ/RXRβ, RARβ/RXRγ, and RXRβ/RXRγ double null mice have decreased expression of D2 receptor (34). This is not true for the corresponding single null mice. Additionally, transcription of tyrosine hydroxylase and dopamine β hydroxylase, the enzymes involved in DA synthesis, is decreased by ATRA in rat superior cervical ganglia neurons (26, 35, 36). However, the tyrosine hydroxylase promoter is activated by ATRA in human neuroblastoma cells (37). Monoamine oxidase B activity, which is primarily responsible for the degradation of DA to dihydroxyphenylacetic acid (DOPAC), is increased by ATRA in chick hepatocytes (38). In addition, the level of homovanillic acid, the final degradative product of DA, appeared to be elevated in the striatal tissue of male rats treated with 13-*cis*-RA (39). Consistent with this, DOPAC was decreased in the striatal tissue of vitamin A deficient mice and DA levels also tended to be reduced in the striatal tissue of vitamin A deficient mice (40).

DEPRESSION

General Overview of Depression

Mood disorders, including major depressive disorder, affect approximately 10% of the population (41). Depression is a very serious, debilitating disease. Symptoms of depression include extreme sadness, feelings of helplessness, lack of interest in pleasure seeking (termed anhedonia), decreased sleep or oversleeping, loss of energy, weight loss or weight gain, irritability, and difficulty focusing and remembering. Additionally, depressed patients may experience headaches or chronic pain that are not responsive to treatment. Ultimately depressed patients may have thoughts of suicide or exhibit suicidal behavior.

Antidepressant treatment for depression usually targets the serotonergic, norepinepherinergic, or dopaminergic systems or some combination thereof. These antidepressants work to increase the levels of the respective monoamine within hours after administration of the drugs (42). However, antidepressant mood-elevating effects are often not observed until about two weeks after antidepressant treatment is initiated (42), indicating that other processes outside of monoamine neurotransmission are involved in mood regulation. Brain regions thought to be involved in depression and relevant to this dissertation include the orbitofrontal cortex, the hippocampus, the habenula, and the raphe nuclei.

Behavioral Tests

Because some of the information about the brain regions involved in depression was gained through behavioral studies in animals, it is important to first discuss the behavioral paradigms. The tail suspension and forced swim tests are two behavioral

despair paradigms in which an animal is placed in an inescapable, stressful situation and the amount of time spent trying to escape the situation is assessed. In both tests, administration of antidepressants to an animal will increase the amount of time the animal spends struggling (43, 44). In the tail suspension test, the animal is suspended by the tail and escape behaviors involve thrashing of the body and both fore- and hindpaw movement. Immobility consists of either hanging straight, but motionless, or curled up with the forepaws holding onto the hindlegs. There is very little movement of the paws in immobility, although grooming may occur.

In the forced swim test, the animal is placed in a cylindrical bath of room temperature water in which the animal cannot touch the bottom of the container to stand, nor can it reach the top of the container to get out. Behaviors in this paradigm are assessed as swimming, climbing, or immobility. Swimming is considered circular movement around the cylinder, while climbing behavior involves the animal becoming vertical and pawing at the walls of the cylinder. Immobility is considered to be movement necessary for the animal to keep its head above water (44).

Because the immobility in these two tests is reduced by antidepressants and antidepressants are mood elevators in humans, the amount of time spent immobile is considered a depression-related behavior. One limitation of this test is that antidepressant treatment to rodents can decrease immobility in these two behavioral tests immediately after administration, while antidepressant efficacy can take weeks in humans. Therefore, it may seem more reasonable to use immobility in the tail suspension and forced swim tests to assess potential antidepressant efficacy of drugs. However, factors known to cause depression in humans can increase the amount of time spent immobile. For example, increased immobility in the forced swim test has been reported to occur in situations that increase vulnerability to depression such as estradiol deficiency due to

aromatase knockout (45), stress due to food restriction (46), magnesium depletion (47), and choline administration (48). The behavior of the animals in the tail suspension test was not assessed in these studies. Increased immobility in both the forced swim and tail suspension tests does occur due to the pro-depressant effects of withdrawal from chronic amphetamine administration (49), centrally administered urotensin-II (50), and interleukin-1 and endotoxin injection (51). Thus, immobility appears to be a good measure of depression-related behavior.

Brain Systems Involved in Depression

Raphe Nuclei

The median and dorsal raphe nuclei are the main serotonin (5-hydroxytryptamine or 5-HT) producing cells in the brain thought to be involved in mood and cognition (52, 53). The serotonergic system is very commonly a target of antidepressant treatments and such treatments work to increase serotonergic signaling. Lesions to the lateral habenula, a major regulator of the monoaminergic systems, increase 5-HT in the dorsal raphe nuclei, and can also decrease depression-related behaviors. Tryptophan is the precursor for 5-HT synthesis and tryptophan depletion studies result in depleted 5-HT levels after approximately 5 hours. Tryptophan depletion induces depression in healthy subjects with a family history of depression (54-56) and in non-medicated, remitted patients with a history of depression (57-59). However, tryptophan depletion does not induce depressive symptoms in healthy patients with no family history of depression (60), suggesting that depression is a multifaceted disease requiring more than just dysfunctional serotonergic signaling. Further confounding the role of 5-HT in depression, rats with denervation of

the dorsal and median raphe nuclei do not exhibit increased depression-related behaviors in the forced swim test (61, 62).

Hippocampus

Neurogenesis in the hippocampus is also thought to be involved in depression and hippocampal volume has been found to be decreased in depressed patients (63-66). Furthermore, antidepressant drugs have been found to increase hippocampal neurogenesis after several weeks of administration (67), which is concordant with the elevation of mood due to antidepressant treatment. However, it is not known if reduced hippocampal neurogenesis causes or results from depression in humans.

Many factors coordinate adult hippocampal neurogenesis including 5-HT, stress, steroids and neurotrophic factors [for reviews see (68, 69)]. 5-HT itself has been implicated in the mechanisms of adult neurogenesis largely on the basis of the actions of antidepressants that elevate 5-HT levels (e.g. fluoxetine) and have been shown to promote neurogenesis (67). In addition, SSRIs and monoamine oxidase inhibitors can also increase brain-derived neurotrophic factor in the hippocampus which could provide an alternative mechanism whereby 5-HT could regulate adult neurogenesis [for reviews see (68, 69)].

Habenula

As a major regulator of the monoaminergic systems, it is not surprising that the habenula might have a role in depression-related behaviors. Although little is known about the possible role of the habenula in depression, the habenula receives afferent projections from the serotonergic and noradrenergic systems (70, 71) as well as sending

efferent projections to the dopaminergic ventral tegmental area (71). In addition, the lateral habenula negatively regulates the dorsal raphe nuclei (72) and lesions of the lateral habenula in stress-induced depressed rats leads to an increase in 5-HT in the dorsal raphe nuclei as well as decreased immobility, due to increased climbing behavior, in the forced swim test (73). The lateral habenula has been found to be significantly hypermetabolic in congenitally learned-helpless rats as compared to congenitally non-helpless rats, a rat line that is resistant to learned helpless behavior (74).

Orbitofrontal Cortex

Metabolic mapping studies have shown that various areas of the frontal cortex may be altered in depression. In depressed patients that are responsive to antidepressant treatment, orbitofrontal cortex metabolism is higher than in healthy individuals (75). However, the orbitofrontal cortex metabolism is either not changed or is decreased in depressed patients that are resistant to antidepressant treatment (75). Additionally, neuronal and glial cell densities are also reduced in the orbitofrontal cortex of depressed suicide victims (76, 77).

ACCUTANE AND DEPRESSION

Human Studies

Since approval of Accutane in 1982 to treat severe cystic acne, numerous reports concerning the ability of Accutane to induce depression and suicidal ideation have appeared throughout the medical literature indicating an incidence of depressive symptoms in approximately 8% of patients (78). Between 1982 and 2002 the US FDA Adverse Event Reporting System received approximately 394 reports of depression and

37 suicides related to the use of Accutane (79). In some cases, depressive symptoms were reported to resolve once Accutane use was discontinued [for review see (80)]. Additionally, some cases report recurrence of symptoms upon rechallenge with 13-*cis*-RA (81). Since the mid-1980s, reports in the literature suggest a relationship between 13-*cis*-RA use and the onset of psychological symptoms including depression, suicidal ideation and psychosis (79, 82-88). However, there are also studies suggesting that there is no evidence of such a link (89-92) and the epidemiological evidence has remained contradictory [e.g. (90) versus (87)]. For instance, Jick et al. (89) conducted an epidemiological study in which no link was found between Accutane and major depressive disorder, although other types of depression were not examined. Another epidemiological study conducted by Hersom et al. (93) examined a pharmacy database to determine if patients that had filled isotretinoin prescriptions had a higher rate of sequentially filling antidepressant prescriptions. These authors reported that patients filling isotretinoin prescriptions do not have a higher incidence of then filling an antidepressant prescription, and thus concluded that there is not an association between isotretinoin use and depression (93). However, the authors did not take into consideration that patients that take isotretinoin and experience depressive symptoms may simply stop taking the medication rather than seeking prescriptions for antidepressants. Additionally, the two above-mentioned studies that did not find a link between isotretinoin and depression were both funded by Roche, the manufacturer of Accutane.

Bremner et al. (94) evaluated humans administered 13-*cis*-RA for acne treatment and compared them to antibiotic controls. PET scans taken before and after four months of treatment revealed a decrease in orbitofrontal cortex glucose metabolism following 13-*cis*-RA treatment (94). Patients who received antibiotic treatment had no change in

orbitofrontal cortex glucose metabolism before or after treatment (94). Although some patients taking 13-*cis*-RA reported headaches and subtle changes in irritability or mood, none of them were found to be clinically depressed, as assessed by the Hamilton Depression Scale (94). This study was done as a small pilot study and therefore the treatment groups were not randomly assigned and the sample size was small. Additionally, patients who had a history of mental illness were excluded from the study. These factors could conceal mood-related changes that may be seen following 13-*cis*-RA treatment in a larger population.

Animal Studies

Decreased neurogenesis has been associated with mood disorders, including depression [for reviews see (63, 64)]. The phenomenon of adult neurogenesis, where new neurons proliferate and become functionally integrated with existing neurons, has been most widely studied in the hippocampus (95, 96). Long-term retinoid treatment *in vivo* decreases adult hippocampal neurogenesis (97). Specifically, when young adult CD1 mice were treated with 13-*cis*-RA (1mg/kg/day) for up to 6 weeks, a significant decrease in hippocampal neurogenesis was observed (97). Although these authors did not examine depression-related behaviors, they did demonstrate that 13-*cis*-RA treatment leads to impaired spatial learning and memory performance in the radial arm maze.

Only one other group has conducted studies examining the effects of 13-*cis*-RA on depression-related behavior in animals. Ferguson et al. (98) treated adult rats with 7.5 or 22.5 mg/kg/day 13-*cis*-RA or 10 or 15 mg/kg/day of ATRA and found no differences in depression-related behavior in the forced swim test. Ferguson et al. (98) examined adult rats with treatment starting at 12 weeks and continuing to approximately 19 weeks of age and 13-*cis*-RA was administered via oral gavage. Although the authors did not

report serum levels, they state that the 7 or 15 mg/kg/day dose of 13-*cis*-RA or ATRA was required to elevate the rat serum level to that measured in humans taking Accutane (98). These doses of 13-*cis*-RA are much higher than the prescribed doses for human patients, which vary between 0.5 and 2 mg/kg/day (6). Additionally, Ferguson et al. (98) used oral gavage to administer the 13-*cis*-RA to the rats and this method of administration requires that the animal be restrained for a longer period of time than other methods of administration, such as intraperitoneal (i.p.) injection. The animals were subjected to a two-day forced swim test, which is typically used to assess learned-helplessness. The second day is utilized as a measure of the animal's learned response to become helpless. Ferguson et al. (98) reported that the animals spent more time swimming on the second day of treatment. In the learned-helpless paradigm, animals usually spend more time immobile on the second day. The fact that Ferguson et al. (98) reported that control rats spend less time immobile on the second day indicates that this test was not performed correctly. However, these authors report the swimming, climbing, and immobility measurements as an average from the two tests, making it difficult for the reader to assess their results.

In a follow-up study by the same group, Ferguson et al. (99) again reported no change in depression-related behaviors due to 13-*cis*-RA treatment. Treatment doses and method of administration were the same as in the first study. In this second study, animals were tested in the two-day forced swim test three separate sessions at 24, 82, and 130 days after treatment with vehicle or 13-*cis*-RA (99). This group reported no effect of treatment on behavior for any of the test sessions. Measurements of climbing, swimming, and immobility were reported as an average of the three test sessions for either day one or day two (99). Due to inappropriate presentation of the forced swim

test, these studies do not offer insight as to whether or not 13-*cis*-RA can induce depression.

OVERVIEW

The work that comprises this dissertation was directed at four aims. The first aim was to determine if 13-*cis*-RA is capable of inducing depression-related behaviors in adolescent mice. This aim is important because the epidemiological data indicating that 13-*cis*-RA could cause depression is controversial. Additionally, whether or not patients taking Accutane might become depressed due to 13-*cis*-RA is confounded by the psychosocial impact of acne on human self-image and self-esteem. The use of an animal model allowed us to establish the effect of 13-*cis*-RA on behavior without the confounding social factor of acne and self-image. The second aim was to determine the effects of 13-*cis*-RA on the serotonergic system. The serotonergic system is commonly disrupted in depressed individuals and many antidepressants work through manipulating the serotonergic system. The third aim was to determine the effects of 13-*cis*-RA administration on brain metabolism in adolescent mice using cytochrome oxidase (CO) as a metabolic measure because brain metabolism in depressed patients is altered in various brain regions. The last aim is directed at determining the effects of 13-cis-RA on serotonergic cell numbers. Retinoids are known to play a role in differentiation, cell cycle, and apoptosis. Additionally, one theory of depression is that apoptosis is increased in depressed patients, thus the effects of 13-cis-RA on serotonergic cell numbers was examined.

Chapter 2 discusses the effects of 13-*cis*-RA administration on depression- and anxiety-related behaviors in adolescent male mice. Chapter 3 investigates the effects that 13-*cis*-RA has on components of the serotonergic system *in vitro*. Chapter 4 examines

the changes in brain metabolism due to 13-*cis*-RA administration. Chapter 5 discusses the effects of 13-cis-RA on the cell death in serotonergic cells *in vivo*. To conclude this study, Chapter 6 summarizes these studies and discusses future work that could be done in this field.

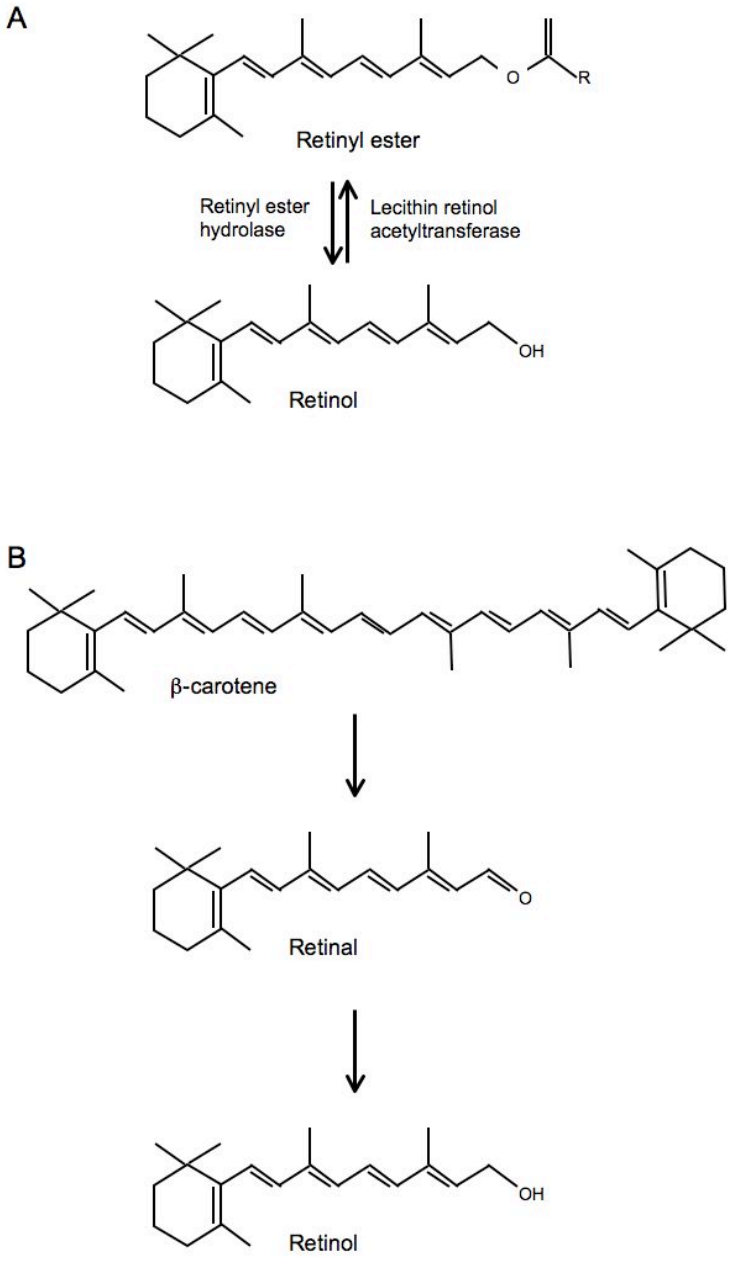

Figure 1.1: Cleavage of dietary vitamin A.

(A) Retinyl Esters are cleaved in the lumen of the intestine and **(B)** β-carotene is cleaved in the intestinal mucosa to form Retinol adapted from (100).

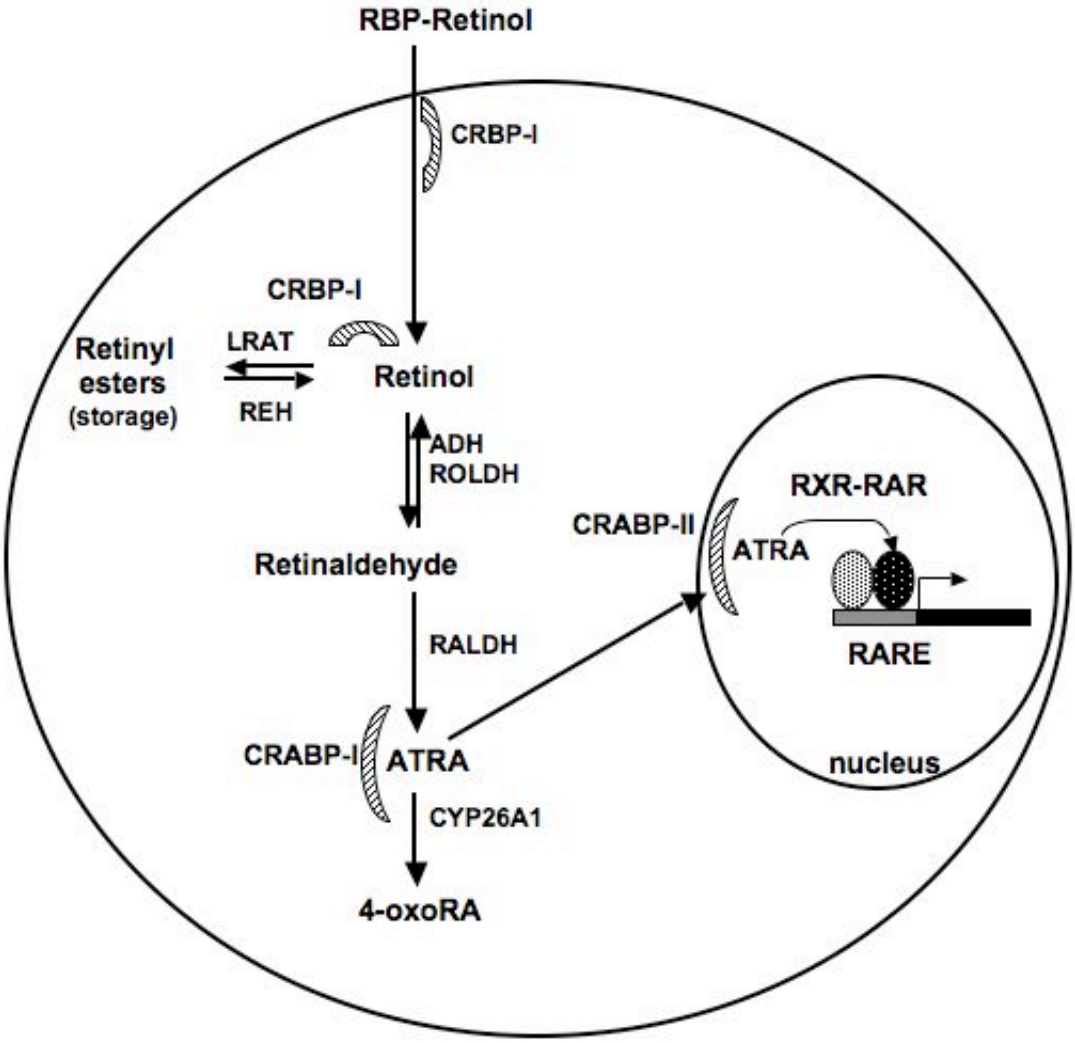

Figure 1.2: Retinoid storage and mechanism of action.

Retinol is transported through the blood bound to retinol binding protein (RBP). Retinol crosses the cell membrane and is either converted to retinyl esters for storage or to *all-trans*-retinoic acid (ATRA) via a retinol dehydrogenase (ROLDH) and retinaldehyde dehydrogenase (RALDH). ATRA is then either further degraded to 4-oxo-retinoic acid (4-oxo-RA) and excreted or shuttled to the nucleus where it binds to the retinoic acid receptor (RAR). In the nucleus, the RAR heterodimerizes with the retinoid X receptor (RXR) and binds to the retinoic acid response element in the DNA. Once ATRA binds to the RXR/RAR heterodimer, transcription is initiated.

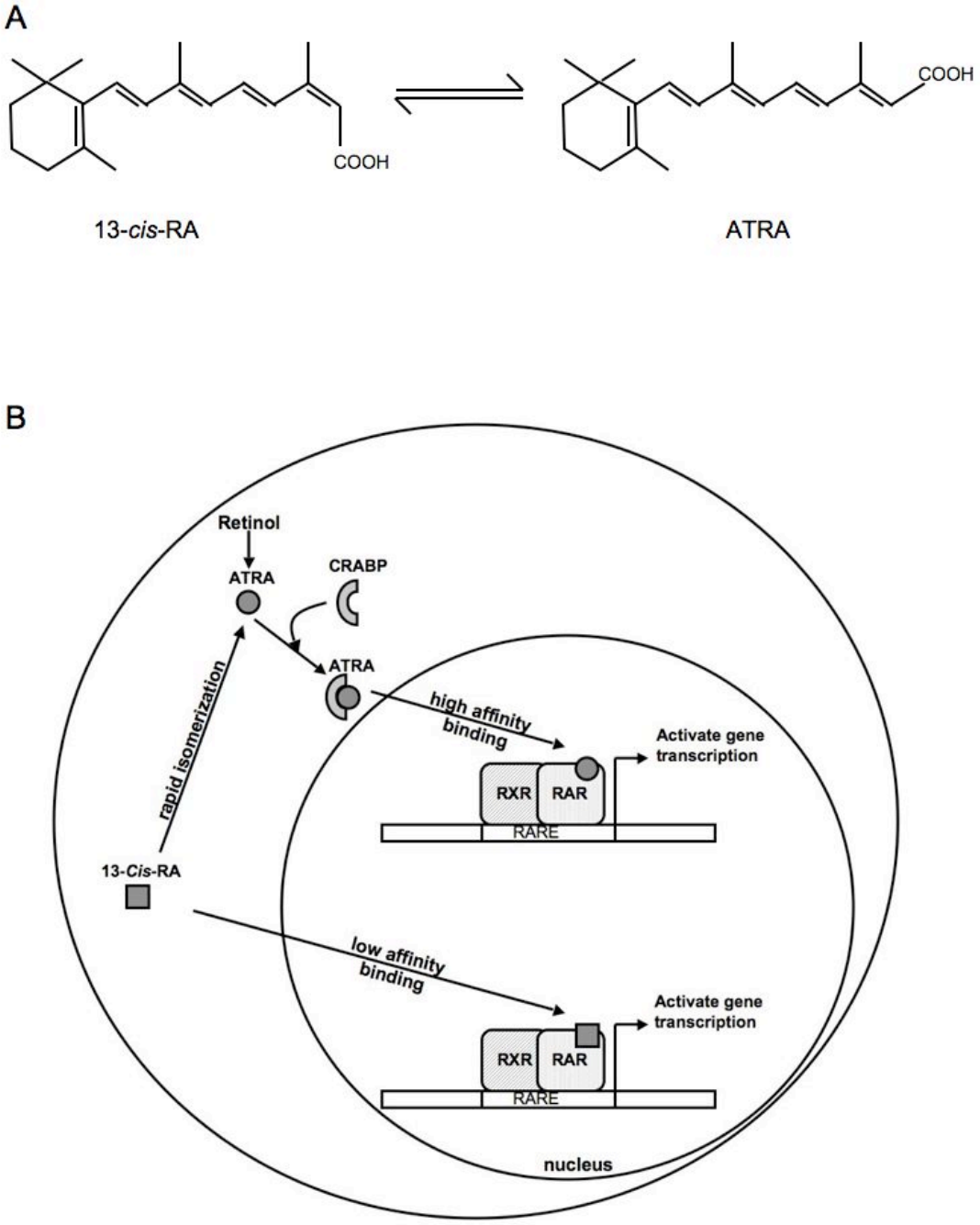

Figure 1.3: 13-*Cis*-RA mechanism of action.

(A) 13-cis-RA is capable of isomerizing to ATRA. **(B)** Once inside the cell, 13-*cis*-RA can isomerize to ATRA and then bind to the RAR in the nucleus to initiate transcription. Alternatively, 13-*cis*-RA can bind to the RAR in the nucleus and initiate transcription.

Chapter 2: Chronic Administration of 13-*Cis*-RA Increases Depression-Related Behavior in Mice

ABSTRACT

The use of 13-*cis*-RA to treat severe acne has been associated with onset of depression in the humans, although whether or not 13-*cis*-RA can cause depression has remained controversial. Because the psychosocial impact of acne may play a factor in adolescent depression, an animal model was used to test the hypothesis that chronic administration of 13-*cis*-RA would lead to depression-related behaviors. Young, adult male mice received 13-*cis*-RA (1 mg/kg) by daily i.p. injection for 6 weeks. This treatment paradigm produced plasma levels of 13-*cis*-RA that are comparable to those reported in human patients taking Accutane. In both the forced swim test and the tail suspension test we found that 13-*cis*-RA treated mice spent significantly more time immobile compared to vehicle treated controls. In the open field test there was no change in anxiety-related behavior in 13-*cis*-RA treated mice. Furthermore, chronic administration of 13-*cis*-RA did not impair locomotion in either the open field or the rotarod test. Taken together these results suggest that administration of 13-*cis*-RA increases depression-related behaviors in mice.

INTRODUCTION

Accutane (13-*cis*-RA) was originally intended to treat severe acne that is resistant to other forms of treatment (7). As mentioned previously, the medical literature indicates there may be a link between 13-*cis*-RA use and depression, although this link remains controversial. Patients with disfiguring acne exhibit problems with self-esteem, self-image, depression and anger (101). These emotional responses to severe acne could, at least in part, be responsible for the depressive symptoms associated with 13-*cis*-RA use, thus confounding depressive symptoms arising due to 13-*cis*-RA treatment. In an attempt to remove the psychosocial variables that could also cause depressive symptoms from our studies, a mouse model was used. The use of an animal model allows for the separation of the effects of acne on self-image and mood from those of 13-*cis*-RA itself on depression-related behavior.

Acne is most prevalent in adolescent populations (102), thus, Accutane is commonly prescribed to adolescents. Adolescence in humans is considered the time of development during which the transition from childhood to adulthood occurs. Hallmarked not only by the greatest amount of growth and the development of sexual characteristics, adolescence is also comprised of the events that lead the individual from dependence on a primary caretaker to the ability to care for themselves [Reviewed in (103)]. Thus, adolescence in humans usually starts around 12 years of age and can end as late as 25 years old [Reviewed in (103)]. Our animal studies utilized the inbred DBA/2J mice strain (Jackson Laboratory, Harbor, MA). Mice were three weeks upon arrival. Mice reach sexual maturity between the ages of six and eight weeks and the growth of the animals does not begin to slow until approximately 9 or 10 weeks of age (104), therefore mice aged 4 to 12 can be considered adolescent.

Retinoids, including vitamin A and its derivatives, have long been studied for their role in embryonic development because excess retinoids induce neural tube defects. Emerging evidence now indicates that retinoid signaling pathways also affect the functioning of the adult brain [For review see (105, 106)]. Inuit populations often consume high levels of vitamin A in the livers of seals, sharks and predatory mammals resulting in the phenomenon termed "pibloktoq", also known as "artic hysteria" (107). Retinoid toxicity, similar to some of the side effects of 13-*cis*-RA treatment, manifests as intense headaches, due to increased intracranial pressure resulting from excess cerebrospinal fluid termed "pseudotumor cerebrei", dry skin and hair loss, bone, joint, and muscle pain, fatigue and anorexia. In addition, hypervitaminosis A has been reported to induce psychosis (108, 109). Specifically, patients experiencing hypervitaminosis A exhibited depression, elevated anxiety, and irritability (107, 110). It is unknown if the toxic effects of excess dietary vitamin A are mediated via ATRA or by retinol. Although circulating retinol concentrations are maintained at 1-2 μM, ingestion of ATRA and 13-*cis*-RA can raise serum levels of these retinoids well above physiological levels. Due to their lipophillic nature, retinoids can cross the blood-brain barrier and affect various cellular processes both inclusive and exclusive of ATRA and RAR-mediated gene transcription (111-113).

Given the role of retinoids in neuronal differentiation, it is not surprising that a large number of neuronal genes have been shown to be retinoid-responsive [For review see (106)]. Neuronal genes containing identified functional RARE in their promoter regions include the dopamine D2 receptor (24, 32, 114), neurogranin (RC3) (115, 116), gonadotrophin-releasing hormone (117, 118) and oxytocin (119). Consequently, retinoid-responsive gene transcription in the central nervous system could have a significant impact on the function of the adult brain. Indeed, such a role for retinoids has

been demonstrated in learning and memory (97, 120, 121). In agreement with a role for retinoids in learning and memory, Crandall et al. (2004) have shown that long-term administration of 13-*cis*-RA in adult mice suppresses hippocampal neurogenesis (97). Deficits in adult neurogenesis in the hippocampus have been proposed to underlie depression (122), especially as they are sensitive to reversal by antidepressant administration (123). Crandall et al. (2004) reported impairments in spatial learning but did not report an effect on depression-related behaviors in mice.

The objective of the present study was to determine whether 13-*cis*-RA, administered in a dose identical to that prescribed to human patients, could alter depression- or anxiety-related behaviors in young adult mice. Here, we report that chronic administration of 13-*cis*-RA increases the time spent immobile in both the forced swim and the tail suspension tests. Increases in immobility in the behavioral despair paradigms are consistent with increased depression-related behavior.

METHODS

Animals

Young, adult male DBA/2J (Jackson Laboratories, Bar Harbor, ME) mice were used in this study. Male mice were chosen to avoid the effects of estrous cycle. Animals were three weeks old at arrival and four weeks old at the start of treatment. Mice were group housed four per cage and maintained under a 12:12 h light/dark cycle. Food and water were provided *ad libitum.* All procedures and tests performed on animals were approved by the University of Texas IACUC, protocol number 04100403, and according to the National Institutes of Health Guide for the Care and Use of Laboratory Animals.

Treatment

Animals were allowed to adapt to the University of Texas animal facility for one week prior to initial injection. Animals were handled during the first week to reduce the stress of receiving daily injections. A 2 mg/mL stock solution of 13-*cis*-RA in DMSO was stored for up to one week at -20 ºC. The stability of 13-*cis*-RA after one week of storage was confirmed by comparing the absorbance at 354 nm to that of a freshly prepared sample (97). Sterile injection samples were prepared in the dark. Injections were performed one hour prior to the start of the dark cycle, to avoid waking the animals in the middle of their sleep cycle, and the injections were kept covered to prevent exposure to light until right before the injection was performed. Injections were given in the same room where the animals were housed and the same person performed all injections. Treated animals (n = 12) received daily intraperitoneal (i.p.) injections of 1 mg/kg/day 13-*cis*-RA (Sigma, St. Louis, MO) dissolved in sterile 50% DMSO/50% saline (0.9%) to a final volume of 200 μL. Control animals (n = 12) were administered 200 μL of vehicle (50% DMSO/50% saline), i.p., daily. Animals were injected for 6 weeks prior to behavioral testing. Daily injections continued throughout the testing period and all animals received injections 14 h before any behavioral testing to eliminate any acute effects of injection. Only one behavioral test was performed each day. The behavioral experiments were conducted in the following order: tail suspension test, forced swim test, open field test, and rotarod test. Approximately 24 h elapsed between each of the following tests.

13-*Cis*-RA Plasma Level Determination

After behavioral testing, blood samples were collected from treated animals immediately postmortem. 13-*Cis*-RA was administered to the mice approximately 16 h

before sacrifice. To prevent retinoid degradation all steps were performed in the dark. The blood was allowed to coagulate for 30 min and then centrifuged at 1000 x *g* for 20 min. The plasma was then removed and stored at –80 ºC until the retinoid extraction was performed. Samples were extracted as described (124). In total, 0.7 volumes of acetonitrile:butanol (1:1) solution was added to the sample and vortexed for 45 s, then 0.6 volumes of saturated K_2HPO_4 was added and vortexed for 10 s. The samples were then centrifuged at 13,000 x g for 10 minutes. The upper layer was removed and the sample volume brought up to 100 μL with 100% acetonitrile. The absorbance of the samples was determined at 354 nm and 13-*cis*-RA concentration was determined by comparison to a standard curve. For the standard curve, a known amount of 13-*cis*-RA was added to plasma from mice not treated with Accutane and extracted as described above. All concentration values were corrected for initial and extracted sample volumes.

Tail Suspension Test

To perform the tail suspension test, animals were suspended by the tail on a horizontal beam 33 cm high. Mice were taped to the bar using adhesive tape placed approximately 1 cm from the tip of the tail. A 6-min test period was used and videotaped for subsequent analysis. The animals engaged in several escape-related behaviors interspersed with periods of immobility. The duration of immobility was measured in seconds. The mice were tested in a randomized, double-blinded manner.

Porsolt Forced Swim Test

The forced swim test is a pharmacologically validated model of depression-related behavior in mice (125). Mice were placed in a Plexiglas, cylindrical tank, 20 cm

x 51 cm, filled to a depth of 35 cm with room temperature water (25 $\pm$ 0.5 ºC) for a total of 6 min and the test was videotaped for subsequent analysis. Mice were scored for each of three behaviors: swimming, climbing, and immobility. Immobility was defined as the absence of escape-related behavior, such as swimming, climbing, or rearing. Swimming behavior was assigned when the animal was moving around the container with all paws, while climbing behavior was assigned when the animal became vertical and clawed at the cylinder walls with its forepaws. The duration of each of these behaviors was measured in seconds over a 6-min period. The mice were tested in a randomized, double-blinded manner.

Open Field Test

The open field test was used to evaluate anxiety-related behaviors (126, 127). Animals were placed in a 16 x 16 cm open field apparatus (Med Associates, St Albans, VT). Ambulatory and stereotypic activity was measured by infrared motion detectors spaced 2.5 cm apart. Rearing and jumping activity was measured by another set of infrared motion detectors 4.6 cm above the floor. The animal activity was monitored by Activity Monitor, version 5.10 (Med Associates, St Albans, VT) over the course of 5 min. The ambulatory time was determined in seconds for each minute spent in the open field as were the total ambulatory, vertical, and stereotypic times. The percent of time the animal spent in the center (38% of the total field area) and the number of entries into the center of the field were also calculated. Motor function was also assessed by considering the total distance traveled in the open field during the 5-min observation period.

Rotarod Test

In order to determine the effect of retinoids on motor coordination, the rotarod test was performed. The rotarod test consisted of placing the animal on a rotating rod, 4 cm in diameter, 35 cm high (Columbia Instruments, Columbus, OH). Low rotation speeds were chosen for this test since DBA/2J mice perform this task relatively poorly at higher speeds (128). The animals were first placed on a rod rotating at 5 rpm for 2 min to acclimate to this novel motor task. Each time an animal fell from the rod during this time period, the animal was placed back onto the rod. After the 2-min acclimation period, the animal was allowed to rest for 1 min and then placed back on the rod rotating at 5 rpm. The latency to fall was then measured in seconds. The animal was then placed on the rod for a second trial at a rotation speed of 10 rpm. The latency to fall was again measured in seconds. In all trials, if the mouse did not fall from the rod, it was removed from the rod after 2 min.

Behavioral Evaluation and Statistical Analyses

All behavioral tests were double-blinded and all were scored prior to decoding any of the tests. Immobility data from the last four minutes of both the tail suspension and forced swim tests were analyzed with a 2 x 2 x 4 (Group x Test x Minute) repeated measures ANOVA, with the two tests and four minutes serving as repeated measures. We analyzed the two immobility tests in this way because they both examine the same construct (depressive behavior) using the same units of measurement (seconds of immobility). This omnibus approach has been successfully applied to other behavioral measures meeting these criteria (129). Only the last four minutes of each test were used in the analysis because of widespread zero values during the first 2 min of each test. The

open-field and rotarod data were analyzed by two-tailed t-tests. Values reported are mean ± SEM of n = 12 observations unless otherwise indicated.

RESULTS

Confirmation of 13-*Cis*-RA plasma levels in treated mice

The human dose of 13-*cis*-RA used to treat acne ranges from 0.5 to 2 mg/kg/d. The mice used in this study received an amount of 13-*cis*-RA within this range and identical to the amount administered to mice in the study by Crandall et al. (97). The plasma level of 13-*cis*-RA in six mice chronically treated with 13-*cis*-RA was 1.5 ± 0.4 μg/mL. This value is higher than that previously observed by Crandall et al. (97), potentially due to the use of different retinoid extraction techniques. However, the plasma levels obtained in the present study are approximately twice that displayed by humans administered 0.5 mg/kg/d of 13-*cis*-RA, one-half the dose used in the present study. Plasma 13-*cis*-RA concentrations in these patients reached 0.74 μg/mL (8) . In addition, the plasma concentration obtained in the present study is similar to that reported in the Accutane capsules package insert were the peak plasma concentration of 13-*cis*-RA in healthy patients aged 12-15 years receiving multiple oral doses of 13-*cis*-RA for the treatment of severe acne ranged from 0.37 to 1.09 μg/mL. Therefore, administration of 1 mg/kg/d of 13-*cis*-RA to young, adult male mice results in plasma 13-*cis*-RA levels similar to those observed in human patients.

13-*Cis*-RA Treatment Had No Effect on Weight Gain

Weight gain over the six weeks of injections was followed to ensure that the animals were not showing overt signs of distress or discomfort. Weekly weighing of the

mice showed that overall weight gain across the experiment was normal and that there was no difference in body weight between the 13-*cis*-RA treated group and the control group. At the start of injections, the 13-*cis*-RA treated group weighed 15.5 $\pm$ 0.4 g and the control group weighed 15.1 $\pm$ 0.3 g. At the beginning of the behavioral testing, the treatment group weighed 23.8 $\pm$ 0.5 g and the control group weighed 23.1 $\pm$ 0.5 g. The behavioral tests had no effect on the weight of the animals. Daily monitoring confirmed that the animals were not showing any signs of distress as a result of the repeated injections, which were given on alternating sides of the abdominal cavity. The injections were verified to be i.p. and not subcutaneous by feeling the skin on the underside of the animals daily for bubbles or scar tissue.

Chronic Administration of 13-*Cis*-RA Increases Immobility in the Tail Suspension and Forced Swim Tests

The effect of chronic administration of 13-*cis*-RA on young adult mouse behavior in the tail suspension (A and B) and forced swim (C and D) tests is shown in Figure 2.1. Both tests are pharmacologically validated models of behavioral despair in which the time spent immobile decreases with antidepressant treatment (43, 130). The 2 x 2 x 4 (Group x Test x Minute) repeated measures ANOVA of the immobility data showed no significant interactions and no significant effect of test, supporting the validity of analyzing the two tests in this way. There was a significant main effect of group, $F(1,21) = 4.8$, $p = 0.039$, with 13-*cis*-RA treated mice showing significantly more immobility than vehicle controls. The estimated marginal means and standard errors for the two groups were 19 ± 2.1 s of immobility per min for the 13-*cis*-RA treated group and 12 ± 2.0 s of immobility per min for the vehicle controls. The increase in immobility due to 13-*cis*-RA treatment observed in the forced swim test appears to be due to a decrease in

swimming behavior (Fig. 2.1C). There was no difference between the groups for the amount of time the animals spent engaged in climbing activity. These data show that chronic 13-*cis*-RA administration increases immobility in both the tail suspension and forced swim tests, which is indicative of increased depression-related behavior.

Chronic Administration of 13-*Cis*-RA has No Effect on Anxiety-related and Motor Behavior in the Open Field Test

Approximately 25-50% of depressed youth also exhibit anxiety. Selective 5-HT reuptake inhibitors have been used successfully to treat both depression and anxiety, potentially indicating a common etiology [For review see(131)]. Also, in mice, anxiety may be one factor that contributes to susceptibility to depression-related behaviors (132). The open field test is an anxiety-related behavioral paradigm that is sensitive to anxiolytic drugs (126, 127). An animal exhibiting anxiety-related behavior will spend less time in the center of the open field. There was no difference between the 13-*cis*-RA treated group and the control group in the number of entries into the inner zone of the field between the two groups ($p = 0.61$) (Fig. 2.2A). 13-*Cis*-RA treated mice made 21 $\pm$ 4 entries into the inner field and control animals made 24 $\pm$ 2 entries.

Retinoid signaling affects locomotion. For example, RARβ–RXRβ, RARβ–RXRγ and RXRβ–RXRγ double null mutant mice (but not the corresponding single mutants) exhibit reduced forward locomotion and rearing frequency in the open field test (34). Also, retinoic acid-mediated effects have been implicated in Parkinson's (133), and Huntington's disease (134) [For review see (106)]. Therefore, to assure that the effects of 13-*cis*-RA on behavior in the tail suspension and forced swim tests were due to a specific increase in despair-related behavior and not to an overall decrease in locomotion or coordination, we conducted the open field and rotarod tests, respectively. There was no

difference in total ambulatory time ($p = 0.68$) or the ambulatory time in the inner zone of the field ($p = 0.68$) between the two groups (Fig. 2.2B). The total ambulatory time of mice treated with 13-*cis*-RA was 55 $\pm$ 3 seconds versus 57 $\pm$ 2 seconds for the control mice. The ambulatory time for the 13-*cis*-RA treated mice in the inner zone of the field was 7 $\pm$ 1 seconds while control mice had 8 $\pm$ 1 seconds of ambulatory time in the inner zone of the open field. Additionally, there was no difference in the ambulatory distance traveled over the entire field ($p = 0.78$) or the inner zone of the field ($p = 0.93$) (Fig. 2.1C). 13-*Cis*-RA treated mice traveled 1426 $\pm$ 98 cm while control mice traveled 1451 $\pm$ 57 cm over the entire field. 13-*Cis*-RA treated mice traveled 211 $\pm$ 30 cm in the inner zone and the control mice traveled 216 $\pm$ 19 cm. Because 13-*cis*-RA treatment did not alter the number of entries into, or the total distance traveled in, the center zone of the open field it is unlikely that 13-*cis*-RA has an effect on anxiety-related behavior. The lack of a difference between groups with respect to total distance traveled or total ambulatory time indicates that 13-*cis*-RA has no effect on overall locomotion compared with vehicle treated controls.

Chronic 13-*Cis*-RA Administration Increases Motor Coordination on the Rotarod

There was no impairment of motor coordination in mice treated with 13-*cis*-RA (Fig. 2.3). There was a trend for mice treated with 13-*cis*-RA to remain on the rotating rod longer than control mice when tested at a rotational speed of 5 rpm ($p = 0.07$). Mice administered 13-*cis*-RA were able to stay on the rod for 105 $\pm$ 10 seconds, whereas control mice were only able to remain on the rod for 75 $\pm$ 13 seconds. However, when tested at 10 rpm, there was no difference between the latency to fall time for the treated and control mice ($p = 0.91$). Retinoids have been implicated in the regulation of locomotion because RARβ-RXRβ, RARβ-RXRγ, and RXRβ-RXRγ double null mutant

mice were shown to have locomotor deficits (34). In contrast, chronic 13-*cis*-RA treatment tends to improve motor coordination at low rotational speeds in the rotarod test without an effect on total locomotion (Fig. 2.3).

DISCUSSION

Here we demonstrate that chronic administration of 13-*cis*-RA to young adult male mice increased the time spent immobile in both the tail suspension and forced swim tests. In the open field test there was no evidence of a change in anxiety-related behavior. Furthermore, there was no impairment of locomotion or motor coordination in 13-*cis*-RA treated animals. Taken together these data indicate that the increased immobility in behavioral despair paradigms is not due to an effect on motor systems, but results from increased depression-related behavior.

Increased immobility in the forced swim test has been reported to occur in situations that increase vulnerability to depression such as estradiol deficiency due to aromatase knockout (45), stress due to food restriction (46), magnesium depletion (47), and choline administration (48). The behavior of the animals in the tail suspension test was not assessed in these studies. However, increased immobility in both the forced swim and tail suspension tests does occur due to the pro-depressant effects of withdrawal from chronic amphetamine administration (49), centrally administered urotensin-II (50), and interleukin-1 and endotoxin injection (51). Interestingly, in the forced swim test, antidepressants that target the serotonergic system increase swimming behavior, thereby decreasing immobility (135). On the other hand, antidepressants that target noradrenergic systems increase climbing behavior. In our experiments, 13-*cis*-RA treatment leads to an increased immobility with a concomitant decrease in swimming behavior, without an

effect on climbing behavior. This may indicate that chronic 13-*cis*-RA administration disrupts serotonergic systems, leading to increased depression-related behavior.

A recent study reported the effects of chronic 13-*cis*-RA administration on adult rats. In the forced swim test, Ferguson et al. (98) reported a marginally significant effect of 13-*cis*-RA treatment on immobility. However, in contrast to our observations, these authors observed less immobility following 13-*cis*-RA administration. This reduced immobility was observed for a successive two-day test in which the immobility for the second day was found to be decreased for all test groups. The fact that immobility was decreased on the second test day is surprising because the forced swim test, when conducted on consecutive days, generally results in increased immobility each day regardless of treatment [for example (136)]. In addition, Ferguson et al. (99) reported that there was no change in voluntary saccharin solution intake in treated rats, reflecting an absence of the depressive symptom anhedonia. The authors concluded that 13-*cis*-RA did not severely affect depression-like behaviors in male or female rats.

There are three important differences between our study and that of Ferguson et al. (98): 1) age and species of test subjects, 2) method of dosing, and 3) dose of drug administered. The adolescent mice used in our study are at a much earlier stage of development than the adult rats used by Ferguson et al. (98); we began dosing between the time of weaning and the onset of sexual maturity. The dose of 13-*cis*-RA we administered was 1mg/kg via i.p. injection in comparison to the much higher doses (7.5 and 22.5 mg/kg) used by Ferguson et al. (98) administered by oral gavage. The dose we used is within the recommended range for treatment of patients (0.5-2.0 mg/kg/day) and we achieved serum levels in treated mice that were equivalent to those seen in patients. Repeated drug administration is a potential stressor and stress has been shown to influence depression-related behavior (137). Ferguson et al. (98) also examined behavior

in the open field and in one treatment group saw that 13-*cis*-RA treated rats were significantly less active than same sex controls. This increase in freezing time in the open field increased with the duration of treatment even in control animals. One explanation for this is that all animals were exhibiting enhanced stress-responses, which can manifest as increased freezing time in the open field test. It is therefore possible that Ferguson et al. (98) were not able to detect changes in depression-related behaviors in 13-*cis*-RA treated animals because they were masked by elevated stress in all treatment groups.

Changes in adult behavior as a result of 13-*cis*-RA administration are perhaps not surprising given the evidence linking retinoid signaling to adult CNS function (105, 106). A large number of neuronal genes have been shown to be retinoid-responsive (106), but it is not yet known whether 13-*cis*-RA can regulate gene transcription in the adult brain. 13-*Cis*-RA could be activating gene transcription by either isomerizing to ATRA and binding to the RAR (9) or directly binding to the RAR itself (10). Although 13-*cis*-RA binds to the RAR with much lower affinity than ATRA, once bound to the RAR, 13-*cis*-RA is very efficient at initiating transcription (10). Given that depression is a complex, multifactorial phenomenon involving dopaminergic, serotonergic, noradrenergic and other transmitter pathways, altered regulation of a subset of target genes by 13-*cis*-RA could produce subtle changes in neuronal function that lead to enhanced depression-related behaviors. For example, a verified RARE has been found in the promoter region of the dopamine D2 receptor and *all-trans*-retinoic acid can upregulate dopamine D2 receptor expression (24). Increased dopamine D2 receptor abundance has been reported in patients with major depression (138). Similarly, the 5-hydroxytryptamine 1A (5-HT_{1A}) receptor, which has a role in regulating the firing of 5-HT neurons and is associated with depression-related personality traits (139), has been shown to be upregulated in response

to *all-trans*-retinoic acid treatment in neuronal cells (140). Altered regulation of either the D2 receptor or the 5-HT_{1A} receptor genes by 13-*cis*-RA, as well as other neuronal genes, could provide a possible mechanism for the changes in depression-related behaviors seen in chronically treated mice.

An alternative mechanism by which 13-*cis*-RA could alter depression-related behaviors is by affecting adult neurogenesis. In animal models, inescapable stress reduces hippocampal neurogenesis, a phenomena that can be reversed with antidepressant treatment (141). Apart from the well documented effects of retinoids on neuronal differentiation during development (142), retinoid signalling has been shown to promote adult neurogenesis in the hippocampus and olfactory bulb (143, 144). A role for retinoids in learning and memory behaviors had previously been established using RAR knockout mice and vitamin A deficient models [for review see (145)]. Interestingly, both RARβ or RARβ-RXRγ double null mutant mice and vitamin A deficiency are associated with deficits in spatial learning and memory (121, 146, 147). In contrast, long-term administration of 13-*cis*-RA suppresses hippocampal neurogenesis and decreases hippocampal cell survival (97). It may seem contradictory that RARβ and RARβ/RXRγ null mice have decreased spatial learning while chronic administration of 1 mg/kg/day of ATRA or 13-*cis*-RA to adolescent male CD1 mice also impairs learning and memory, but this may be a case where the dose makes the poison. Although physiological levels of retinoids and retinoid signaling pathways are required for neuronal differentiation and ultimately, learning and memory, pharmacological levels of retinoids may initiate other processes that inhibit neurogenesis. Thus, the ability of 13-*cis*-RA to increase depression-related behavior in the present study may be due to decreased hippocampal neurogenesis and cell survival and likely involves altered regulation of neuronal gene expression. Interestingly, adult neurogenesis requires functional serotonergic signaling

(148, 149), further suggesting that 13-*cis*-RA mediates its effects by specifically regulating serotonergic gene expression and/or hippocampal neurogenesis.

13-*Cis*-RA is an effective treatment for severe recalcitrant acne (150). Diagnosing depressive symptoms in acne patients following 13-*cis*-RA treatment is complicated by the psychological effects of severe acne itself. Clinically significant anxiety and depression symptoms have been reported in both adolescents and adults with chronic acne (101, 151). Additionally, adolescents under social stress may be on the border of clinical depression and 13-*cis*-RA treatment may be a precipitating event (152). Despite the possible confounding effects of existing conditions, there are some instances where patients with no previous history of psychiatric symptoms develop depression and suicidal ideation following 13-*cis*-RA treatment (7). Use of a mouse model allowed us to examine the effects of 13-*cis*-RA on depression-related behaviors independent of pre-existing conditions, self-image, and other factors that confound human studies. This report is the first to demonstrate that 13-*cis*-RA administration enhances depression-related behaviors in mice. These depression-related behaviors may be due to changes in brain metabolism, altered hippocampal neurogenesis, and altered serotonergic function.

ACKNOWLEDGEMENTS

I would like to thank Chris Bailey, Doug Barrett, and Elizabeth Johnson for technical assistance. I would also like to thank Jason Shumake for his assistance with the statistical analysis and Sarah Bailey for assistance in scoring the behavioral tests. I would also like to thank Dr. Yuri Blednov for the use of the rotarod. This research was supported by a University of Texas at Austin Fiscal Year Research Grant FY 2004-2005.

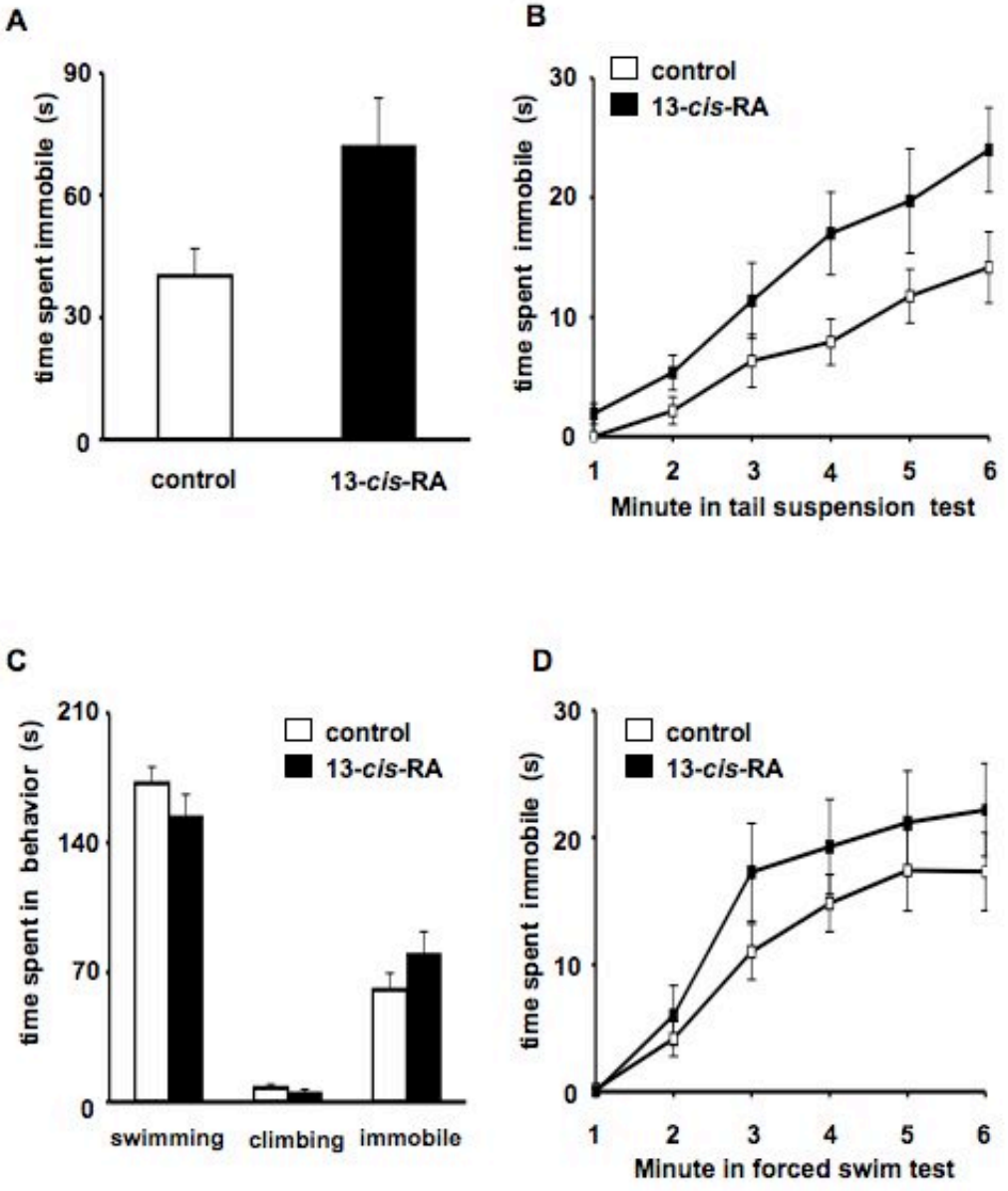
A
time spent immobile (s)
90
60
30
0
control
13-cis-RA
B
control
13-cis-RA
time spent immobile (s)
30
20
10
0
1
2
3
4
5
6
Minute in tail suspension test
C
time spent in behavior (s)
210
140
70
0
control
13-cis-RA
swimming
climbing
immobile
D
control
13-cis-RA
time spent immobile (s)
30
20
10
0
1
2
3
4
5
6
Minute in forced swim test

Figure 2.1: 13-C*is*-RA increases immobility in the tail suspension and forced swim tests.

Total time spent immobile in the tail suspension **(A)** and forced swim **(C)** tests are expressed as the mean ± SEM for the last four minutes of the observation period. The development of immobility during the tail suspension **(B)** and forced swim **(D)** tests are shown as mean ± SEM seconds per each minute of the six minute observation period. Overall immobility time from both tests (as assessed by repeated measures ANOVA) showed a significant main effect of group, $F(1,21) = 4.8$, $p = .039$, with 13-*cis*-RA treated mice showing significantly more immobility than vehicle controls. n = 11 13-*cis*-RA treated mice and n = 12 control mice.

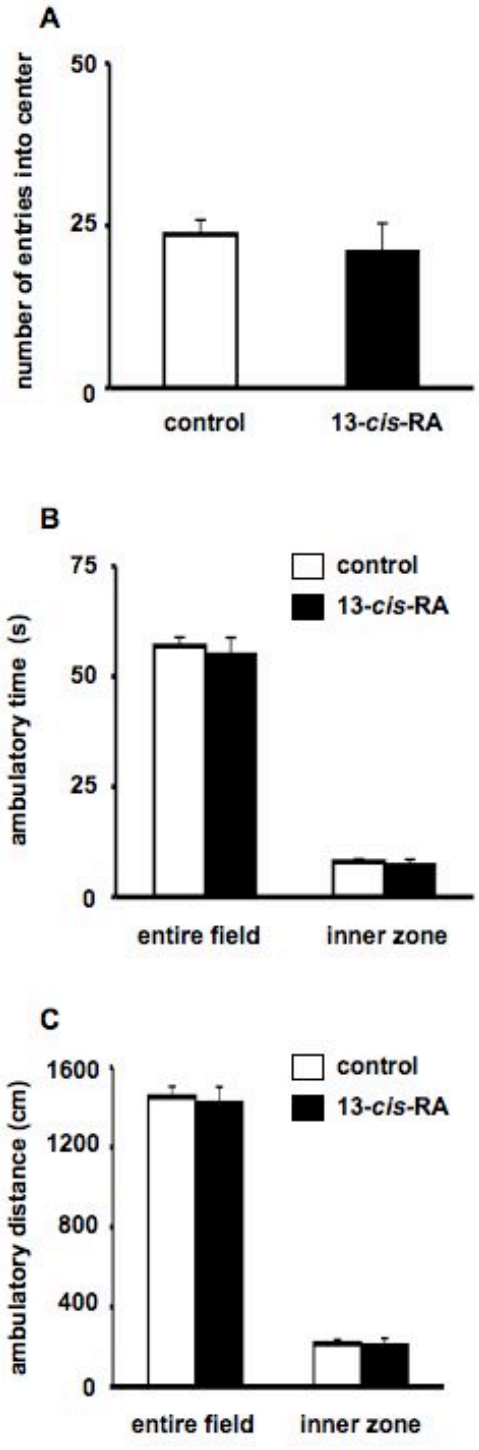
A
number of entries into center
50
25
0
control
13-cis-RA
B
ambulatory time (s)
75
50
25
0
control
13-cis-RA
entire field
inner zone
C
ambulatory distance (cm)
1600
1200
800
400
0
control
13-cis-RA
entire field
inner zone

Figure 2.2: 13-*Cis*-RA does not affect performance in the open field test.

The number of entries into the center **(A)**, the total ambulatory time **(B)** and the total ambulatory distance **(C)** measured during a five minute observation period in the open field test. In each case there was no difference between 13-*cis*-RA treated mice and vehicle treated controls. Values are mean $\pm$ SEM with n = 12 for each group.

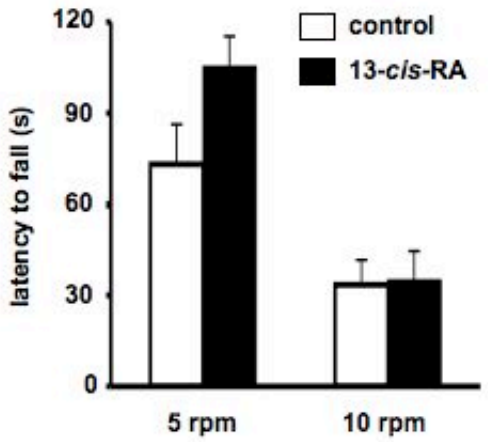

Figure 2.3: 13-*Cis*-RA does not impair motor performance in the rotarod test.

The mean latency to fall from a rod rotating at 5 rpm or at 10 rpm is shown during a two-minute test period. The 13-*cis*-RA treated mice tended to remain on the rotarod longer at 5 rpm. Treatment had no effect on rotarod performance at 10 rpm. Values are mean $\pm$ SEM with n = 12 for each group.

Chapter 3: 13-*Cis*-RA Alters Intracellular Serotonin, Increases 5-HT_{1A} Receptor and Serotonin Reuptake Transporter Levels *In Vitro*

ABSTRACT

As shown in chapter 2, chronic administration of 13-*cis*-RA to adolescent male mice increased depression-related behaviors. Here, we have examined whether 13-*cis*-RA regulates components involved in serotonergic neurotransmission *in vitro*. We used the RN46A-B14 cell line, derived from rat embryonic raphe nuclei. This cell line synthesizes serotonin (5hydroxytryptamine, 5-HT) and expresses the 5-HT_{1A} receptor and the serotonin reuptake transporter (SERT). Cells were treated with 0, 2.5, or 10 μM 13-*cis*-RA for 48 or 96 h and the levels of 5-HT, its metabolite 5-hydroxyindoleacetic acid (5-HIAA), 5-HT_{1A} receptor and SERT determined. Treatment with 13-*cis*-RA for 96 h increased the intracellular levels of 5-HT and tended to increase intracellular 5-HIAA levels. Furthermore, 48 h of treatment with 2.5 and 10 μM 13-*cis*-RA significantly increased 5-HT_{1A} protein to 168.5 ± 20.0 and 148.7 ± 2.2 % of control respectively. SERT protein levels were significantly increased to 142.5 ± 11.1 and 119.2 ± 3.6 % of control by 48 h of treatment with 2.5 and 10 μM of 13-*cis*-RA respectively. Increases in both 5-HT_{1A} receptor and SERT proteins may lead to decreased 5-HT availability at synapses. Such an effect of 13-*cis*-RA could contribute to the increased depression-related behaviors we have shown in mice.

INTRODUCTION

The Serotonergic System

5-HT (serotonin) is a monoamine neurotransmitter in the brain and gastrointestinal tract. 5-HT is also present in the blood and was discovered in 1948 and named for its role in vascular tone, "sero" for serum and "tonin" for tone. 5-HT is produced from tryptophan in a two-step process (Fig. 3.1). Tryptophan is first converted to 5-hydroxytryptophan by the rate limiting enzyme tryptophan hydroxylase. 5-Hydroxytryptophan is then converted to 5-hydroxytryptamine, or 5-HT, by the enzyme 5-HTP decarboxylase. 5-HT is then broken down to its inactive catabolite, 5-hydroxyindole acetic acid (5-HIAA), by monoamine oxidase A (MAOA). Intracellular levels of 5-HT are controlled by 5-HT synthesis from tryptophan, 5-HT degradation to 5-hydroxyindole acetic acid (5-HIAA), vesicular packaging and release of 5-HT into the synapse, and reuptake of 5-HT into the cell by serotonin reuptake transporter (SERT or 5-HTT) (Fig. 3.1). An additional regulator of 5-HT release is the somatodendritic serotonin receptor 1A (5-HT_{1A}) (Fig. 3.1). This autoreceptor is activated by 5-HT to inhibit firing of serotonergic raphe neurons (153).

The raphe nuclei are the main 5-HT producing cells in the central nervous system and the raphe nuclei and have processes that project widely throughout the brain. The processes of the dorsal raphe nuclei innervate, *inter alia*, the frontal cortex, the lateral septum and the ventral tegmental area (154). The median raphe nuclei project to the lateral habenula and the interpeduncular nucleus (155), among other regions of the brain. The hypothalamus and the septum receive input from both the dorsal and median raphe nuclei (154, 155) and the dorsal and median raphe nuclei send processes to each other (154, 155). Additionally, the molecular layer of the hippocampus receives input from

dorsal raphe nuclei while the hilus of the dentate gyrus receives input from the median raphe nuclei (148).

The 5-HT_{1A} receptor is a presynaptic autoreceptor found predominately in the raphe nuclei and a postsynaptic receptor found in the hippocampus, prefrontal cortex and caudate of the forebrain (156, 157). This metabotropic receptor is inhibitory in both the presynaptic and postsynaptic neurons of serotonergic circuits. The 5-HT_{1A} receptor is a G-protein coupled receptor that inhibits adenylate cyclase activity in postsynaptic neurons. However, in presynaptic neurons it is thought to activate an inwardly rectifying potassium channel (156). The inhibition of raphe nuclei neuron firing due to activation of the 5-HT_{1A} receptor directly inhibits neurotransmitter release [Reviewed in (158)].

The SERT is responsible for removing 5-HT from the synaptic cleft to terminate 5-HT signaling. SERT uses co-transport of sodium and chloride ions as a driving force for 5-HT transport into the cell [Reviewed in (159)]. The electrochemical gradient that drives sodium and chloride ions into the cell facilitates 5-HT transport, while the movement of potassium ions out of the cell through the transporter is what renders it competent for the next cycle of 5-HT transport [Reviewed in (159)]. Thus, SERTs are activated when the cell is hyperpolarized. Therefore inhibitory effects mediated by the 5-HT_{1A} receptor not only inhibit 5-HT release, but also enhance the reuptake of 5-HT from the synaptic cleft (156).

Serotonin and Depression

Although the etiology of depression is still unknown, the serotonergic system has long been a target of antidepressant drugs (160). 5-HT was discovered to have a role in the pathogenesis of depression in the 1950s when an antidepressant response was noticed in tuberculosis patients taking iproniazide (a monoamine oxidase inhibitor, or MAOI) and

imipramine (a selective serotonin reuptake transporter inhibitor, or SSRI) [Reviewed in (161)]. 5-HT reuptake and metabolism are targets of antidepressants, with the net result being increased levels of 5-HT in the synaptic cleft (Fig. 3.1). SERT inhibitors block the transport of 5-HT into the cell from the synaptic cleft while MAOA inhibitors block the metabolism of 5-HT to its inactive catabolite 5-HIAA. The role of 5-HT in human depression is further supported by studies showing reduced 5-HIAA levels in the cerebrospinal fluid (162) and polymorphisms in 5-HT1A receptor (163) and SERT (164, 165).

Evidence is accumulating that suggests the role of the 5-HT_{1A} receptor in regulating mood disorders. For example, altered expression of and polymorphisms in the 5-HT_{1A} receptor are implicated in depression [Reviewed in (166)] and 5-HT_{1A} receptor levels are increased in the midbrain of suicide victims with major depression (163). Chronic antidepressant treatment reduces the electrophysiological response to 5-HT_{1A} autoreceptors (162, 167) disinhibiting the action potential firing of the raphe nuclei and enhancing serotonergic neurotransmission (167)

Altered expression of the SERT is also implicated in depression [Reviewed in (166)] and regulation dysfunction of SERT has been associated with neuropsychiatric disorders and psychological traits such as bipolar disorder, anxiety, obsessive compulsive disorder, schizophrenia, and eating disorders (168).

Both the 5-HT_{1A} null mouse and the SERT knockout mouse exhibit decreased immobility time in the tail suspension test ((169) and (170) respectively). In contrast, the SERT knockout mouse has increased immobility in the forced swim test (170). SERT knockout mice also display significant impairment in shock avoidance (170) and treatment of mice between postnatal days 4 and 21 via i.p. injection with fluoxetine to block SERT activity replicated the impairment in shock avoidance seen in SERT

knockout mice even though testing was done nine weeks after the last fluoxetine injection (171). Perhaps the increased immobility in the forced swim test exhibited by SERT knockout mice is due to abnormal development of serotonergic signaling circuits in early life.

Retinoid Signaling and Depression-Related Behaviors

All-trans-retinoic acid (ATRA) is the endogenous ligand for retinoic acid receptors (RAR) and is synthesized from dietary vitamin A (retinol) (172). 13-*Cis*-RA is a synthetic retinoid capable of either binding to RAR itself (10) or being isomerized to ATRA prior to RAR binding (9). RAR heterodimerize with retinoid X receptors (RXR) and together they bind to specific DNA sequences termed retinoic acid response elements (RARE) (172). Binding of ligand to the RAR initiates transcription (172) and this has led to the view that retinoids are primarily regulators of gene transcription, either directly or via intermediate genes. The expression of many neuronal genes is affected by ATRA and a few have been reported to have functional RARE suggesting that retinoids act as transcriptional regulators in neuronal cells [for review see (106)]. However, retinoids can also influence cellular function by altering protein levels via non-transcriptional mechanisms, such as increasing mRNA (14, 15) or protein stability (16).

As shown in chapter 2, 13-*cis*-RA administration increases depression-related behaviors in mice (173). Adolescent, DBA/2J mice treated with 1 mg/kg/d of 13-*cis*-RA, the same dose prescribed to human patients, exhibited significantly more immobility than vehicle-treated controls in both the tail suspension test and the forced swim test (173). Further analysis of data in the forced swim test reveals that the increase in immobility is accompanied by a decrease in swimming, but not climbing behavior (173). For rodents, in the forced swim test, antidepressants that target the serotonergic system decrease

immobility due to an increase in swimming time (135). In contrast, antidepressants that target the noradrenergic system, decrease immobility and increase time spent climbing (135).

The ability of 13-*cis*-RA to cause depression-related behavior in adolescent mice led us to hypothesize that serotonergic function may be altered in the raphe nuclei in response to 13-*cis*-RA treatment. In this study we used a cell line derived from rat raphe nuclei, RN46A-B14, as our model. These cells are serotonergic and express the 5-HT_{1A} receptor and SERT (174, 175). We show that treatment of RN46A-B14 cells with 13-*cis*-RA increases intracellular 5-HT content. Intracellular 5-HIAA content also tends to be increased. In addition, both the 5-HT_{1A} receptor and SERT are increased following 13-*cis*-RA treatment.

METHODS

Tissue Culture

The *in vitro* studies were performed in the RN46A-B14 cell line. The RN46A parent cell line was derived from medullary raphe nuclei of an embryonic day 13 rat and immortalized with the temperature sensitive mutant of the SV40 large T-antigen. At the permissive temperature of 33˚C, the cells are prolific. Although these cells are from the raphe nuclei, they are not serotonergic until they undergo a differentiation process. To differentiate these cells, they are shifted to 39˚C and grown in a low serum medium. These cells require the addition of brain derived neutrophic factor (BDNF) for the duration of their differentiation process in order to become serotonergic (176), thus the RN46A parent cell line was transfected with the human clone of the BDNF gene and the RN46A-B14 cell line derived to constitutively expresses BDNF (174). An additional part

of the differentiation process is the addition of 40 mM KCl to the growth media four days after the temperature shift occurs. This depolarizing condition is continued throughout the duration of the experiment. Although the RN46A-B14 cell line expresses TPH, the addition of 40 mM KCl is required for TPH phosphorylation, and thus activation of the enzyme (176). Without the addition of 40 mM KCl, the cells do not produce very large amounts of 5-HT, even if exposed to the higher temperature and BDNF (176). The cells used for all of the *in vitro* studies were differentiated as described here prior to treatment with retinoids.

RN46A-B14 cells (a gift from Dr. Scott Whittemore, University of Louisville, Louisville, KY) were used to investigate the effects of 13-*cis*-RA on components of the serotonergic system. RN46A-B14 cells were maintained in DMEM/F12 medium containing 10% FBS and antibiotics (1,000 units/mL penicillin and 1,000 μg/mL streptomycin) at 33°C. Prior to differentiation, cells were plated at a density of 4 x 10^6 cells/plate in 100 mm dishes and allowed to grow for 2-3 d until reaching approximately 70% confluency. Cells were differentiated as described (174) by incubation at 39°C in DMEM/F12 medium containing 1% FBS, antibiotics (1,000 units/mL penicillin and 1,000 μg/mL streptomycin), 5 μg/mL insulin, 20 nM progesterone, 100 μM putrescine, 1 μg/mL transferrin, and 1% ovalbumin (w/v). Media was changed every d for the first 4 d and on d 4, 40 mM KCl was added. Depolarization with KCl enhances the serotonergic phenotype of these cells (175, 176). Media was then changed every 48 h and contained 40 mM KCl for the duration of the experiment. After 8 d at 39°C, differentiated cells were treated with 0, 2.5, or 10 μM 13-*cis*-RA dissolved in ethanol vehicle for 48 or 96 h. The Accutane package insert reports that the steady state plasma concentration of 13-*cis*-RA ranges from a minimum (mean ± SD) of 352.32 ± 184.44 ng/mL (1.2 μM) to a maximum of 731.98 ± 361.86 ng/mL (2.5 μM) (6). Thus, the 2.5 μM concentration of

13-*cis*-RA was chosen to reflect the average steady state concentration of 13-*cis*-RA and the 10 μM concentration of 13-*cis*-RA may be reached soon after 13-*cis*-RA administration. All cells, including control, were treated with an equal amount of vehicle. All retinoid manipulations were performed under subdued light.

HPLC Analysis of Intracellular 5-HT and 5-HIAA Content

Isocratic high performance liquid chromatography (HPLC) with electrochemical detection was used to examine the effect of 13-*cis*-RA on 5-HT production in RN46A-B14 cells. Cells were grown and differentiated as described above. Although the media contained 66 μM tryptophan, to ensure adequate levels of 5-HT for detection by HPLC analysis, after 48 or 96 h of 13-*cis*-RA treatment, cells were incubated with 10 μM tryptophan and 10 μM chlorgyline for 30 min and then with 10 μM fluoxetine for an additional 30 min as described (175). Tryptophan is the precursor for 5-HT synthesis, chlorgyline inhibits monoamine oxidase A and fluoxetine blocks SERT and therefore 5-HT entry into the cell, thereby allowing for detection of 5-HT. Cells were left attached to the plate and washed 2X with phosphate buffered saline (PBS) and lysed by freezing at -80°C. The next day, 200 μL of e-pure water was added to the plate, the plate was scraped and the lysed cells harvested, transferred to an eppendorf tube, and centrifuged at 13,000 *x g* for 10 min. The supernatant was stored at -20°C until analysis. The protein content of each sample was determined using a portion of the supernatant and the BioRad DC protein assay kit (Hercules, CA).

5-HT and 5-hydroxyindoleacetic acid (5-HIAA) levels in the lysate were determined in the College of Pharmacy Analytical Instrumentation Facility Core (University of Texas at Austin, Austin, TX) by HPLC electrochemical method modified from (177). Briefly, the samples (60 to 100 μL) were injected into the HPLC system

which consisted of a Shimadzu SCL-10A system controller and a LC-10AD pump equipped with a SIL-10A auto-sampler (Shimadzu, Columbia, MD), coupled to a four-channel CoulArray electrochemical detector (ESA, Chlemsford, MA). The isocratic mobile phase consisted of 4 mM citrate, 8 mM ammonium acetate, 20 mg/L EDTA, and 120 μM 1-octanesulfonic acid sodium salt (SOS), pH 3.5, and 5% methanol. 5-HT and 5-HIAA were separated by a 4.6 x 80 mm reverse phase HR-80, 3 μm particle size, 120Å, column (ESA Biosciences Inc., Chelmsford, MA) at a flow rate of 1 mL/min and analyzed by electrochemical detection using a CoulArray electrochemical detector (ESA Biosciences Inc., Chelmsford, MA). The potential of channels one through four of the CoulArray were set at -50, 0, 300, and 400 mV respectively (Fig. 3.2A). Peak area (nC) of 5-HT or 5-HIAA at the corresponding retention time on the chromatogram resulting from 300 mV was obtained using CoulArray for Windows, version 1.12 software (ESA, Chlemsford, MA). The peak area was used to quantify the 5-HT or 5-HIAA in each sample injected, based on the standard curve. The total 5-HT or 5-HIAA concentration was corrected for sample volume loaded and normalized to protein content.

Northern Blot Analysis of 5-HT_{1A} and SERT mRNA

For probe generation, total RNA was isolated from differentiated vehicle control-treated RN46A-B14 cells or adult rat hippocampus with RNA Stat-60 (Tel-Test, Friendswood, TX). Two μg of RN46A-B14 or rat hippocampal total RNA were reverse-transcribed with oligo-dT primers and the Reverse Transcription System (Promega, Madison, WI) as per manufacturer's instructions. Amplification of the 5-HT_{1A} and GAPDH cDNA were performed using RN46A-B14 cDNA and the following primers: 5-HT_{1A} forward primer: 5'- AGC ATC TCC GAC GTG ACC TTC AGC TAC CA -3' reverse primer, 5'- GCT CCC TTC TTT TCC ACC TTC CTG ACA GT -3', resulting in

a 635-bp product (178). GAPDH forward primer: 5'- CGT CTT CAC CAC CAT GGA GA -3' reverse primer, 5'- CGG CCA TCA CGC CAC AGT TT -3', resulting in a 260-bp product (179). Amplification of SERT cDNA was performed using hippocampal cDNA and the following primers. SERT forward primer: 5'- TGA CCA GCA GCA TGG AGA CC -3' reverse primer: 5'- CCA CGG CAT AGC CAA TGA C -3', resulting in a 304 bp product (180). 5-HT_{1A}, GAPDH, and SERT cDNA were amplified using Taq polymerase (New England Biolabs Inc. Ipswich, MA) as per manufacturer's instructions under the following PCR conditions: 95°C for 5 min followed by 50 cycles of 95°C for 30 sec, 60°C for 30 sec, and 72°C for 30 seconds, with a final extension period of 7 min at 72°C. PCR reactions were then electrophoresed in a 1.8% agarose gel and products of the appropriate size were purified using the Qiagen Gel Extraction kit (Qiagen, Valencia, CA) as per the manufacturer's instructions. All products were sequenced to confirm their identity.

Total RNA was isolated from cells differentiated and treated with 0, 2.5, or 10 μM 13-*cis*-RA for 48 or 96 h as described above using RNA Stat-60 (Tel-Test, Friendswood, TX). RNA was electrophoresed through 1.2% agarose/2.2 M formamide gels, transferred to nylon filters, and cross-linked to the filters with a UV-Stratalinker (Stratagene) as described (124). The cDNA probes for 5-HT_{1A}, SERT, and GAPDH were labeled with [α-^{32}P]dCTP using the Random Primed DNA Labeling Kit (Roche Applied Science, Indianapolis, IN) as per the manufacturer's instructions. Membranes were prehybridized overnight at 42°C in hybridization solution [50% (w/v) deionized formamide/0.2% BSA/0.2% polyvinyl pyrrolidone/2% Ficoll (molecular weight 400,000 g/mol)/50 mM Tris·HCl, pH 7.5/0.1% sodium pyrophosphate/1% SDS/10% dextran sulfate/100 μg/ml salmon sperm DNA] and then hybridized overnight at 42°C in hybridization solution containing radiolabled probe. After hybridization, the membranes

were washed and processed as described previously (124). The membranes were then exposed to film for 24 h. All membranes were stripped and re-hybridized with GAPDH to control for loading differences. Autoradiographs were quantitated using a BioRad Gel Documentation System (Hercules, CA).

Western Blot Analysis of 5-HT_{1A} and SERT Protein

The effect of 13-*cis*-RA on 5-HT_{1A} and SERT protein levels in serotonergic cells was examined using semi-quantitative western blot analysis. RN46A-B14 cells were differentiated as described above and treated with 13-*cis*-RA for 48 or 96 h. For 5-HT_{1A} and SERT analysis, cells were lysed in RIPA buffer (150 mM NaCl, 1% NP-40, 0.5% deoxycholate, 0.1% SDS, 50 mM Tris, 1 mg/ml leupeptin, 1 mM DTT, 2 mM $NaOV_4$, 1 mg/ml PMSF, 1 mg/ml trypsin inhibitor, and 10 mM aprotinin) and equal amounts of protein (50 μg for 5-HT_{1A} or 75 μg for SERT) were electrophoresed on 12% (5-HT_{1A}) or 10% (SERT) SDS-PAGE gels. Protein was quantitated using BioRad DC protein assay kit (Hercules, CA). After electrophoresis, protein was transferred to a nitrocellulose membrane.

For analysis of 5-HT_{1A} levels, the blots were prehybridized with 5% milk in TBST (10 mM Tris, pH 8, 150 mM NaCl, and 0.5% Tween-20) for 1 h at room temperature before overnight incubation at 4°C with 5-HT_{1A} polyclonal antibody (catalogue #sc-10801, Santa Cruz Biotechnology Inc., Santa Cruz, CA) at a 1:300 dilution. For analysis of SERT levels, blots were prehybridized 5% milk in TBST prior to incubation with a 1:200 dilution of polyclonal anti-SERT antibody (catalogue #sc-1458, Santa Cruz Biotechnology Inc., Santa Cruz, CA) in 1% BSA in TBST at 4°C overnight. Secondary antibodies were goat anti-rabbit (catalogue #0031460, Pierce, Rockford, Il) or bovine anti-goat (catalogue #sc-2350, Santa Cruz Biotechnology Inc., Santa Cruz, CA), for 5-

HT_{1A} or SERT respectively, and were incubated in 5% milk for one hour at room temperature. Immunoreactivity was detected using the Horseradish Peroxidase Super Signal West Pico Chemiluminescent Substrate kit (Pierce, Rockford, IL). The membranes were then stripped and re-probed with polyclonal β-actin antibody (catalogue #A2066 Sigma, St. Louis, MO) at a 1:10,000 dilution to control for differences in loading. Densitometry was performed using a BioRad Gel Documentation System (Hercules, CA).

RT-PCR analysis of RAR/RXR expression

RN46A-B14 cells were grown and differentiated for eight days as described, and on the eighth day, total RNA was extracted from RN46A-B14 cells as described above. DNA was removed by DNase digestion and total RNA (1 μg) was reverse-transcribed with oligo-dT primers and the Reverse Transcription System (Promega, Madison, WI) as per manufacturer's instructions. cDNA was then subjected to 40 PCR cycles, Tm = 60 °C, with the primers listed below. For adult rat dorsal raphe tissue, total RNA was extracted using Trizol reagent (Invitrogen, Carlsbad, CA). DNA was removed by means of a DNase digest and total RNA (0.25μg) was reverse-transcribed using RT/ Platinum® *Taq* Mix (Superscript™ One-Step RT-PCR with Platinum® *Taq*, Invitrogen, Carlsbad, CA) as per manufacturer's instructions, with the gene specific primers listed. Amplification of RARα, RARβ, RARγ, RXRα and RXRβ/γ cDNA were achieved using the following primers: RARα forward: 5'- CTG GAG ATG GAC GAT GCT GAG ACT -3' reverse: 5'- CAC AGA TGA GGC AGA TGG CAC TGA -3' resulting in a 54-bp product (181); RARβ forward: 5'- CAA AGC CTG CCT CAG TGG ATT CA -3' reverse: 5'- AGT GGT AGC CCG ATG ACT TGT CCT -3' resulting in a 178-bp product (181); RARγ forward: 5'- GGA ACT CAT CAC CAA GGT CAG CAA -3'

reverse: 5'- CGC TTC GCA AAC TCC ACA ATC TT -3' resulting in a 175-bp product (181); RXRα forward: 5'- CTT TGA CAG GGT GCT AAC AGA GC -3' reverse: 5'- ACG CTT CTA GTG ACG CAT ACA CC -3' resulting in a 172-bp product (182); RXRβ/γ forward: 5'- AGG CAG GTT TGC CAA GCT TCT G -3' reverse: 5'- GGA GTG TCT CCA ATG AGC TTG A -3' resulting in a 102-bp product (183).

Statistical Analyses

Statistical analyses were performed using Excel (XP 2002; Microsoft). Two-tailed, Student's *t*-tests were performed to test for differences between vehicle control and 13-*cis*-RA treatments. Data are expressed as mean ± SEM, n = 3, unless otherwise indicated, and differences were considered significant at $p < 0.05$.

RESULTS

Effect of 13-*Cis*-RA Treatment on Intracellular 5-HT and 5-HIAA Levels

HPLC was used to determine the effect of 13-*cis*-RA treatment on intracellular 5-HT levels in RN46A-B14 cells. The levels of 5-HIAA, the primary metabolite of 5-HT, were also determined. 5-HT and 5-HIAA peak retention times reflect their respective standards at 300 mV (Fig. 3.2A and B). We found that 48 h of 2.5 μM 13-*cis*-RA treatment did not increase intracellular 5-HT (Fig. 3.2C) or 5-HIAA (Fig. 3.2D) levels in RN46A-B14 cells. However, treatment with 10 μM 13-*cis*-RA for 48 h decreased (p = 0.01) intracellular 5-HT levels to 77.8 ± 6.2% of control (Fig. 3.2C), but had no effect on 5-HIAA (Fig. 3.2D). Extending treatment for 96 h with 10 μM 13-*cis*-RA significantly increased the intracellular 5-HT concentration to 206.9 ± 37.1% of vehicle control (p = 0.03) (Fig. 3.2C). Both 2.5 and 10 μM 13-*cis*-RA tended to increase intracellular 5-

HIAA levels to 132.4 ± 18.8% (p = 0.14) and 181.7 ± 38.1% of vehicle control (p = 0.07), respectively, after 96 h of treatment (Fig. 3.2D). These data indicate that prolonged treatment of RN46A-B14 cells with 13-*cis*-RA tends to increase intracellular 5-HT and 5-HIAA content.

Effect of 13-*Cis*-RA Treatment on 5-HT_{1A} mRNA and Protein Levels

Because retinoids are well known for their ability to induce gene transcription (172), northern blot analysis was used to examine the effect of 13-*cis*-RA on 5-HT_{1A} mRNA levels in RN46A-B14 cells. 13-*Cis*-RA treatment tended (p = 0.06) to slightly decrease 5-HT_{1A} mRNA levels (91.2 ± 3.8 %) after 48 h of treatment with 2.5 μM 13-*cis*-RA (Fig. 3.3A). 10 μM 13-*cis*-RA treatment had no effect on 5-HT_{1A} mRNA levels after 48 h (93.9 ± 5.5% of control) and there were no differences in 5-HT_{1A} mRNA levels due to either 2.5 or 10 μM 13-*cis*-RA treatment after 96 h (104.9 ± 5.6 and 104.9 ± 5.8% of vehicle control, respectively, Fig. 3.3A).

To determine the effect of 13-*cis*-RA on 5-HT_{1A} protein levels in RN46A-B14 cells, semi-quantitative western blotting was performed. Treatment of RN46A-B14 cells with 2.5 μM and 10 μM 13-*cis*-RA for 48 h significantly increased 5-HT_{1A} levels to 168.5 ± 20.0 and 148.7 ± 2.2% of control, respectively (Fig. 3.3B). This increase was maintained after 96 h of 13-*cis*-RA treatment. Thus, treatment of serotonergic cells with 13-*cis*-RA increases 5-HT_{1A} protein levels as early as 48 h after drug administration but does not affect 5-HT_{1A} mRNA levels.

Effect of 13-*Cis*-RA Treatment on SERT mRNA and Protein Levels

Northern blot analysis was also used to determine the effect of 13-*cis*-RA treatment on SERT mRNA levels. Treatment of RN46A-B14 cells with 2.5 or 10 μM 13-*cis*-RA for 48 h did not affect SERT mRNA levels (Fig. 3.4A). In contrast, 96 h of treatment with 10 μM 13-*cis*-RA tended ($p = 0.10$) to increase SERT mRNA levels to 144.8 ± 20.7% of vehicle control. In addition to the increase in mRNA levels, semi-quantitative western blotting revealed that SERT protein levels were significantly increased after treatment with 2.5 μM and 10 μM 13-*cis*-RA for 48 h, reaching 142.5 ± 11.1 and 119.2 ± 3.6% of vehicle control, respectively (Fig. 3.4B). SERT protein levels tended to remain elevated after 96 h of treatment with 13-*cis*-RA (Fig. 3.4B). Therefore, treatment of serotonergic cells with 13-*cis*-RA leads to increased levels of SERT protein as early as 48 h after treatment and later to an increase in SERT mRNA.

RAR and RXR expression

RAR and RXR mediate gene transcription in response to retinoic acid. Therefore, RT-PCR was used to examine RAR and RXR expression in RN46A-B14 cells and adult rat dorsal raphe tissue. RARα, β, and γ as well as the RXRα, and β/γ isoforms were expressed in both RN46A-B14 cells and the raphe nuclei (Fig. 3.5), indicating that retinoid-mediated gene transcription via RAR/RXR/RARE can occur. In RN46A-B14 cells, the RARα expression level may be lower than RARβ and γ. However, this RT-PCR method is not quantitative.

DISCUSSION

We show here that prolonged treatment with 13-*cis*-RA increases intracellular 5-HT and 5-HIAA levels, although the effect of 13-*cis*-RA on 5-HIAA levels was not significant. Additionally, 13-*cis*-RA treatment increased 5-HT_{1A} receptor and SERT protein levels, although it had little effect on their mRNA levels. Previously, we showed that 13-*cis*-RA administration induced depression-related behavior in adolescent male mice (173). Disturbances in the serotonergic system are known to be involved in depression, including changes in expression of the 5-HT_{1A} autoreceptor and SERT (166). An increase in expression of the 5-HT_{1A} autoreceptor and SERT levels in the raphe nuclei following 13-*cis*-RA treatment may lead to decreased serotonergic availability at the synapse and thus contribute to the increase in depression-related behavior observed *in vivo* (173).

We examined whether 13-*cis*-RA alters intracellular 5-HT levels or the levels of its metabolite, 5-HIAA and saw that 13-*cis*-RA increased 5-HT and tended to increase 5-HIAA *in vitro*. The increase in intracellular 5-HIAA parallels the increase in intracellular 5-HT, thus we suspect the increase in intracellular 5-HIAA is due to the increase in intracellular 5-HT levels and occurred prior to chlorgyline treatment. Ferguson et al. (39) examined the effects of 13-*cis*-RA treatment on monoaminergic systems in adult rats. While they found no effect on 5-HT or 5-HIAA content in brain tissue homogenates of either hippocampus or frontal cortex, 5-HIAA levels in the striatum were increased in male rats administered 13-*cis*-RA. These data indicate that there are likely to be brain-region specific effects of 13-*cis*-RA on 5-HT/5-HIAA levels. Ferguson et al. (39) did not examine the raphe nuclei and thus it remains possible that 13-*cis*-RA may cause an increase in 5-HT and 5-HIAA in the raphe *in vivo*. Although we did not examine release, recycling, or reuptake of 5-HT in this study, we speculate that increased levels of

intracellular 5-HT due to 13-*cis*-RA treatment could occur as a result of increased reuptake. In these experiments we pre-treated the cells with fluoxetine prior to HPLC analysis, this SERT inhibitor was not added until we had preloaded the cells with tryptophan for 5-HT synthesis. Therefore, greater 5-HT reuptake may be due to the ability of 13-*cis*-RA to increase SERT protein levels. Alternatively, increased intracellular 5-HT levels could result from increased 5-HT synthesis due to the effects of 13-*cis*-RA on the levels of synthetic enzymes such as tryptophan hydroxylase or amino acid decarboxylase.

Although retinoids are known for their ability to alter gene transcription when binding to RAR/RXR heterodimers on RARE, other roles for retinoids are becoming evident. ATRA has been shown to affect mRNA stability. Although the mechanism is not completely understood, ATRA can reduce TNF-α mRNA stability in a RXR-mediated manner in hepatocytes (14) increase keratin 19 mRNA stability in cultured keratinocytes (15) and increase protein stability in P19 cells (16). Adult raphe and RN46A-B14 cells express RARα/β/γ and RXRα/β/γ (Fig. 4), indicating the presence of the cellular mechanisms for both retinoid receptor-mediated gene transcription. We observed an increase in 5-HT_{1A} protein after 48 and 96 h treatment with 13-*cis*-RA without an increase in mRNA. It is possible that the increase in 5-HT_{1A} protein level in response to 13-*cis*-RA treatment is due to increased translation of 5-HT_{1A} mRNA or increased stability of the 5-HT_{1A} protein. We observed an increase in SERT mRNA after 96 h of 13-*cis*-RA treatment. This may reflect an increase in stability of the mRNA, but given the delay in increase of mRNA with treatment, it is possible that the SERT gene is not directly regulated by 13-*cis*-RA. Instead, perhaps an intermediate gene, such as a transcription factor or a derepressor element, which regulates SERT expression, is transcriptionally activated by 13-*cis*-RA. Because SERT protein but not mRNA levels

are changed after 48 h of treatment, 13-*cis*-RA treatment, in RN46A-B14 cells, may initially increase SERT protein stability or mRNA translation. Increased transcription of early response genes that are transcription factors for SERT would then lead to the increase seen in SERT mRNA at 96 h and thus be the underlying cause of later elevated levels of SERT protein.

Functionally, the 5-HT_{1A} autoreceptor is involved in regulation of serotonergic neuron firing (153). Activation of 5-HT_{1A} autoreceptors residing on raphe nuclei by 5-HT results in reduced firing of the raphe nuclei and therefore the amount of 5-HT in the synaptic cleft. Both increased and decreased expression of the 5-HT_{1A} receptor has been reported in depressed and suicidal patients (166). In addition, polymorphisms in the human 5-HT_{1A} promoter region have been linked to depression in some (163) but not all patients (184). Interestingly, 5-HT_{1A} null mice exhibit a decrease in immobility in both the forced swim test and the tail suspension test, consistent with an antidepressant-like effect in the tail suspension test (185). In these knockout mice there is an increase in basal firing of serotonergic neurons (186) that is accompanied by enhanced extracellular 5-HT release *in vivo* in hippocampus and frontal cortex (187), but not in striatum (188).

Abnormalities in SERT expression may also contribute to depression (166). SERT removes 5-HT from synaptic cleft to regulate 5-HT signaling. Two functional polymorphisms in the human SERT gene are associated with increased vulnerability to depression and that affect the response to antidepressants (189). These polymorphisms of the SERT gene are associated with reduced SERT expression, reduced 5-HT reuptake rate (164, 190, 191) and increased susceptibility to depression (164, 165, 192). Also, SERT null mice exhibit decreased immobility in the tail suspension test (170) and siRNA knockdown of SERT in adult mice reduced time spent immobile in the forced swim test (193). Interestingly, SERT knockout mice exhibit a gene dose-dependent decrease in

SERT protein levels, 5-HT uptake and an increase in extracellular 5-HT levels (194-196). Since the function of SERT is to remove 5-HT from the synaptic cleft, both increases and decreases in SERT may disrupt 5-HT signaling, affecting downstream neuronal targets, which may eventually result in depression.

Given that the roles of the presynaptic 5-HT_{1A} receptor and SERT are to regulate 5-HT signaling, increases of the 5-HT_{1A} presynaptic-receptor and SERT due to 13-*cis*-RA treatment may inhibit firing and reduce 5-HT signaling from the raphe to other brain regions. Such impairment in serotonergic neurotransmission could contribute to the 13-*cis*-RA-induced increase in depression-related behaviors observed in mice.

ACKNOWLEDGMENTS

The RN46A-B14 cells were generously provided by Dr. Scott Whittemore, University of Louisville, Louisville, Kentucky. Neurotransmitter HPLC was performed by Dr. Herng-Hsiang Lo in the University of Texas at Austin CRED Analytical Instrumentation Facility Core supported by NIEHS center grant ES07784. The PCR for the RARs and RXRs in the rat raphe nuclei tissue was completed by Simon Trent. This work was supported in part by the National Institute of Environmental Health Sciences/NIH (ES09145), NIEHS toxicology training grant (T32 ES007247, K.O.) and the University of Texas at Austin Fiscal Year Research Grant FY 2004-2005.

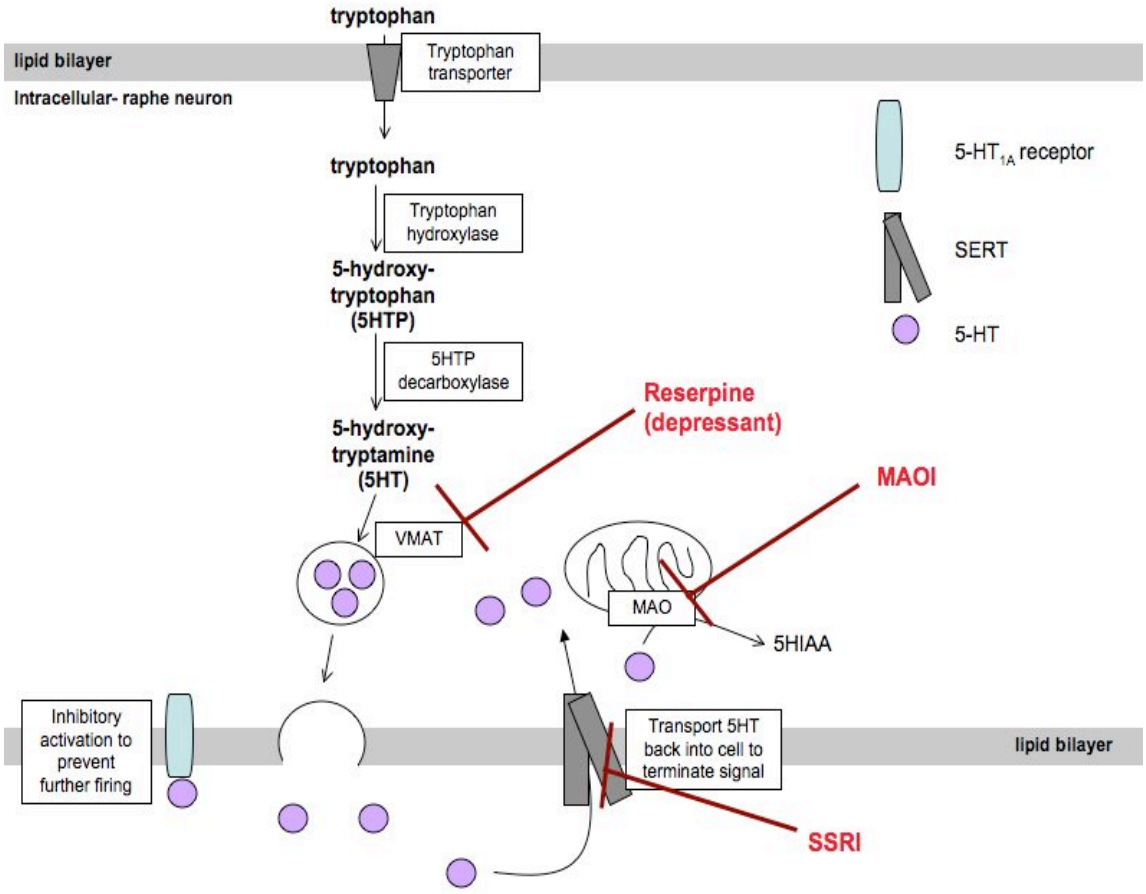

Figure 3.1: Regulation of 5-HT in a raphe neuron and antidepressant activity.

5-HT content within a raphe neuron is controlled by synthesis, packaging into vesicles for release, reuptake by SERT, and breakdown by MAO. The 5-HT_{1A} receptor is one receptor that regulates 5-HT release. Activation of the 5-HT_{1A} receptor by 5-HT prevents 5-HT release by preventing depolarization and thus raphe neuron firing. Antidepressants that target the serotonergic system work to increase the amount of 5-HT in the synaptic cleft. Reserpine, which is a depressant, prevents packaging of 5-HT into vesicles for release upon firing and therefore reduces the amount of 5-HT in the synaptic cleft.

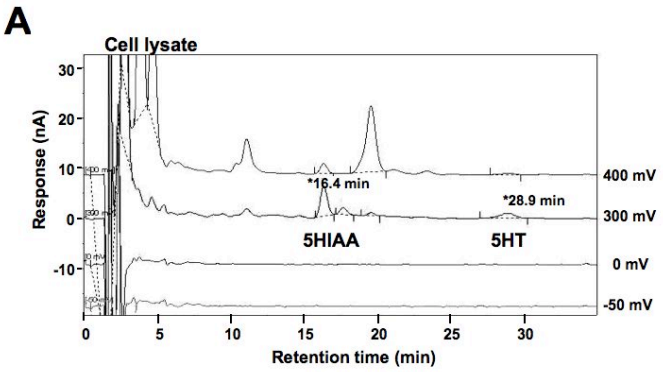
A
Cell lysate
Response (nA)
*16.4 min
*28.9 min
5HIAA
5HT
400 mV
300 mV
0 mV
-50 mV
Retention time (min)

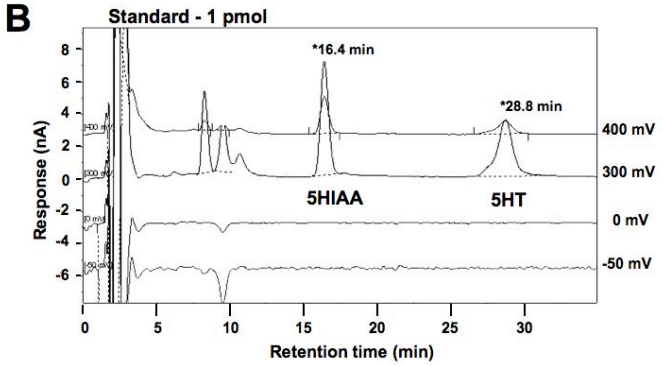
B
Standard - 1 pmol
Response (nA)
*16.4 min
*28.8 min
5HIAA
5HT
400 mV
300 mV
0 mV
-50 mV
Retention time (min)

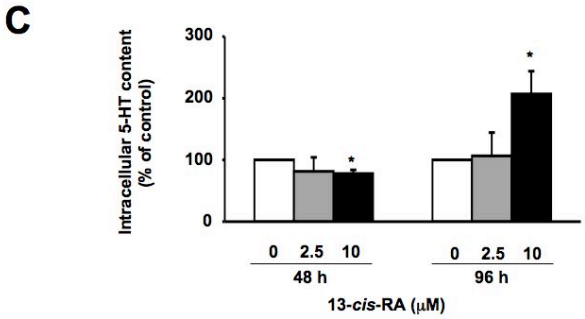
C
Intracellular 5-HT content (% of control)
48 h
96 h
13-cis-RA (μM)

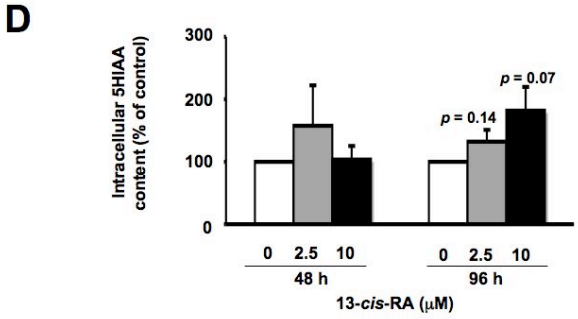
D
Intracellular 5HIAA content (% of control)
p = 0.14
p = 0.07
48 h
96 h
13-cis-RA (μM)

Figure 3.2: Effect of 13-*cis*-RA treatment on intracellular 5-HT and 5-HIAA levels in cultured serotonergic cells.

Representative HPLC tracing for cell lysate (**A**) and 1 pmol standard (**B**). 5-HT and 5-HIAA retention times are indicated. Intracellular 5-HT and 5-HIAA content (**C** and **D**). Cells were differentiated for 8 d before treatment with 0, 2.5, or 10 μM 13-*cis*-RA for 48 or 96 h. Prior to harvesting, cells were incubated with 10 μM tryptophan and 10 μM chlorgyline for 30 min, then 10 μM fluoxetine was added for another 30 min. Cells were lysed and 5-HT and 5-HIAA content were detected electrochemically via HPLC . Results shown 5-HT **(C)** and 5-HIAA **(D)** are mean ± SEM for four separate experiments. Statistical analysis was performed using *t*-tests comparing each 13-*cis*-RA concentration to control.

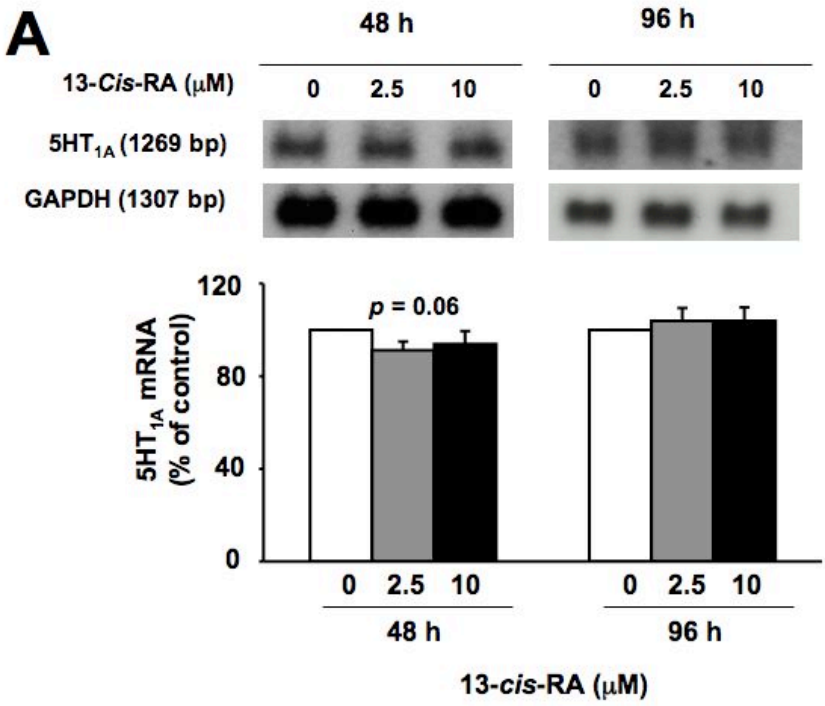
A
48 h
96 h
13-Cis-RA (μM)
0
2.5
10
0
2.5
10
5HT1A (1269 bp)
GAPDH (1307 bp)
5HT1A mRNA (% of control)
120
80
40
0
p = 0.06
0
2.5
10
0
2.5
10
48 h
96 h
13-cis-RA (μM)

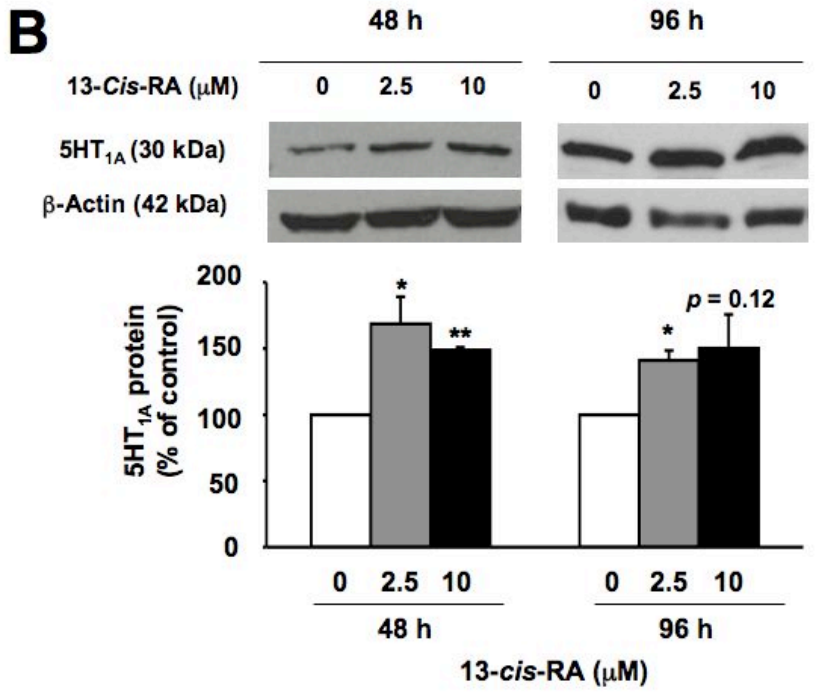
B
48 h
96 h
13-Cis-RA (μM)
0
2.5
10
0
2.5
10
5HT1A (30 kDa)
β-Actin (42 kDa)
5HT1A protein (% of control)
200
150
100
50
0
*
**
*
p = 0.12
0
2.5
10
0
2.5
10
48 h
96 h
13-cis-RA (μM)

Figure 3.3: Effect of 13-*cis*-RA on 5-HT_{1A} mRNA and 5-HT_{1A} protein levels.

Cells were differentiated for 8 d and then cultured with 0, 2.5, or 10 μM 13-*cis*-RA for 48 or 96 h. **(A)** Total RNA was harvested and subjected to northern blot analysis for 5-HT_{1A} and GAPDH mRNA (1269 and 1307 bp respectively) as described in Materials and Methods. GAPDH was used to correct for loading differences. Northern blot analysis was repeated four separate times with similar results; a representative northern blot is shown. **(B)** Total protein was harvested and subjected to western blot analysis for 5-HT_{1A} and β-actin (30 and 42 kDa respectively) as described in Materials and Methods. β-actin was used to correct for loading differences. Western blot analysis was performed three separate times with similar results; a representative western is shown. Values reported are mean ± SEM. Statistical analysis was performed using *t*-tests comparing each 13-*cis*-RA concentration to control. $*P < 0.05$, $**P < 0.01$; significantly different from control.

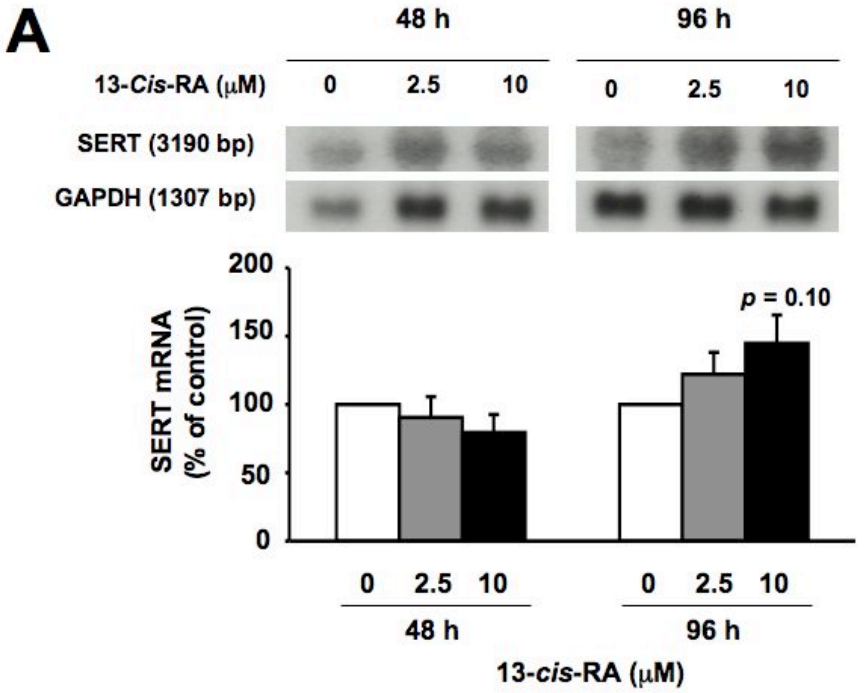
A
48 h
96 h
13-Cis-RA (μM)
0
2.5
10
0
2.5
10
SERT (3190 bp)
GAPDH (1307 bp)
SERT mRNA (% of control)
200
150
100
50
0
p = 0.10
0
2.5
10
0
2.5
10
48 h
96 h
13-cis-RA (μM)

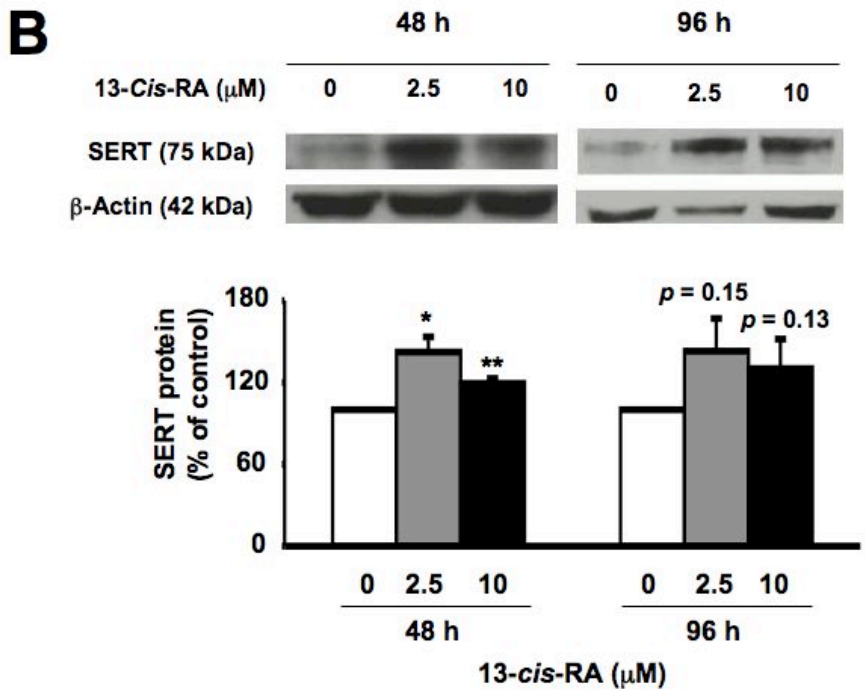
B
48 h
96 h
13-Cis-RA (μM)
0
2.5
10
0
2.5
10
SERT (75 kDa)
β-Actin (42 kDa)
SERT protein (% of control)
180
120
60
0
*
**
p = 0.15
p = 0.13
0
2.5
10
0
2.5
10
48 h
96 h
13-cis-RA (μM)

Figure 3.4: Effect of 13-*cis*-RA treatment on SERT mRNA and protein levels.

Cells were differentiated for 8 d and then cultured with 0, 2.5, or 10 μM 13-*cis*-RA for 48 or 96 h. **(A)** Total RNA was harvested for northern blot analysis of SERT and GAPDH mRNA (3190 and 1307 bp respectively) as described in Materials and Methods. GAPDH was used to demonstrate equal loading. **(B)** Total protein was harvested and subjected to western blot analysis for SERT and β-actin (75 and 42 kDa respectively) as described in Materials and Methods. β-actin was used to demonstrate equal loading. These experiments were performed three separate times with similar results; representative western and northern blots are shown. Results are mean ± SEM for three separate experiments. Statistical analysis was done using *t*-tests comparing each 13-*cis*-RA concentration to control. $*P < 0.05$, $**P < 0.01$; significantly different from control.

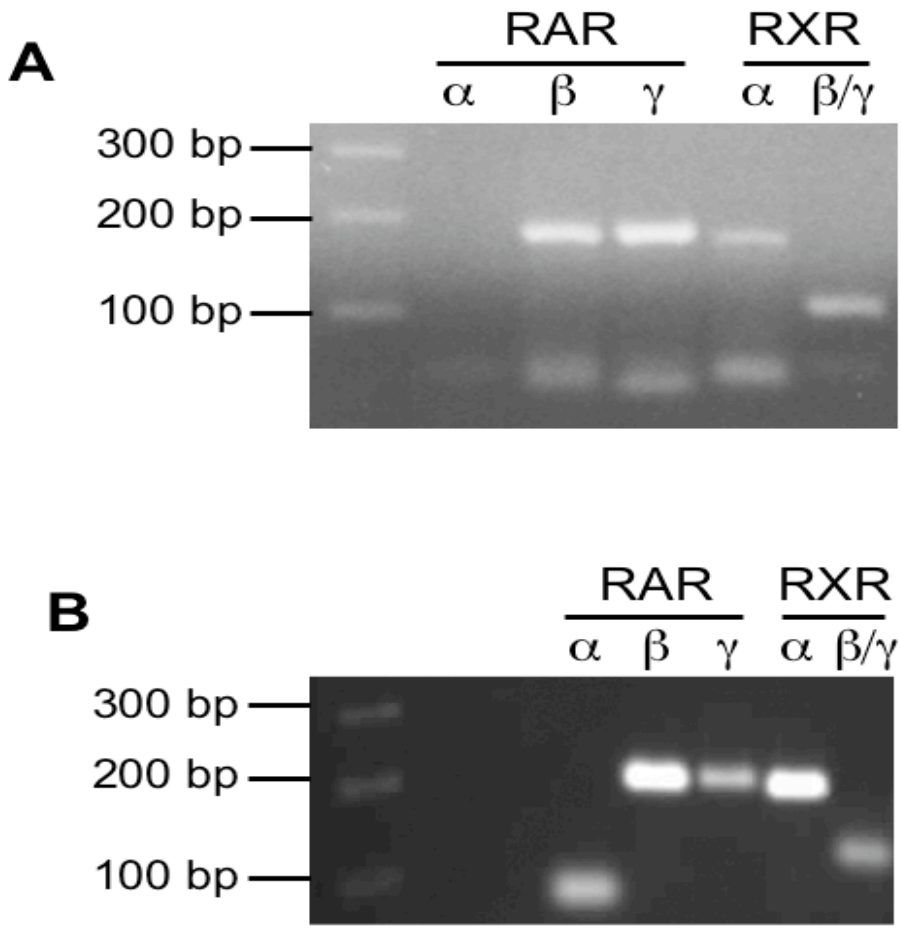

Figure 3.5: Expression of RAR and RXR in RN46A-B14 cells and rat raphe tissue.

(A) RN46A-B14 cells were differentiated for eight days and total RNA was reverse transcribed. cDNA was then amplified with primers specific for RAR and RXR. **(B)** Total RNA from rat raphe tissue was reverse-transcribed in a one-step RT-PCR with the same primers for RAR and RXR. All isoforms of RAR and RXR were expressed in RN46A-B14 cells and rat raphe tissue. The RARα, RARβ, RARγ, PCR amplicons were 54, 178, and 175 bp in length. The RXRα and RXRβ/γ amplicons were 172 and 102 bp in length.

Chapter 4: Chronic 13-*Cis*-RA Administration Disrupts Functional Connections between the Serotonergic and Hippocampal Systems in Adolescent Male Mice

ABSTRACT

We previously showed that chronic administration of 13-*cis*-RA induces depression-related behaviors in adolescent male mice and that 13-*cis*-RA can alter components of the serotonergic system *in vitro*. Other work has shown that hippocampal neurogenesis is reduced by chronic 13-*cis*-RA treatment in young-adult male mice. Furthermore, orbitofrontal cortex metabolism is decreased due to 13-*cis*-RA treatment in humans. In the current study, cytochrome oxidase (CO) activity, a metabolic marker that reflects steady state neuronal firing, was measured in various regions of the brain to determine the effects of 13-*cis*-RA on neuronal activity. Adolescent male mice were administered vehicle or 1 mg/kg/day 13-*cis*-RA, i.p., for 6 weeks, tested for depression-related behaviors, and then CO activity was analyzed. We show that chronic 13-*cis*-RA administration tended to decrease CO activity in the median raphe nuclei and significantly decreased the CO activity in the inferior rostral linear nucleus of the raphe. Although there was no change in CO activity in the dorsal raphe nuclei or the hippocampal regions in 13-*cis*-RA treated animals, these regions become functionally uncoupled by 13-*cis*-RA treatment. Furthermore, a path analysis of the connectivity between the hippocampus to the lateral habenula through the dorsal raphe nuclei showed that this circuit is disrupted in 13-*cis*-RA treated animals. Interestingly, total immobility in the tail suspension and forced swim tests inversely correlated to the CO activity in the dentate gyrus in 13-*cis*-RA treated mice, but not control treated mice. Taken together these data show that 13-*cis*-RA is capable of altering brain metabolism and disrupting

functional connectivity between the serotonergic system and the hippocampus possibly leading to the previously observed increase in depression-related behaviors.

INTRODUCTION

We previously showed that chronic 13-*cis*-RA administration to adolescent male mice induced depression-related behaviors as measured by total immobility in the last four minutes of the tail suspension and forced swim tests. We also showed that 13-*cis*-RA treatment of serotonergic cells *in vitro* increased protein levels of the 5-HT_{1A} receptor and SERT (197), two components of the serotonergic system that regulate neuronal firing. Increases in the 5-HT_{1A} receptor and SERT proteins *in vivo* could lead to decreased serotonergic signaling. 13-*Cis*-RA administration has also been shown to decrease hippocampal neurogenesis in mice (97) and decrease metabolism in the orbitofrontal cortex of human patients taking Accutane (94).

Metabolic differences in the brain due to depression have been shown using human neuroimaging studies as well as animal models. Human studies have shown abnormalities in blood flow and metabolism of the frontal cortex regions of depressed patients. For instance, depressed patients have a pattern of decreased orbitofrontal cortical metabolism (198) and anterior cingulate cortex metabolism (199) and increased infralimbic cortical metabolism (199).

Several animal models of depression have also begun to elucidate metabolic differences in the brain. For instance, alpha-methyl-para-tyrosine (a catecholamine synthesis inhibitor) administration, chronic stress, and short term withdrawal from amphetamine all produce decreased ^{14}C-2-deoxyglucose uptake in the prefrontal motor cortex and increased ^{14}C-2-deoxyglucose uptake in the lateral habenula (200). The congenitally learned helpless rat is an inbred strain that exhibits increased vulnerability to learned helplessness and has also proven to be a useful model for human depression. The congenitally learned helpless rat has altered cortex metabolism that mimics the

metabolism abnormalities seen in the frontal and cingulate regions of depressed humans. Further characterization of metabolic differences in the congenitally learned helpless rat compared to normal rats has revealed differences in CO activity throughout the brain [reviewed in (137)]. In the congenitally helpless rats, regions that were hypometabolic compared to controls include the orbitofrontal cortex, the lateral septal nucleus, the raphe nuclei, and the ventral tegmental area [reviewed in (137)]. Brain regions that were hypermetabolic in the congenitally helpless rats when compared to controls include the subgenual cingulate cortex, the infralimbic cortex, the hippocampus, the habenula, the paraventricular hypothalamus, the interpeduncular nucleus, and the subiculum [Reviewed in (137)].

Cytochrome oxidase (CO) is the terminal enzyme in the electron transport chain that catalyzes the transfer of electrons from ferrocytochrome C to oxygen to form water and, ultimately, ATP (201). Other commonly used measures of brain metabolic activity, such as positron emission tomography (PET) or functional magnetic resonance imaging (fMRI), measure glucose uptake and/or blood flow to specific regions of the brain, and PET imaging is similar to the autoradiographic ^{14}C-2-deoxyglucose uptake used to measure glucose uptake in animals. However, while glucose uptake and blood flow represent state dependent neuronal activity spanning approximately 45 minutes, CO activity reflects cumulative long term neuronal activity (201).

Because the serotonergic, hippocampal, and frontal cortical systems are involved in depression, alterations in metabolism in the serotonergic and hippocampal regions due to 13-*cis*-RA treatment may elucidate the underlying mechanism by which 13-*cis*-RA induces depression-related behaviors. Therefore, the objective of this study was to determine the effect of chronic 13-*cis*-RA treatment on brain metabolism in the same adolescent animals that were treated with 13-*cis*-RA or vehicle and then tested for

depression-related behaviors. We used CO activity to measure metabolic activity and therefore long term neuronal activity in the brain. Our goal was to determine if 13-*cis*-RA induces long-term brain metabolic changes consistent with those seen in depressed humans and in rat models of depression.

METHODS

Animals

The animals used for the metabolic mapping were the same as those used in Chapter 2 of this dissertation. Briefly, young, adult male DBA/2J (Jackson Laboratories, Bar Harbor, ME) mice were three weeks old at arrival and four weeks old at the start of treatment. Mice were group-housed four per cage and maintained under a 12:12 h light/dark cycle. Food and water were provided *ad libitum*. All procedures and tests performed on animals were approved by the University of Texas IACUC, protocol number 04100403, according to the National Institutes of Health Guide for the Care and Use of Laboratory Animals.

Treatment

Animals were allowed to adapt to the University of Texas animal facility for one week prior to initial injection. Animals were handled during the first week to reduce the stress of receiving daily injections. A 2 mg/mL stock solution of 13-*cis*-RA in dimethyl sulfoxide (DMSO) was stored for up to one week at -20 ºC. The stability of 13-*cis*-RA after one week of storage was confirmed by comparing the absorbance at 354 nm to that of a freshly prepared sample (97). Sterile injection samples were prepared in the dark. Injections were performed one hour prior to the start of the dark cycle in the same room

where the animals were housed and the same person performed all injections. Treated animals (n = 12) received daily i.p. injections of 1 mg/kg/day 13-*cis*-RA (Sigma, St. Louis, MO) dissolved in sterile 50% DMSO/50% saline (0.9%) to a final volume of 200 μL. Control animals (n = 12) were administered 200 μL of vehicle (50% DMSO/50% saline), i.p., daily. Animals were injected for 6 weeks prior to behavioral testing. Daily injections continued throughout the testing period and all animals received injections 14 h before any behavioral testing to eliminate any acute effects of injection. Only one behavioral test was performed each day. The behavioral experiments were conducted in the following order: tail suspension test, forced swim test, open field test, and rotarod test. Approximately 24 h elapsed between each of the tests.

Tissue Processing

After cervical dislocation, animals were decapitated and the brains were removed intact, frozen rapidly in isopentane, and stored at -40˚C until they were sectioned at -20˚C using a cryostat (Leica, Bannockburn, IL) into 40 μm sections and thaw mounted onto slides. The slides were then kept frozen at -40˚C until they were processed using quantitative CO histochemistry.

CO histochemical staining was performed as described in (202), the slides were first incubated in 0.1 M phosphate buffer (with 10% w/v sucrose and 0.5% gluteraldehyde, pH 7.6) for five min. The tissues were then transferred to a series of four exposures to 0.1 M phosphate buffer (containing 10% w/v sucrose) for five min each. The tissues then underwent metal intensification (0.05 M Tris buffer, pH 7.6, with 275 mg/L cobalt chloride, 10% w/v sucrose, 0.5% dimethylsulfoxide) for 10 min. These buffers were stored at 4˚C and poured prior to the first incubation so that the tissues could

gradually warm to room temperature. Following the metal intensification incubation, the tissues were placed in a room temperature phosphate buffer rinse.

The CO staining was done with a 60 min incubation in 0.1 M phosphate buffer containing 350 mg diaminobenzidine tetrahydrochloride, 52.5 mg cytochrome c, 35 g sucrose, 14 mg catalase, and 1.75 mL DMSO in 700 mL total volume, at 37˚C. The reaction was stopped by fixing the tissue in 0.1 M phosphate buffer containing 4% formalin and 10% w/v sucrose. Finally, the tissues were dehydrated in a series of ethanol baths (30%, 50%, 70%, 95%, 95%, 100%, 100%, five min each) and then cleared with xylene and coverslipped with permount.

Preparation of CO Standards and Densitometric Analysis

In order to quantify enzyme activity and to control for staining variability across batches of CO staining, sets of tissue homogenate standards were included in each batch of slides. The tissue homogenate was prepared as described previously (202) and the enzymatic activity of CO activity was assayed as described in (203). Activity units were defined at pH 7 and 37˚C, where one unit oxidizes one μmol of reduced cytochrome c/min (μmol/min/g tissue wet weight). The remaining tissue homogenate was frozen and stored at -40˚C.

Prior to the CO staining procedure, the standard homogenate was sectioned into 10, 20, 40, 60, and 80 μm sections, and thaw mounted onto slides, with two replicates of each thickness per slide. Two slides of standards were incubated with each batch during the CO staining procedure. The activity values determined by the spectophotometric method were correlated with the corresponding optical density (OD) measurements of each standard, taken with an image-processing system as described in (203). The resulting linear regression equations ($r^2 > 0.95$) were used to convert OD readings from

chosen brain regions into CO activity values. The activity values were then used in the statistical analysis of this study.

The image processing system (JAVA, Jandel Scientific, Corte Madera, CO) was used to record OD readings from 15 brain regions as described in the next section. Microscope slides of the stained tissue were placed on a DC-powered light box and the image captured with a black and white video camera (Javelin JE2362). The signal was then transmitted to a Targa M-8 frame grabber mounted in an Everex 486 computer where the image was digitized. To correct for background and optical distortions within the camera, a coverslipped glass slide and a calibrated optical density tablet (Kodak, Rochester, NY) were used to calibrate the system. The sampling window (square-shaped) was adjusted for each region so that it would be as large as possible to take two to three readings over the region of interest in one hemisphere per slice per subject and three brain slices per subject were examined. These readings were then averaged to represent CO activity for each region for an individual animal. Prior to performing the image analysis, the slides were coded so that the person performing the image analysis was blinded to the treatment group.

Morphometric Analysis

Morphometric analysis of the hippocampus was performed on the cytochrome oxidase stained slides as described previously in (204). Briefly, images of the brain slices were captured as in the densitometric analysis above and the Jandel software's algorithm calculated areas of the right and left hemi-brain section as well as the right and left hemi-hippocampus. The first section measured was the first appearance of the hippocampus at the bregma level -0.94, as determined with a mouse brain atlas (205), and every third section was measured until bregma level -4.04. The hemi-hippocampal area was normalized to the hemi-brain section area (hemi-hippocampal area/hemi-brain section

area x100) for each bregma level. The bregma levels were collapsed mathematecally to seven bregma levels and each bregma level consited of the following levels: -1 (-0.94 to -1.06), -1.5 (-1.22 to -1.58), -2 (-1.70 to -2.08), -2.5 (-2.18 to -2..54), -3 (-2.70 to -3.08), -3.5 (-3.16 to -3.52), and -4 (-3.64 to -4.04) mm from bregma. The % hippocampal area for each bregma level was determined by averaging the % hemi-hippocampal area for the bregma levels within the main bregma level for both the right and left sides of the brain.

Hippocampal volumes were estimated by the Cavalieri principle (206) using a grid printed on acetate overlay. Each square on the grid corresponded to an area of 0.56 mm^2. The grid was placed over the image on the computer screen and each grid crossing was counted for each hemi-section of the hippocampus. The area of the grid was corrected for the magnification (area/magnification^2). To calculate the hippocampal volume, the number of grid crossings was multiplied by 180.65 μm, which was the corrected grid area, and then by 120 μm, which was the tissue thickness of the three sections until the next section that was analyzed. The total hippocampal volume was the sum of the hippocampal volumes across all sections for the left and right sides.

Selection of Regions for Imaging

Because our animals exhibited depression-related behaviors (173), we chose to examine the areas of the brain that have metabolic differences in the above mentioned models of induced depression, learned helplessness, and areas known to be affected by 13-*cis*-RA. Specifically, we chose to look at the following regions: orbitofrontal cortex, raphe nuclei, hippocampus, cingulate cortex 2, infralimbic cortex, lateral septal nucleus, habenula, paraventricular hypothalamus, ventral tegmental area, interpeduncular nucleus, and subiculum (Fig. 4.1). Regions were identified with the help of a mouse brain atlas (205).

Statistical Analyses

Regional Mean CO Activity

The average CO activity for each region of interest was calculated on a group basis. Two-tailed, Student's *t*-tests were performed to test for differences between vehicle control and 13-*cis*-RA treated animals in Excel (XP 2002; Microsoft). Tissue quality was poor in some regions of interest and thus the number of animals (n) for the regions varied. Data are expressed as mean ± SEM μmol/min/g wet tissue weight.

Interregional Correlations

SPSS was used to determine the Pearson product moment correlations and whether or not these correlations were significantly different from zero using a two-tailed Student's *t*-test. A modified jackknife approach was performed to verify that the significant correlations were not driven by a single animal. In this modified jackknife approach, one animal at a time is removed from the correlation and the correlation is recomputed with n-1 data points. That animal is then placed back in the group and the next animal is removed and the correlation recalculated with the new n-1 data points. This process is repeated until each animal has been removed and the respective correlation is calculated. The highest *p*-value is then reported and the correlations are evaluated from the jackknife approach. If the *p*-value for the original correlation was less than 0.05 and the *p*-value for the correlation after the modified jackknife remained less than 0.1 the correlation was considered significant and the original correlation and *p*-value were reported. Positive correlations indicate that the CO activity of both regions move in the same direction, i.e. lower CO activity in region A predicts lower CO activity in region B and vice versa. Negative correlations indicate the CO activities of the regions

move in opposite directions, i.e. lower CO activity in region A predicts higher CO activity in region B.

To determine if the correlations from the 13-*cis*-RA treated group were different from the correlations of the control treated group, the correlations for each group were first converted to a z score. The between group z scores were then determined to be different from each other using the Fischer's z test. Correlations for the 13-*cis*-RA treated group were considered to be different from the control correlations if the *p*-value reported for the Fisher's z-test was less than 0.05.

Path Analysis

Path analysis, also called structural equation modeling, was performed similar to that described in (207). Briefly, a path was first identified using known anatomical connectivity based on previous literature. The path we chose to analyze is presented in Fig. 4.2. In path analysis, causal relationships between regions are represented by path coefficients for connecting regions, denoted by the arrow. The path coefficients represent a numeric weight, or influence, of one brain region on a connected brain region. The path coefficients are determined in an iterative process whereby a theoretical model is data-fitted to the interregional correlation data that resulted from the experimental CO values. In this particular model, the path coefficient from the lateral habenula to the dorsal raphe nuclei represents the proportion of CO activity in the dorsal raphe nuclei that is predicted by the CO activity of the lateral habenula. Likewise, the path coefficient between the dorsal raphe nuclei and the hippocampus represents the proportion of CO activity of the hippocampus determined by the CO activity of the dorsal raphe nuclei. The path coefficients were determined for each of the control and 13-*cis*-RA treated groups using LISREL (version 8.54, Scientific Software). LISREL first estimates the

unknown parameters of path coefficients and residuals using a least-squares estimation. The residuals reflect external influence from regions not included in the model, as well as the influence of a region upon itself. For instance, because the lateral habenula does not have inputs that would influence the CO activity in our model, the residual is 1.0, indicating that all of the CO activity in the lateral habenula is influenced by an outside source or by itself. Iterations of calculated path coefficients and residuals are then used to determine the optimal parameters that minimize the deviation of the theoretical covariances from the experimental covariances.

A stacked model approach was used to compare the theoretical model generated for the control group versus the theoretical model generated for the 13-*cis*-RA treated group. To perform this approach, two more models are determined, a null model and an alternative model. The null model is generated by forcing the path coefficients for the control group and the 13-*cis*-RA treated group to be equal. The alternative model is the model derived if the coefficients for each group are allowed to vary. A χ^2 goodness-of-fit statistic is computed for the ability of each model to fit the original correlation matrix and then summed for each group. The degrees of freedom (df) for each group were also summed. The summed χ^2 for the alternative model was then subtracted from the χ^2 of the null model and the degrees of freedom of the alternative model subtracted from the degrees of freedom of the null model. The $\chi^2_{diff}(df_{diff})$ was then used to determine the probability that the two models are different from each other, expressed as a *p*-value, based on the null hypothesis that the path coefficients of the control group model and the 13-*cis*-RA group model are not different.

Brain-Behavior Correlations

The immobility of the last four min of both the tail suspension and forced swim tests were summed and called "Total Immobility". SPSS was used to determine the Pearson product moment correlation between the Total Immobility and each region of interest and whether or not these correlations were significantly different from zero using a two-tailed Student's *t*-test. Again, the correlations were subjected to the modified jackknife approach to verify the correlations were not driven by a single animal. The same criteria as before were used to determine significant correlations, i.e. the original correlation *p*-value was less than 0.05 and the modified jackknife *p*-value was less than 0.01. Positive brain-behavior correlations indicate that the Total Immobility is increased with the CO activity the region of interest, i.e. higher CO activity in region A predicts more Total Immobility and vice versa. Negative correlations indicate the Total Immobility and CO activity in the region of interest move in opposite directions, i.e. lower CO activity in region A predicts more Total Immobility. Correlations were considered significant if $p < 0.05$.

Morphometric Analysis

Group comparisons of % hippocampal areas at the various bregma levels were evaluated using a repeated measures ANOVA in SPSS. Comparison of total hippocampal volumes between groups were made using a Student's t-test in Excel. Differences were considered significant at $p < 0.05$.

RESULTS

13-*Cis*-RA Tends to Decrease CO Activity in the Median Raphe Nuclei

CO activity was measured to assess the effect of 13-*cis*-RA on brain metabolism in regions thought to be involved in depression (Table 4.1). Although Bremner et al. found decreased metabolism in the orbitofrontal cortex due to 13-*cis*-RA administration in humans (94), 13-*cis*-RA treatment had no effect on CO activity in the orbitofrontal cortex in this study. However, consistent with the ability of 13-*cis*-RA to alter serotonergic components *in vitro* (197), 13-*cis*-RA treatment tended to decrease CO activity in the median raphe nuclei. The CO activity of the control group was 294.1 ± 9.8 μmol/min/g wet tissue weight, while the CO activity of the 13-*cis*-RA treated group was 267.7 ± 11.3 μmol/min/g wet tissue weight (p = 0.09). We also found a significant decrease in CO activity in the inferior rostral linear nucleus of the raphe (p = 0.03) a region that was previously thought to be a part of the serotonergic system and that receives input from the dorsal raphe nuclei (208). However, other work indicates that this region may also be associated with the ventral tegmental area (209-211). The somatosensory 1 barrel field region receives input from the whiskers and is not known to be involved in depression-related behaviors, thus CO activity in this region was used as a negative control. There was no difference in CO activity in the somatosensory 1 barrel field region as expected. Furthermore, whole brain activity was not different between groups. These data show that chronic 13-*cis*-RA administration is capable of disrupting serotonergic activity, not only at the serotonergic cell bodies, but also at sites of efferent serotonergic projections such as the rostral linear nucleus of the raphe.

13-*Cis*-RA Reverses the Correlations between the CO Activity of Hippocampal Regions and CO Activity of the Dorsal Raphe Nuclei

The dorsal and median raphe nuclei contain the main 5-HT producing cells in the brain thought to be involved with mood and cognition (52, 53). There were no significant metabolic differences in the dorsal raphe nuclei between the 13-*cis*-RA treated and control groups. However, because the serotonergic system is thought to be involved in depression, and because 13-*cis*-RA has been shown to decrease hippocampal neurogenesis, we wanted to determine the effects of 13-*cis*-RA on interregional CO activity correlations between the dorsal or median raphe nuclei and the hippocampus. In control animals, the CO activity of the dorsal raphe nuclei is significantly correlated to the CO activity of the CA1 ($r = 0.83$, $p = 0.003$) and the CA3 regions of the hippocampus ($r = 0.82$, $p = 0.004$) as well as to the dentate gyrus ($r = 0.70$, $p = 0.02$) (Fig. 4.3A-C). Interestingly, in 13-*cis*-RA treated animals, these correlations are lost. Specifically, the correlations between the CO activity of the dorsal raphe nuclei and the CO activities of the CA1 and CA3 hippocampal regions and the dentate gyrus in 13-*cis*-RA treated animals were $r = -0.14$ ($p = 0.71$), $r = -0.07$ ($p = 0.84$), and $r = 0.02$ ($p = 0.96$), respectively (Fig. 4.3A-C). Furthermore, the correlations between the dorsal raphe nuclei and the CA1 and CA3 regions in control animals are significantly different from the correlations in 13-*cis*-RA treated animals ($p = 0.01$ and $p = 0.02$, respectively). However, correlations between the dorsal raphe nuclei and the dentate gyrus were not significantly different between control and 13-*cis*-RA treated mice ($p = 0.11$) (Fig. 4.3D). These data show that chronic 13-cis-RA treatment uncouples the dorsal raphe nuclei from the hippocampus, revealing that 13-*cis*-RA is targeting multiple brain systems thought to be involved in depression.

13-*Cis*-RA Significantly Disrupts the Communication Path between the Lateral Habenula and the Hippocampus

Although there is little known about the relationship between the lateral habenula and the hippocampus, Ferraro et al. (212) showed that the lateral habenula can affect the hippocampus by regulating the dorsal raphe nuclei. Specifically, the lateral habenula has an excitatory effect on the CA1 region of the hippocampus by exerting an inhibitory effect on the dorsal raphe nuclei (212). The dorsal raphe nuclei also sends projections to the CA3 region of the hippocampus as well (208). Because the dorsal raphe nuclei became uncoupled from the regions of the hippocampus, we wanted to determine the effects of 13-*cis*-RA treatment on the following network: lateral habenula → dorsal raphe nuclei → hippocampus, and we included the known anatomical connections of the intrinsic pathway of the hippocampus: dentate gyrus → CA3 → CA1 (Fig. 4.2). We conducted a path analysis to determine if these paths were different in control versus 13-*cis*-RA treated animals. Bivariate correlations for the lateral habenula, dorsal raphe nuclei, and hippocampus were used to calculate the path coefficients for the control (Fig. 4.4A) and 13-*cis*-RA (Fig. 4.4B) treated groups. The χ^2 analysis revealed that the alternate model, where the correlations were allowed to vary, was significantly different from the null model with fixed paths ($\chi^2_{diff}(8) = 17.03$, $p = 0.03$). This indicates that the interactions between the lateral habenula and the dorsal raphe nuclei and the hippocampus are significantly different between the control and 13-*cis*-RA treated groups. Additionally, the intrinsic pathway of the hippocampus is significantly changed by 13-*cis*-RA treatment. In the control group, the lateral habenula has a positive influence on the dorsal raphe nuclei whereas the influence of the lateral habenula on the dorsal raphe nuclei in 13-cis-RA treated animals is negative. Furthermore, the residual influence on the dorsal raphe nuclei is increased after 13-*cis*-RA treatment.

The dorsal raphe nuclei has a positive influence on both the CA1 and CA3 region of the hippocampus in control animals. This influence is reduced and is negative after 13-*cis*-RA treatment, indicating that these two regions, the dorsal raphe nuclei and the hippocampus, are operating independently of one another. The influences of the dentate gyrus on the CA3 region and the CA3 region on the CA1 region are increased by 13-*cis*-RA treatment. These data show that chronic 13-*cis*-RA treatment is capable of altering functional paths, not just correlations, in the mature brain.

Total Immobility is Correlated to CO Activity in the Dentate Gyrus

Because the brains were extracted from the same animals that were subjected to behavioral testing, we wanted to know if the behaviors correlated to CO activity in any region that we measured. Additionally, since we evaluated the activity in the tail suspension and forced swim tests together as one measure of depression (173), we decided to compare total immobility to the CO activities of the various regions. The Total Immobility did not correlate to any region in the control group. Interestingly, in the 13-*cis*-RA treated group, the Total Immobility significantly and inversely correlated to the CO activity in the dentate gyrus ($r = -0.94$, $p < 0.001$) (Fig. 4.5A-B). The fact that the decreased CO activity in the dentate gyrus strongly predicts Total Immobility in the 13-*cis*-RA treated group, but not the control group, indicates that the more 13-*cis*-RA decreased dentate gyrus activity, the more it increased depression-related immobility.

13-*Cis*-RA Has No Effect on Hippocampal Volume or Morphology

The results discussed above have indicated that 13-*cis*-RA is targeting the hippocampus. Because 13-*cis*-RA effects neurogenesis in the hippocampus (97) and

because hippocampal volumes are thought to be reduced in depressed patients (63-65) the volumes of the hippocampus were determined and the % hippocampal area at various bregma levels were calculated and compared between groups. 13-*Cis*-RA had no effect on hippocampal volume. The hippocampal volume was 29006128 ± 1086737 μm^3 in control animals (n = 10) and 29697935 ± 786124 μm^3 in 13-*cis*-RA treated animals (n = 12). There was also no effect on % hippocampal area at any bregma level (Figure 4.6).

DISCUSSION

CO activity in the brain represents long-term neuronal activity and interregional correlations of CO activity indicate functional connectivity between these regions. Decreased CO activity due to 13-*cis*-RA treatment therefore represents decreased neuronal firing in the region of interest. Furthermore, differences in interregional correlations between control and 13-*cis*-RA treated mice represent alterations in communication within the brain regions due to 13-*cis*-RA treatment. We show here that chronic treatment of adolescent male mice for 6 weeks with 1 mg/kg/day of 13-*cis*-RA tends to decrease CO activity in the median raphe nuclei and significantly decreases the CO activity in the rostral linear nucleus of the raphe when compared to animals administered an equal volume of vehicle. Additionally, in control animals, the CO activity in the dorsal raphe nuclei significantly correlates to the CO activity in the CA1 region, CA3 region, and dentate gyrus of the hippocampus. These correlations are lost in the 13-*cis*-RA treated animals. Furthermore, a path analysis evaluating the connectivity of the lateral habenula to the hippocampus via the dorsal raphe nuclei revealed that this path is also disrupted by 13-*cis*-RA as seen by a disconnect of the dorsal raphe nuclei from each of the hippocampal regions and from the lateral habenula. Additionally, the path analysis revealed that the regional influences of the dentate gyrus on the CA3 region

and the influence of the CA3 region on the CA1 region is increased by 13-*cis*-RA treatment. Moreover, the Total Immobility in the tail suspension and forced swim tests correlated inversely to the CO activity in the dentate gyrus of 13-*cis*-RA treated, but not control, animals. Although 13-*cis*-RA seems to be disrupting communication to the hippocampus, there was no effect on volume or % hippocampal area due to 13-*cis*-RA treatment. A summary of the CO activity changes, as well as the correlation changes can be seen in Fig. 4.7. The behavior-region and region-region correlations, as well as the differences between the group correlations are summarized in Table 4.2. Combined, these data show that 13-*cis*-RA treatment alters serotonergic and hippocampal function, which could be responsible for the depression-related behaviors we observed previously.

Only one previous study examined the effects of 13-*cis*-RA on brain metabolism. Bremner et al. (94) found that four months of 13-*cis*-RA treatment decreased orbitofrontal cortex metabolism when compared to baseline metabolism in each individual. In contrast, there was no change in orbitofrontal cortex metabolism in antibiotic treated control patients over the four month period (94). None of the 13-*cis*-RA treated patients were depressed, according to the Hamilton depression rating scale. However, patients exhibiting decreased orbitofrontal cortex metabolism reported mood changes as observed by themselves, their family, or the staff conducting the study (94). Although we found increased depression-related behaviors in the adolescent male mice that received chronic 13-*cis*-RA treatment (173), we did not find altered metabolism in the orbitofrontal cortex of 13-*cis*-RA treated animals. This may be due to differences in homology between these brain regions in humans and mice, or it may be due to differences in technique. The PET scans measure glucose uptake, which is representative of neuronal response to environmental conditions that span over about 45 min (203). In contrast, the CO activity denotes steady state activity of a given brain region (201, 203).

Therefore, although steady state orbitofrontal cortex neuronal demands may not be different due to 13-*cis*-RA treatment, orbitofrontal cortex response to environmental cues may be suppressed due to 13-*cis*-RA treatment.

We expected chronic 13-*cis*-RA administration to alter CO activity according to the available models of depression. We were surprised to see very few differences in the regional group average CO activities of the 13-*cis*-RA treated mice when compared to control mice because there was a significant difference in depression-related behaviors, specifically increased immobility, in the 13-*cis*-RA treated mice when compared to control mice (173). However, we did find that the CO activity in the median raphe nuclei, one of the main 5-HT producing systems in the brain, of 13-*cis*-RA treated mice tended to be lower than that of the control mice.

The ability of 13-*cis*-RA to reduce CO activity in the inferior rostral linear nuclei may, in part, account for the depression related behaviors induced by 13-*cis*-RA. The dorsal raphe nuclei projects to the rostral linear nucleus of the raphe (208). Additionally, the rostral linear nucleus of the raphe has been found to have efferent projects directly to the lateral habenula, the dorsal raphe nuclei and to the ventral tegmental area, a largely dopaminergic area involved in reward (209). Historically, this region has been considered to be a part of the raphe nucleus, and brain atlases continue to call it the rostral linear nucleus of the raphe. Furthermore, although a mouse atlas was used to identify brain regions within the slices analyzed, the Paxinos rat atlas states that regions called the raphe were identified consistently with serotonergic labeling (213). From the stereological study performed in Chapter 5, we found that serotonergic labeling of the raphe nuclei cell bodies did not occur until approximately bregma level -4.04, where the median raphe nuclei begins (Fig. 5.1A). Additionally, the rostral linear nucleus of the raphe has been suggested to be a GABAergic containing component of the ventral

tegmental area (209). The ventral tegmental area is involved in reward, and depressive symptoms such as anhedonia implicate that this regions is disrupted in depression. The ventral tegmental area has decreased CO activity in congenitally learned-helpless rats (74). However, raphe nuclei and the ventral tegmental area did not exhibit covaried CO activity with the inferior rostral linear nucleus of the raphe. Whether the rostral linear nucleus of the raphe is a component of the serotonergic raphe nuclei or the dopaminergic ventral tegmental area, decreased CO activity in the inferior rostral linear nucleus may be important to depression, but the exact role of the rostral linear nucleus of the raphe in depression-related behaviors remains to be elucidated.

As mentioned in Chapter 1, hippocampal neurogenesis is thought to be compromised in depression [reviewed in (63, 64)]. Hippocampal neurogenesis is decreased by 13-*cis*-RA administration in male CD1 mice (97). Although we don't fully understand the role of the hippocampus or neurogenesis in depression-related behaviors, hippocampal volume is decreased in depressed patients as assessed with MRI (63-66). However, hypermetabolism has been observed in the hippocampus in the congenitally-learned helpless rat (214) and human patients with major depressive disorder (215). Additionally, hippocampal metabolism is reduced following antidepressant treatment in humans (216). This may indicate that there is some metabolic mechanism that compensates for neurogenesis loss.

Interestingly, 5-HT appears to have a role in hippocampal neurogenesis and the removal of 5-HT reduces hippocampal neurogenesis (148). Furthermore, in rats, serotonergic denervation reduces hippocampal neurogenesis (217), a phenomena that can be reversed by transplantation of fetal raphe nuclei cells into the hippocampus (218). We were interested to find that dorsal raphe nuclei metabolism correlated to the hippocampal regions in the control mice but not the in the 13-*cis*-RA treated mice. Perhaps this

uncoupling of the serotonergic system from the hippocampal system is, at least in part, responsible for the effects of 13-*cis*-RA on neurogenesis observed by others (97).

Increases in somatodendritic autoinhibitory 5-HT_{1A} levels may reduce serotonergic cell firing and thereby decrease 5-HT signaling. Increases in SERT protein levels would lead to increased removal of 5-HT from the synaptic cleft, and therefore also decrease serotonergic signaling. Since 13-*cis*-RA increased both the 5-HT_{1A} and SERT proteins *in vitro* (197), it seems likely that should these two proteins be increased *in vivo*, they would lead to a decrease in serotonergic signaling that may ultimately decrease hippocampal neurogenesis. However, more experiments would need to be done to determine if, in the 13-*cis*-RA treated animals, compromised hippocampal neurogenesis due to 13-*cis*-RA treatment leads to, or results from, uncoupling of the hippocampal regions from the dorsal raphe nuclei. Interestingly, rats that underwent partial serotonergic denervation had increased CO levels in the CA3 region of the hippocampus (219). However, when partial serotonergic denervation was combined with chronic variable stress, CO activity in the CA3 region was not different from control rats (219). Thus, although 13-*cis*-RA may be leading to decreased serotonergic function, which could lead to increased metabolism in the CA3 region, the stress of the behavioral testing may have masked hippocampal hypermetabolism expected for a model of depression.

As mentioned in Chapter 1, the habenula is a major regulator of monoaminergic transmission and receives inputs from the serotonergic and the norepinephrinergic systems as well as sending output to the serotonergic dorsal raphe nuclei (70, 71) and to the dopaminergic ventral tegmental area (71). The ability of the lateral habenula to regulate monoaminergic function, which is often disrupted in depression, makes the lateral habenula a likely candidate for involvement in depression. Additionally,

metabolic activity in the lateral habenula has been shown to be increased using ^{14}C-2-deoxyglucose uptake in three animal models of depression: chronic-stress, amphetamine withdrawal, and alpha-methyl-para-tyrosine administration (200). Moreover, the congenitally learned-helpless model of depression was found to have increased metabolism in the lateral habenula as assessed by CO activity (74).

The lateral habenula has been found to negatively regulate the dorsal raphe nuclei (72, 212) and this inhibitory regulation of the dorsal raphe nuclei ultimately results in an excitatory regulation of the hippocampus by the lateral habenula (212). A recent study by Yang et al. (73) used two models of depression in rats, chronic mild stress and neonatal exposure to clomipramine, to observe the effect of lateral habenula lesions on immobility in the forced swim test. Lesions to the lateral habenula decreased immobility in the forced swim test in both models of depression and also led to an increase in 5-HT in the dorsal raphe nuclei (73). Given that, in control animals, the lateral habenula is coupled to the dorsal raphe nuclei, which is coupled to the hippocampal CA1 region, the lateral habenula may be regulating the CA1 region of the hippocampus consistent with the pathway outlined by Ferraro et al. (212). Additionally, the dorsal raphe nuclei sends projections to the CA3 region as well (208) and so this connection was included in the path analysis. We also wanted to determine more specifically what the effects of 13-cis-RA are on the hippocampus and we therefore included the hippocampal intrinsic pathway in the path analysis. The path analysis performed here indicates that this excitatory control of the lateral habenula on the hippocampus via inhibition of the dorsal raphe nuclei may be disrupted by 13-*cis*-RA treatment. However, the lateral habenula remains coupled to the CA1, perhaps representative of other pathways involved in lateral habenula/hippocampal regulation. It is interesting to see that the intrinsic dentate gyrus → CA3 → CA1 pathway within the hippocampus is increased after 13-*cis*-RA treatment

and may explain why the hippocampus seems to be functioning independently of the dorsal raphe nuclei.

Decreased hippocampal neurogenesis may be responsible for the uncoupling of the hippocampus and the dorsal raphe nuclei and the disruption of the lateral habenula → dorsal raphe nuclei → hippocampal paths. Decreased hippocampal neurogenesis may also account for the increased influences of the dentate gyrus on the CA3 region and the CA3 region on the CA1 region in 13-*cis*-RA treated animals. However, it is difficult to determine if decreased hippocampal neurogenesis or decreased serotonergic signaling is caused by 13-*cis*-RA first, thereby leading to lateral habenula → dorsal raphe nuclei → hippocampal dysregulation, or if effects are happening simultaneously. It is possible that 13-*cis*-RA could target the lateral habenula first. However, since 13-*cis*-RA increases 5-HT_{1A} and SERT protein levels in an isolated serotonergic cell system *in vitro* (197), 13-*cis*-RA may have the ability to disrupt serotonergic signaling directly without having to disrupt serotonergic control by the lateral habenula first, ultimately resulting in the uncoupling of the dorsal raphe nuclei from the lateral habenula.

It seems as though a loss of the lateral habenula → dorsal raphe nuclei → hippocampus pathway should lead to increased activity in the hippocampus since the inhibitory effect of the dorsal raphe nuclei is not present. We expect that this would especially be true given that hippocampal activity is thought to be increased in depression (214) as mentioned above. Ultimately, one might also expect the lateral habenula and the hippocampal regions to become functionally uncoupled, an outcome not observed in the interregional correlations calculated here. Perhaps the loss of serotonergic function leading to decreased neurogenesis was not great enough to lead to the expected increased hippocampal activity in these mice, although the effects of 13-*cis*-RA are enough to lead to depression-related behaviors in these animals.

Lack of altered metabolism in the hippocampal regions may maintain the functional connectivity between the lateral habenula and the hippocampus. However, loss of serotonergic to hippocampal functional connectivity may still result in depression-related behaviors. This especially seems to be the case because we saw an inverse correlation between the CO activity in the dentate gyrus and Total Immobility in the tail suspension and forced swim tests, indicating that the lower the dentate gyrus CO activity, the more immobility the animal exhibited. Furthermore, this was only true in 13-*cis*-RA treated animals, where decreased neurogenesis is expected. However, it is unknown if CO activity in the dentate gyrus is reflective of the level of neurogenesis occurring in the dentate gyrus. We did not find a difference in hippocampal volume due to 13-*cis*-RA treatment here even though others have shown that 13-*cis*-RA treatment decreases the number of new neurons throughout the hippocampus (97). Although 13-*cis*-RA may still be affecting neurogenesis in the animals in this study, volume measurements are probably not sensitive enough to reflect the effect of 13-*cis*-RA on neurogenesis.

Evaluation of CO activity in the various brain regions of control and 13-*cis*-RA treated mice showed very few alterations in metabolic activity. However, the serotonergic system and coupling of the serotonergic system to the hippocampus were affected by 13-*cis*-RA administration. Specifically, not only did 13-*cis*-RA tend to decrease CO activity in the median raphe nuclei, but 13-*cis*-RA treatment uncoupled the functional connectivity of the dorsal raphe nuclei to the hippocampus. This uncoupling of the dorsal raphe nuclei and the hippocampus may be a result of, or lead to, decreased hippocampal neurogenesis previously observed due to 13-*cis*-RA treatment. Additionally, animals with lower dentate gyrus CO activity exhibited higher levels of total immobility in the tail suspension and forced swim tests in the 13-*cis*-RA treated group. Previously, we showed that 13-*cis*-RA increased 5-HT_{1A} receptor and SERT

protein levels *in vitro* (197). Ultimately, increased 5-HT_{1A} and SERT protein levels *in vivo* may be decreasing serotonergic signaling, leading to decreased hippocampal neurogenesis, uncoupling of the lateral habenula from the dorsal raphe nuclei, and most importantly, increased depression-related behaviors.

ACKNOWLEDGEMENTS

I would like to thank Sarah Bailey, Chris Bailey, Doug Barrett, and Penny Riha for technical assistance. I would also like to thank Jason Shumake for his help with statistical analysis and Francisco Gonzalez-Lima for help in tissue analysis. This research was supported by a Roaccutane Research Grant (M.L.), NIEHS toxicology training grant (T32 ES007247, K.O.) and the University of Texas at Austin Fiscal Year Research Grant FY 2004-2005 (M.L.).

Table 4.1: Mean ± S.E.M. CO activity (μmol/min/g wet tissue weight) for control versus 13-*cis*-RA treated animals.

Brain region	*Bregma level*	*Control*	*n*	*13-cis-RA*	*n*	*p*
Orbitofrontal Cortex	2.68	224.0 ± 10.5	12	231.2 ± 12.9	12	0.67
Cingulate Cortex 2	1.42	195.2 ± 14.7	11	211.9 ± 11.6	12	0.38
Infralimbic Cortex	1.42	202.3 ± 10.8	11	213.6 ± 9.5	12	0.44
Lateral Septal Nucleus	1.42	215.5 ± 8.0	11	221.2 ± 9.0	12	0.64
Hippocampus						
CA1	-1.94	240.8 ± 10.1	10	235.4 ± 10.6	11	0.72
CA3	-1.94	267.0 ± 8.7	10	280.0 ± 10.2	11	0.35
Dentate Gyrus	-1.94	311.4 ± 10.2	10	310.2 ± 11.6	11	0.94
Habenula						
Median	-1.94	268.9 ± 10.6	10	260.2 ± 8.9	11	0.54
Lateral	-1.94	348.9 ± 9.9	10	347.6 ± 9.0	11	0.92
Paraventricular hypothalamus	-1.94	259.7 ± 10.0	12	266.0 ± 8.2	12	0.63
Ventral Tegmental Area	-3.52	204.7 ± 7.8	12	195.2 ± 9.3	12	0.44
Rostral Linear Nucleus of the Raphe						
Superior	-3.52	147.6 ± 10.1	12	143.8 ± 8.5	12	0.78
Inferior	-3.52	152.7 ± 9.6	12	124.9 ± 8.1	12	0.03*
Raphe Nuclei						
Dorsal	-4.36	313.8 ± 10.2	12	306.5 ± 13.5	11	0.67
Median	-4.36	294.1 ± 9.8	12	267.7 ± 11.3	11	0.09†
Subiculum	-3.52	248.9 ± 8.4	12	254.1 ± 6.9	12	0.64
Interpeduncular Nucleus	-3.52	351.0 ± 16.6	11	355.7 ± 20.0	12	0.86
Somatosensory 1, barrel field	-1.94	278.9 ± 8.5	11	297.4 ± 9.5	11	0.18
Whole brain averages		202.2 ± 1.9	12	202.0 ± 2.9	12	0.96

*P < 0.05.
†0.05<P < 0.10.

Table 4.2: Summary of behavior to CO correlations and interregional correlations in control and 13-*cis*-RA treated animals

Behavior and Regions Correlated	*Correlation*				
	Control	*n*	*13-Cis-RA treated*	*n*	*Compared to control (p-value)*
TST immobility –					
Dentate gyrus	-0.32 ($p = 0.38$)	10	-0.94 ($p < 0.001$)	11	< 0.001**
Dorsal raphe nuclei –					
CA1	0.83 ($p = 0.003$)	10	-0.14 ($p = 0.71$)	10	0.01*
CA3	0.82 ($p = 0.004$)	10	-0.07 ($p = 0.84$)	10	0.02*
Dentate gyrus	0.70 ($p = 0.02$)	10	0.02 ($p = 0.96$)	10	0.11
Lateral Habenula –					
CA1	0.78 ($p = 0.007$)	10	0.91 ($p < 0.001$)	11	0.35
Dorsal raphe nuclei[§]	0.62 ($p = 0.06$)	10	-0.33 ($p = 0.36$)	10	0.04*

*Correlation for 13-*cis*-RA treated group is significantly different from correlation for control treated group as determined by the Fischer's z test ($p < 0.05$).
** Correlation for 13-cis-RA treated group is significantly different from correlation for control treated group as determined by Fisher's z test ($p < 0.001$)
[§]Correlations between dorsal raphe nuclei and lateral habenula were not significant in the control group after performing the modified jackknife ($r = 0.51$, $p = 0.34$) and correlations were not significantly different between groups for the dorsal raphe and lateral habenula after performing the modified jackknife ($p = 0.17$)

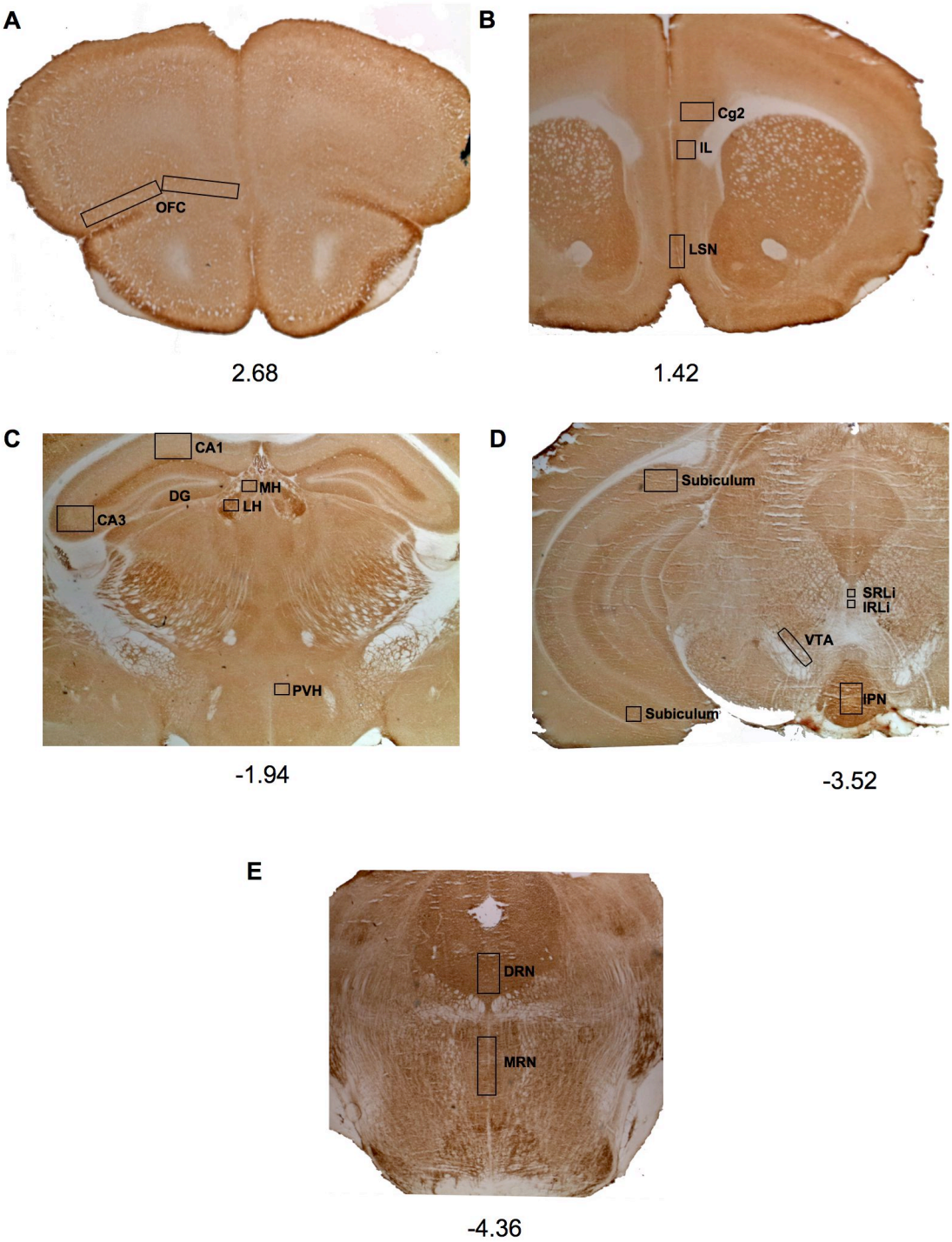
A
OFC
2.68
B
Cg2
IL
LSN
1.42
C
CA1
MH
DG
LH
CA3
PVH
-1.94
D
Subiculum
SRLi
IRLi
VTA
IPN
Subiculum
-3.52
E
DRN
MRN
-4.36

Figure 4.1: Bregma levels for CO readings.

Slices are representative of the CO readings taken for each brain region. **(A)** Bregma level 2.68. OFC = orbitofrontal cortex. **(B)** Bregma level 1.42. Cg2 = cingulate cortex 2, IL = infralimbic cortex, LSN = lateral septal nucleus. **(C)** Bregma level -1.94. CA1 = Cornu Ammonis field 1 of the hippocampus, CA3 = Cornu Ammonis field 3 of the hippocampus, DG = dentate gyrus of the hippocampus, MH = median habenula, LH = lateral habenula, PVH = paraventricular hypothalamus. **(D)** Bregma level -3.52. SRLi = superior rostral linear nuclei of the raphe, IRLi = inferior rostral linear nuclei of the raphe, VTA = ventral tegmental area, IPN = interpeduncular nucleus. **(E)** Bregma level -4.36. DRN = dorsal raphe nuclei, MRN = median raphe nuclei.

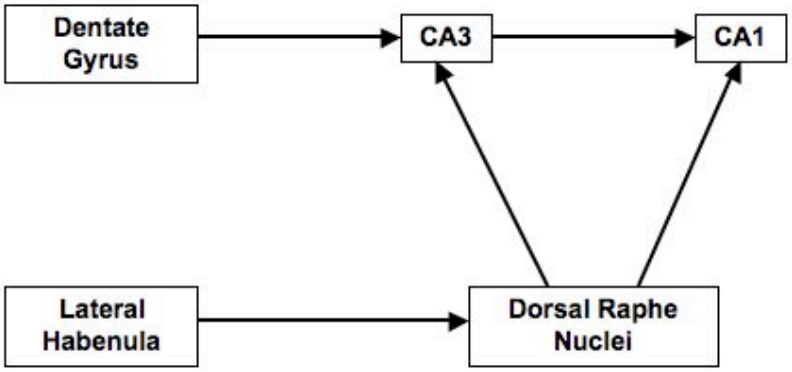

Figure 4.2: Proposed path of control of hippocampus by lateral habenula via the dorsal raphe nuclei.

Anatomical connections are represented by arrows. The lateral habenula is known to have an effect on the CA1 region by acting on the dorsal raphe nuclei, but the dorsal raphe nuclei also send input to the CA3 region.

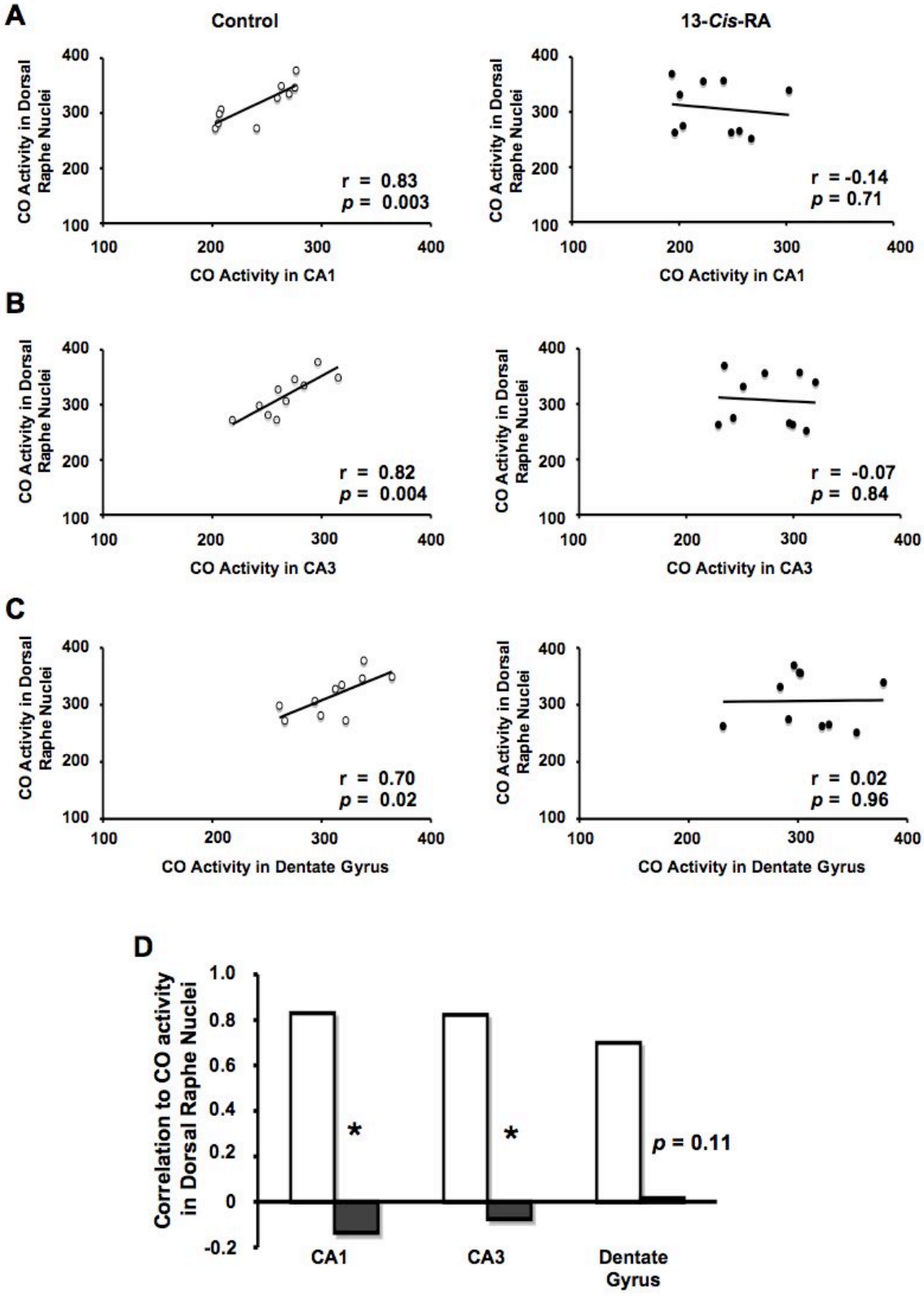
A
Control
13-Cis-RA
CO Activity in Dorsal Raphe Nuclei
CO Activity in CA1
r = 0.83
p = 0.003
r = -0.14
p = 0.71
B
CO Activity in CA3
r = 0.82
p = 0.004
r = -0.07
p = 0.84
C
CO Activity in Dentate Gyrus
r = 0.70
p = 0.02
r = 0.02
p = 0.96
D
Correlation to CO activity in Dorsal Raphe Nuclei
1.0
0.8
0.6
0.4
0.2
0
-0.2
*
*
p = 0.11
CA1
CA3
Dentate Gyrus

Figure 4.3: 13-*Cis*-RA treatment uncouples the dorsal raphe nuclei from the hippocampal regions.

Interregional correlations between CO activity in the dorsal raphe nuclei and each of the hippocampal regions were determined as Pearson product moment correlations for control treated animals (A, B, C left column) or 13-*cis*-RA treated animals (A, B, C right column). **(A)** The CO activity in the dorsal raphe nuclei significantly correlates to the CO activity of the CA1 region in control animals but not in 13-*cis*-RA treated animals. **(B)** The CO activity of the dorsal raphe nuclei significantly correlates to the CO activity of the CA3 region in control animals but not in 13-*cis*-RA treated animals. **(C)** The CO activity of the dorsal raphe nuclei significantly correlates to the CO activity of the dentate gyrus in control but not 13-*cis*-RA treated animals. **(D)** Comparisons of the correlations between control and 13-*cis*-RA treated animals. *Correlation in 13-*cis*-RA treated animals is significantly different from correlation in control animals ($p < 0.05$).

Control

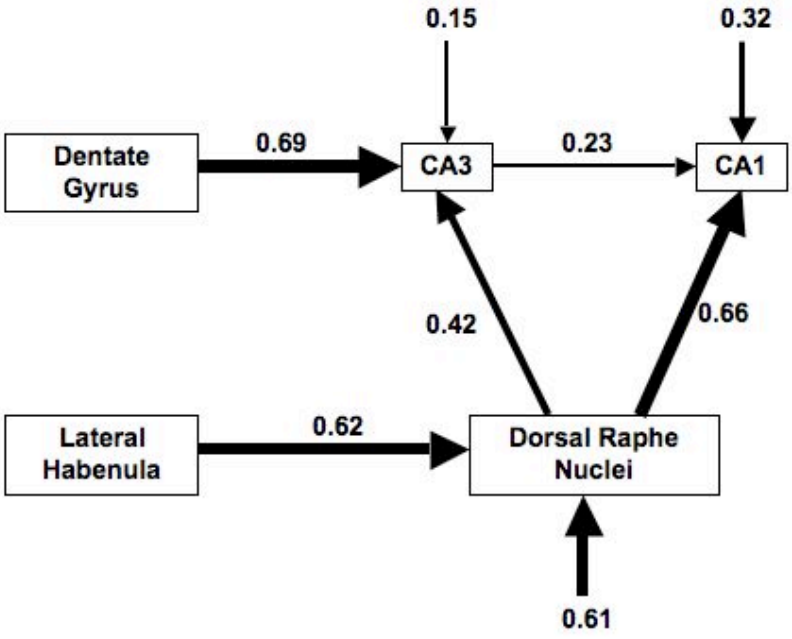

13-*Cis*-RA

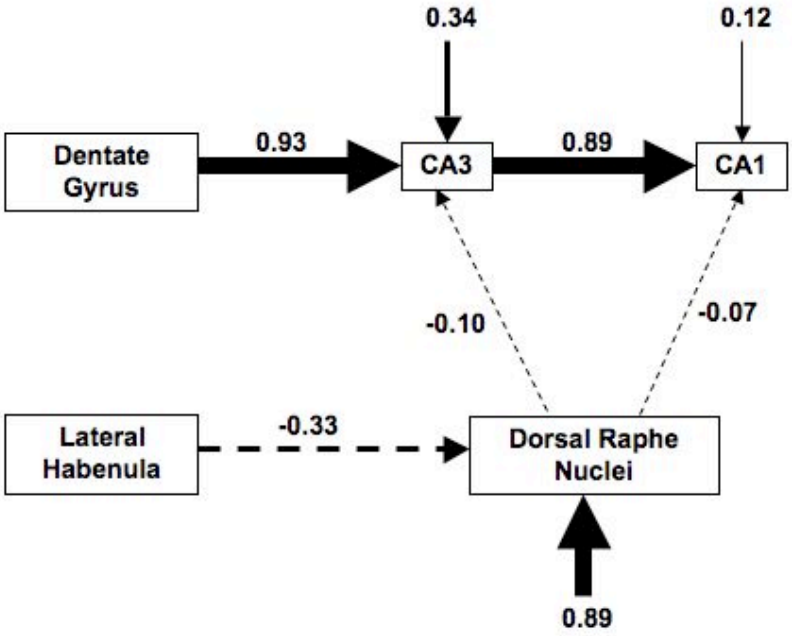

Figure 4.4: Communication between the hippocampus, the lateral habenula, and the dorsal raphe nuclei is lost due to 13-*cis*-RA treatment.

The pathway by which the lateral habenula controls the CA1 region of the hippocampus via the dorsal raphe nuclei and the communication between the dorsal raphe nuclei and the hippocampus in **(A)** control animals and **(B)** 13-*Cis*-RA treated animals. Positive path coefficients are shown as solid lines. Negative path coefficients are shown as dashed lines. Path coefficients are indicated next to each arrow. Magnitude of effect is represented by the thickness of lines. The lines coming into each region without an annotated region themselves are the residual influence into the lateral habenula, hippocampus, or the dorsal raphe nuclei. The regions exerting the residual influences are unknown. n = 10 for both groups. $\chi^2_{diff}(8) = 17.03$, $p = 0.03$.

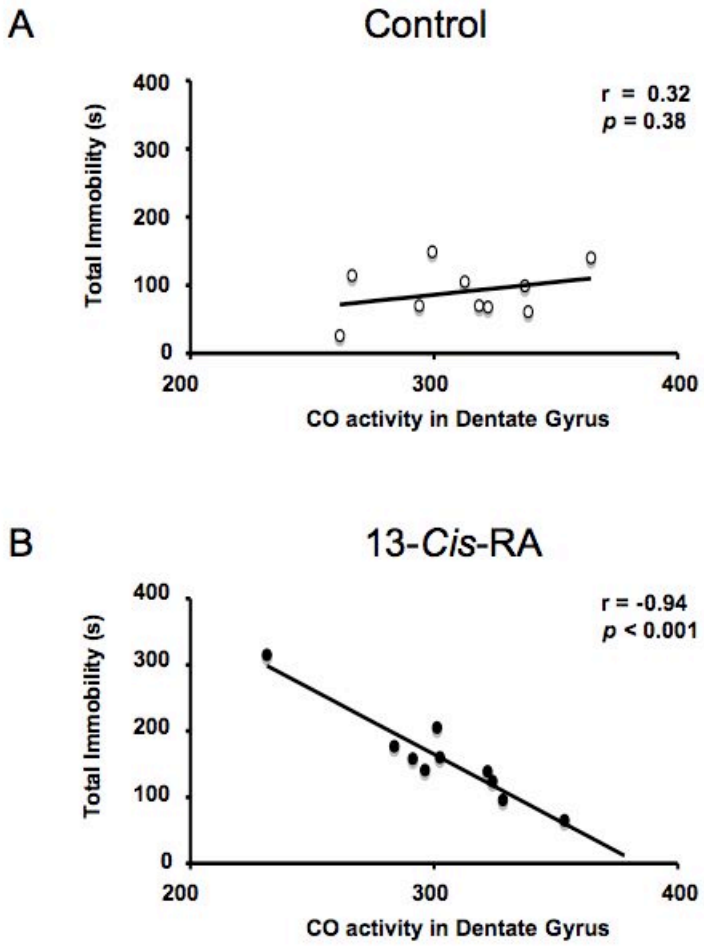

Figure 4.5: Total time spent immobile in the tail suspension and forced swim tests correlates to the CO activity of the dentate gyrus in 13-*cis*-RA treated animals.

The Total Immobility is the sum of the immobility during the last four min of the tail suspension and the forced swim tests. Correlations between the Total Immobility and the CO activity of the dentate gyrus are Pearson product moment correlations for **(A)** control group and **(B)** 13-*cis*-RA treated group.

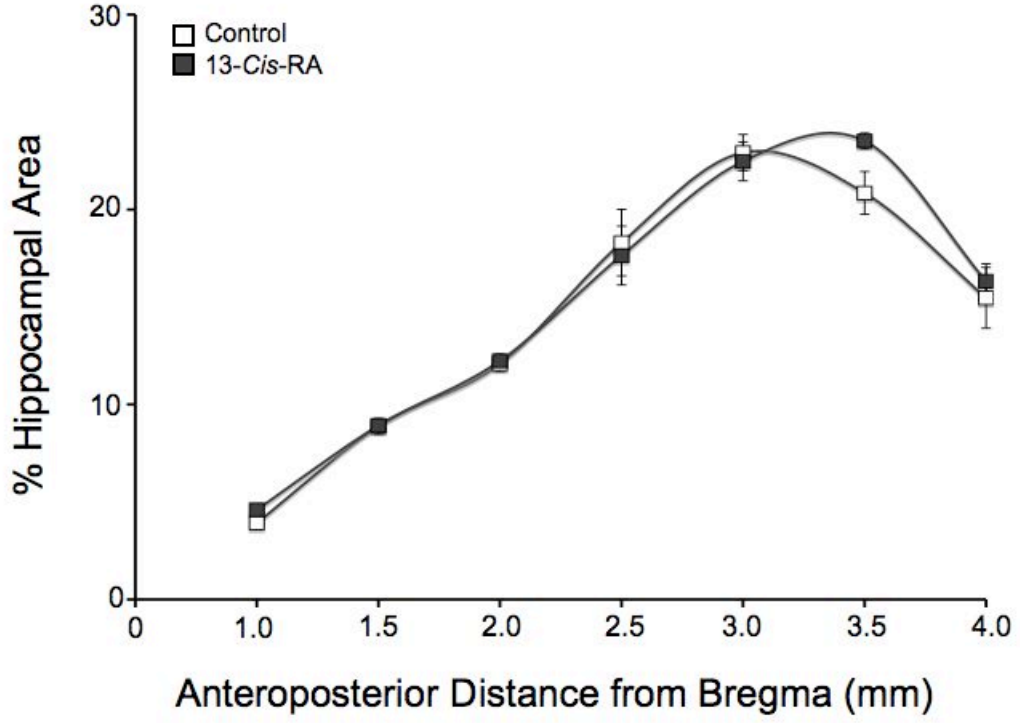

Figure 4.6: 13-*Cis*-RA has no effect on percent hemi-hippocampal area of hemi-section area.

The percent hemi-hippocampal area was calculated at each bregma level for control and 13-*cis*-RA treated mice. There was no effect of treatment on % area as determined by a repeated measures ANOVA with an alpha level of 0.05. For control animals, n = 7. For 13-*cis*-RA treated animals, n = 11.

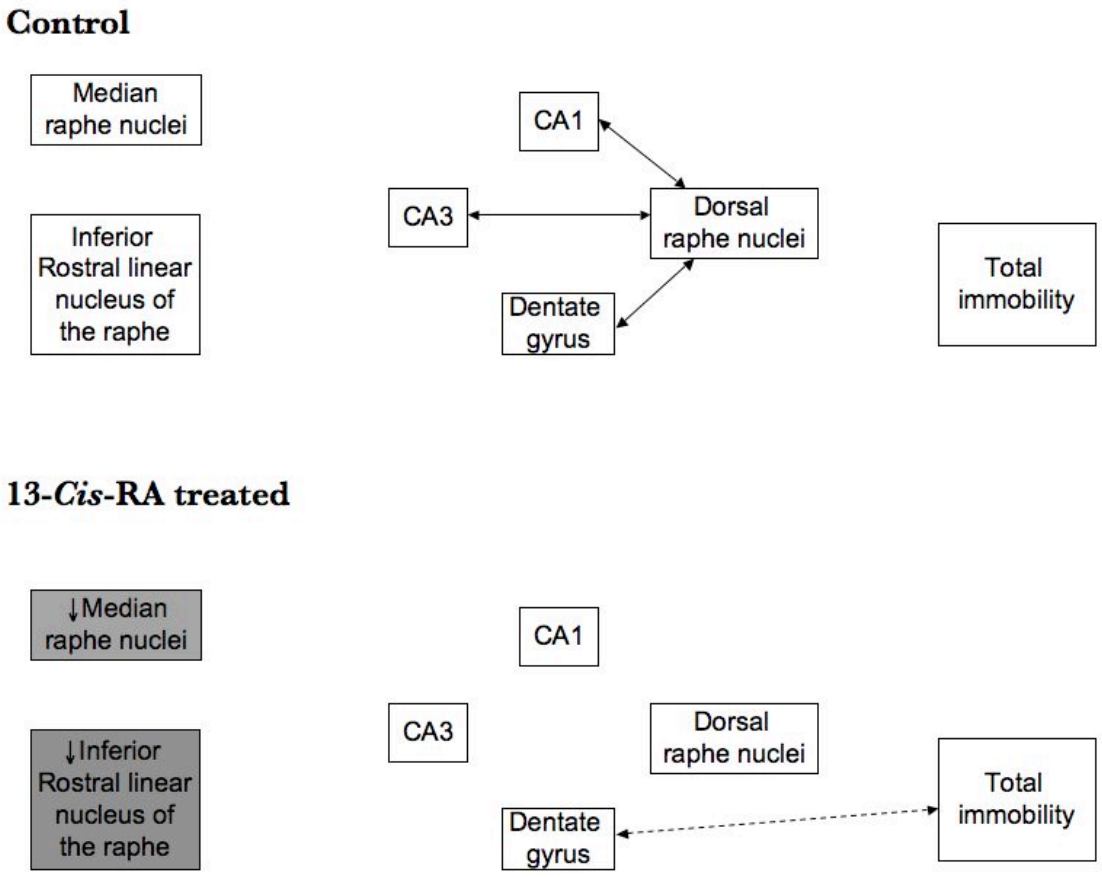

Figure 4.7: Summary of the effects of 13-*cis*-RA on brain metabolism and functional connectivity.

The lines represent correlations between brain regions and thickness of the line is representative of the correlation. Solid lines represent positive correlations while dashed lines are negative correlations. **(A)** Control group: The hippocampal CA1 and CA3 regions are coupled to the dorsal raphe nuclei. Additionally, the dentate gyrus is also coupled to the dorsal raphe nuclei. There was no correlation between immobility in the tail suspension and forced swim tests to any brain region in the control animals. **(B)** 13-*Cis*-RA treatment tends to decrease the CO activity in the median raphe nuclei and significantly decreased CO activity in the inferior rostral linear nucleus of the raphe. 13-*Cis*-RA treatment also uncouples the dorsal raphe nuclei from the CA1 and CA3 regions of the hippocampus and uncouples the dorsal raphe nuclei from the dentate gyrus, where neurogenesis occurs. Lastly, total immobility in the tail suspension and forced swim tests is negatively correlated to the dentate gyrus in 13-*cis*-RA treated animals only.

Chapter 5: 13-*Cis*-RA Has No Effect on Estimated Volume or Number of Serotonergic Neurons in the Median or Dorsal Raphe Nuclei

ABSTRACT

13-*Cis*-RA, a synthetic retinoid, is capable of inducing depression-related behaviors in adolescent male mice and tends to reduce median raphe nuclei CO activity. Because CO activity is tightly coupled to energy requirements for neuronal activity, reductions in CO activity represent decreased neuronal firing. 13-*Cis*-RA administration to male mice also uncouples the dorsal raphe nuclei from the hippocampus *in vivo*. In serotonergic cells *in vitro*, 13-*cis*-RA treatment leads to increased protein levels of 5-HT_{1A} and SERT, two components of the serotonergic system that regulate serotonergic signaling. Increases in these proteins *in vivo* could lead to decreased serotonergic signaling. Interestingly, 5-HT is involved in hippocampal neurogenesis and removal of 5-HT reduces hippocampal neurogenesis. Others have found that 13-*cis*-RA decreases hippocampal neurogenesis. Because 13-*cis*-RA is capable of inducing apoptosis, as are many retinoids, we hypothesized that reduction in the number of serotonergic cells in the dorsal and median raphe nuclei could account for the decrease in CO activity in the median raphe nuclei and the decreased hippocampal neurogenesis. Adolescent male mice were treated with 1 mg/kg/day of 13-*cis*-RA for six weeks prior to examination of the median and dorsal raphe nuclei via stereological analysis of 5-HT immunopositive neurons. There were no differences in the volumes or serotonergic cell densities in either the median or dorsal raphe nuclei, indicating that while 13-*cis*-RA is capable of disrupting the serotonergic system and its functional connectivity to the hippocampus, these disruptions are not due to decreased serotonergic cell numbers in the dorsal or median raphe nuclei.

INTRODUCTION

Previously we showed that chronic 13-*cis*-RA administration induces depression-related behaviors (173), tends to decrease CO activity the median raphe nuclei, and uncouples the dorsal raphe nuclei from the hippocampal region in adolescent male mice. Additionally, 13-*cis*-RA increases intracellular levels of 5-HT and the 5-HIAA and increases protein levels of the 5-HT_{1A} receptor and SERT in serotonergic cells *in vitro* (197). Furthermore, 13-*cis*-RA treatment decreases hippocampal neurogenesis *in vivo* (97).

13-*Cis*-RA, a synthetic retinoid, is a member of the vitamin A family. Hypervitaminosis A is also thought to have effects on the mature nervous system and can cause headaches and psychosis. Prior to our work, there have been relatively few studies examining the effects of retinoids in the mature central nervous system. Instead, the retinoid field has historically focused on the role of retinoids in development and cancer chemotherapy where retinoids regulate cell differentiation and apoptosis (220).

Postmortem stereological studies of depressed patients show decreased orbitofrontal cortex volume and decreases in glial cell number and size in the orbitofrontal cortex (221, 222), a region that has been shown to have decreased metabolism after four months of 13-*cis*-RA treatment (94). Additionally, hippocampal volume is decreased in depressed humans (63-66). It is not known if these volume reductions and decreases in glial cell numbers are due to atrophy or cell loss (222). However, antidepressant treatments are capable of upregulating cellular protective factors, such as Bcl-2, which blocks apoptosis (77). Although very few studies have looked at volume changes in the dorsal and median raphe nuclei, one study found that while the volume of dorsal raphe nuclei was not different between suicide victims and

controls, the density of serotonergic cells in the dorsal raphe nuclei of suicide patients was higher than that of controls (223).

5-HT is involved in regulation of neurogenesis and loss of 5-HT leads to decreased neurogenesis (148). Denervation of median and dorsal raphe neurons by 5, 7-dihydroxytryptamine decreased cell proliferation in the dentate gyrus as measured by 5-bromo-2'-deoxyuridine immunostaining (217) and grafts of fetal serotonergic cells restored neurogenesis in denervated rats (218). Thus, although the decreased hippocampal neurogenesis due to 13-*cis*-RA treatment may, in part, be due to direct effects of 13-*cis*-RA on differentiation in the dentate gyrus, decreased serotonergic signaling may also play a part in reducing neurogenesis.

Given the effects that 13-*cis*-RA has on the serotonergic system (197), hippocampal neurogenesis (97), and the interactions between serotonergic and hippocampal functional connectivity (chapter 4), we asked what is the mechanism by which 13-*cis*-RA is disrupting these two systems. To our knowledge, this is the only study that has taken a stereological approach to compare the effects of 13-*cis*-RA on number of 5-HT-labeled cells within the median and dorsal raphe nuclei and the volumes of these two regions. Specifically, we determined if 13-*cis*-RA affected median and dorsal raphe nuclei volume and serotonergic cell numbers.

METHODS

Animals

Young, adult male DBA/2J (Jackson Laboratories, Bar Harbor, ME) mice were used in this study. Animals were three weeks old at arrival and four weeks old at the start of treatment. Mice were group housed four per cage and maintained under a 12:12 h

light/dark cycle. Food and water were provided *ad libitum*. All procedures and tests performed on animals were approved by the University of Texas IACUC, protocol number 04100403, and according to the National Institutes of Health Guide for the Care and Use of Laboratory Animals.

Treatment

Animals were treated in the same way as described in Chapter 2 of this dissertation. Briefly, animals were allowed to adapt to the University of Texas animal facility for one week prior to initial injection. Animals were handled during the first week to reduce the stress of receiving daily injections. A 2 mg/mL stock solution of 13-*cis*-RA in DMSO was stored for up to one week at -20 ºC. Sterile injection samples were prepared in the dark. Injections were performed one hour prior to the start of the dark cycle in the same room where the animals were housed and one person performed all injections. Treated animals (n = 11) received daily i.p. injections of 1 mg/kg/day 13-*cis*-RA (Sigma, St. Louis, MO) dissolved in sterile 50% DMSO/50% saline (0.9%) to a final volume of 200 μL. Control animals (n = 11) were administered 200 μL of vehicle (50% DMSO/50% saline), i.p., daily. Animals were injected for 6 weeks. No behavioral testing was performed on these animals.

Perfusions

Perfusions were performed as described in (224). Briefly, mice were deeply anesthetized with 0.05 mL each ketamine (100 mg/mL)/xylazine (20 mg/mL) and then perfused transcardially with 1% paraformaldehyde for 30 s at a rate of 7.5 mL/min, followed by 4% paraformaldehyde for 10 min. The brains were immediately removed

intact and postfixed in paraformaldehyde overnight followed by storage in phosphate buffer saline (PBS) with 0.1% sodium azide at 4°C. Forty μm sections were then cut using a vibratome (Leica, Bannockburn, IL) and stored in PBS with 0.1% sodium azide at 4°C until immunohistochemistry was performed.

Immunohistochemistry for Stereological Analysis

Sections were from a 1:3 series across the region containing both the dorsal and median raphe nuclei. All washes were done in PBS, three times for 10 min each. Sections were washed at room temperature and then blocked for endogenous peroxides containing 3:1 methanol: 3% hydrogen peroxide for 15 min. The sections were then washed and blocked in SuperBlock (Pierce, Rockford, IL) containing 10% natural goat serum (NGS), 2% bovine serum albumin (BSA), and 0.2% Triton X. The tissues were incubated in blocking solution (BS) consisting of PBS containing 10% Superblock, 10% NGS, 2%BSA, and 0.2% Triton X with a 1:10,000 dilution of anti-5-HT antibody (Cat # S5545, Sigma, Saint Louis, MO) for 24 h. The sections were then washed and incubated for 1 h in biotinylated goat anti-rabbit IgG antibody at a 1:600 dilution in BS. The sections were washed and incubated for 1 h in PBS containing 0.1% Triton X and avidin-biotin-peroxidase (Vectastain ABC kit, Vector Labs, Burlingame, CA) according to manufacturer instructions. Sections were washed and developed with diaminobenzidine (DAB) (Vector Labs, Burlingame, CA) for 6 min, rinsed twice in PBS for five min each and then washed overnight in PBS. The tissues were then mounted on Superfrost Plus slides (Fisher Scientific, Pittsburg, PA) and allowed to dry for two days before counterstaining and dehydration.

To Nissl counterstain, the slides were dipped in water 15 times, incubated in toliduline blue for 15 s, followed by 3 water washes for 30 s, each. The sections were

then dehydrated (75% ethanol, 95% ethanol containing acetic acid, 95% ethanol, 100% ethanol, 100% ethanol), cleared in xylenes and coverslipped with permount.

Stereological Analysis

For stereological analysis, the Nissl-counterstained median and dorsal raphe nuclei regions were outlined at a low magnification (4X) on a live image with the help of a mouse atlas (205). To demark the median raphe nuclei, the anterior or ventral tegmental nucleus was used to determine the most dorsal region of the median raphe nuclei, while the paramedian raphe nuclei and the tectospinal tract were used to determine the edges along the dorsal-ventral axis. The most ventral region of the median raphe nuclei was identified by locating the pericentral reticulotegmental nucleus of the pons. The slices of the median raphe nuclei used for the stereological analysis started at approximately -4.04 mm from Bregma and continued posterior to -4.96 mm from Bregma (Fig. 5.1A-K).

The landmark used to help identify the most ventral region of the dorsal raphe nuclei was the superior cerebellar peduncle and the caudal linear nucleus of the raphe. The dorsal raphe nuclei extends into the periaqueductal gray area and the aqueduct was used as a landmark to determine the dorsal boundary of the dorsal raphe nuclei. Because the 5-HT-labeled cells labeled similarly to the drawn regions of the dorsal raphe nuclei in the mouse brain atlas, 5-HT-labeled cells were also used to help determine the boundaries along the dorsal-ventral axis of the dorsal raphe nuclei. The slices used for stereological analysis of the dorsal raphe nuclei started approximately -4.04 mm from Bregma and continued until approximately -5.02 mm from Bregma. (Fig. 5.1A-K).

5-HT-labeled cells appeared brown and were easily identified (Fig. 5.1L-M). A 100X immersion oil, 1.35 numerical aperture objective was used to count cells during

stereological analysis. The stereological analysis was performed similarly to that described in (225) using a computer-assisted morphometry system consisting of an Olympus BX61 photomicroscope (Center Valley, PA) equipped with a Mac5000 Manual joystick control (Ludel Electronic Products, Hawthorne, NY), a MicroFire S99808 video camera (Optronics, Goleta, CA), a Dell microcomputer (Dimension 4550 Series, Austin, TX), Cintiq 15X screen (Wacom, Vancouver, WA), and StereoInvestigator morphometry and stereology software (MicroBrightField, Inc., Colchester, VT) for both the control and 13-*cis*-RA treated groups. The StereoInvestigator software placed dissector frames using a systematic random design within each contour outlining each region on a 90 x 90-μm^2 grid for the median raphe nuclei and a 90 x 130-μm^2 grid for the dorsal raphe nuclei. 5-HT-labeled cells were counted within 45 x 45 μm optical dissector frames on the x-/y-axis and the final post-processing thickness of each section was measured by the microcator in the StereoInvestigator program. The average height of the tissue was 15.65 μm and 5-HT-labeled cells were counted over the whole thickness. Although guard zones are often used in stereological analyses to prevent double-counting cells, most of the 5-HT labeling occurred in the tissue region closest to the edges and all tissues were counted the same way in both control and 13-*cis*-RA treated subjects, therefore the lack of guard zone should not affect the analysis.

The 5-HT-labeled cells in the median and dorsal raphe nuclei were counted as two separate categories. The neuronal number estimates were made using the optical fractionator and did not depend on a direct measurement of the volume of reference of the region considered. Therefore tissue shrinkage during histological processing should not influence the neuronal number estimates. Stereological microscope analyses were performed at high power (100X) in a live computer image.

The volumes of the median and dorsal raphe nuclei were measured by drawing the contour plot of each region at 10X and then multiplying the contour area by the total thickness of the interslice distance. Volume estimates were calculated based on postsprocessing tissues that have shrunk in all three directions. No attempts were made to correct for shrinkage because shrinkage most likely differs in the z and x-y directions. Approximately nine slices were analyzed per subject for the median raphe nuclei and 10 slices were analyzed per subject for the dorsal raphe nuclei. The observer was blinded as to which treatment group the subject belonged during the stereological analysis.

Statistical Analyses

The average neuronal number estimate, volume, and neuronal density for the median or dorsal raphe nuclei were calculated on a group basis. Two-tailed, Student's *t*-tests were performed to test for differences between vehicle control and 13-*cis*-RA treated animals in Excel (XP 2002; Microsoft). Due to poor tissue quality in some of the subjects the final number of subjects for the regions varied. For the median raphe nuclei, the analysis consisted of n = 8 and n = 10 for the control and 13-*cis*-RA treated groups, respectively. For the dorsal raphe nuclei, the control group consisted of n = 7 subjects and the 13-*cis*-RA group contained n = 10. Data are expressed as mean ± SEM.

RESULTS

13-*Cis*-RA Has No Effect on Number of 5-HT-labeled Neurons in the Median or Dorsal Raphe Nuclei

There was no difference between the estimated number of 5-HT-labeled cells in either the median ($p = 0.51$) or dorsal ($p = 0.53$) raphe nuclei between the control and 13-

cis-RA treated groups (Fig. 5.2). Control animals exhibited an estimated 1815 ± 194 5-HT-labeled cells in the median raphe nuclei while 13-*cis*-RA treated animals had and estimated 1954 ± 111 5-HT-labeled cells in the median raphe nuclei. In the dorsal raphe nuclei, the estimated number of 5-HT-labeled cells was 7148 ± 377 in the control group and 7578 ± 424 in the 13-*cis*-RA treated group (Fig. 5.2A). There was no difference in volume of the median or dorsal raphe nuclei between control and 13-*cis*-RA treated groups. The median raphe nuclei volume was 0.14 ± 0.02 mm^3 in the control group and 0.14 ± 0.01 mm^3 in the 13-*cis*-RA treated group ($p = 0.91$). In the control group, the volume of the dorsal raphe nuclei was 0.28 ± 0.02 mm^3 while the volume of the dorsal raphe nuclei was 0.29 ± 0.01 mm^3 in 13-*cis*-RA treated animals ($p = 0.42$) (Fig. 5.2 B).

The total number of 5-HT-labeled cells/mm^3 in the median raphe nuclei was not different between groups ($p = 0.34$) with the control group containing an estimated 12873 ± 743 cells/mm^3 and the 13-*cis*-RA treated group containing 14119 ± 982 cells/mm^3 (Fig. 5.2C). Lastly, the total number of 5-HT-labeled cells/mm^3 in the dorsal raphe nuclei was not different between groups ($p = 0.91$) with the control group containing 26250 ± 748 cells/mm^3 and the 13-*cis*-RA treated group containing 26040 ± 1500 cells/mm^3 (Fig. 5.2C). These data show that while 13-*cis*-RA is capable of disrupting serotonergic function, thereby leading to decreased serotonergic-hippocampal connectivity, this decreased connectivity is not due to decreased numbers of 5-HT-containing neurons in the median or dorsal raphe nuclei.

DISCUSSION

Chronic treatment with 13-*cis*-RA induces depression-related behaviors, decreases CO activity in the median raphe nuclei and uncouples the functional connectivity of the dorsal raphe nuclei and the hippocampus. The tendency for CO

activity in the median raphe nuclei and loss of functional connectivity between the dorsal raphe nuclei to the hippocampus possibly leads to decreased hippocampal neurogenesis. However, the effects of 13-*cis*-RA on the mature brain and behavior are not due to serotonergic neuronal loss in the median or dorsal raphe nuclei. There was no difference in estimated total serotonergic neuronal numbers between the control and 13-*cis*-RA treated groups for either the median or dorsal raphe nuclei. Furthermore, there was no difference in estimated volume of median or dorsal raphe nuclei between control and 13-*cis*-RA treated groups. Lastly, serotonergic neuronal density was not different between groups in either the median or dorsal raphe nuclei.

The etiology of depression remains unknown, but a current theory is that neuron loss due to apoptosis is an underlying cause of depression. Because retinoids are such well-known mediators of cell cycle, differentiation, and apoptosis (220), the apoptotic theory seems very plausible in the case of 13-*cis*-RA induced depression. Neuron loss due to apoptosis seems likely if orbitofrontal and hippocampal volumes are decreased (63, 64, 222) and glial cell numbers are reduced in depression (221, 222). It should be noted that in the case of volume reduction of the hippocampus, many of these studies report that severity of volume reduction is proportional to the length of time the subject has had depression, and is not necessarily associated with age of the patient (226). Thus, we do not know if the loss of neurons causes, or results, from depression. Perhaps in an animal model of depression it is difficult to measure neuronal cell number or volume differences due to the shorter duration of animal studies. This may especially be true if apoptosis is a result of depression.

Apoptosis in the median raphe nuclei could account for the reduction of CO activity in the median raphe nuclei if neuronal loss also resulted in reduced dendritic input into this region. Additionally, loss of serotonergic neurons in the dorsal raphe

nuclei could lead to the functional uncoupling of the dorsal raphe nuclei from the hippocampal regions. Given that denervation of the serotonergic median and dorsal raphe nuclei leads to decreased hippocampal neurogenesis (217), it seems possible that serotonergic cell loss due to 13-*cis*-RA treatment could lead to the decrease in hippocampal neurogenesis also caused by 13-*cis*-RA treatment (97). However, inhibition of 5-HT synthesis by parachloraphenylalanine leads to decreased hippocampal neurogenesis as well (148). The reduction of hippocampal neurogenesis due to inhibition of 5-HT synthesis without denervation of the serotonergic neurons implies that it is the loss of 5-HT itself, and not the loss of the neuron that decreases neurogenesis (148).

When considering the ways in which 5-HT might be reduced in the hippocampus, thereby leading to a decrease in neurogenesis, loss of 5-HT containing cell bodies due to 13-*cis*-RA treatment is only one possible mechanism. 13-*Cis*-RA is capable of increasing protein levels of 5-HT_{1A} receptor and SERT *in vitro* (197). Since the 5-HT_{1A} receptor is an autoinhibitory receptor, which prevents future firing of raphe neurons, and the SERT removes 5-HT from the synapse, increases in both of these proteins *in vivo* could lead to decreased 5-HT signaling in the hippocampus. Increases in protein levels of the 5-HT_{1A} receptor and SERT, if they were to occur *in vivo*, by 13-*cis*-RA treatment may account for the uncoupling of the functional connections between the dorsal raphe and the hippocampus observed with our CO activity assays (chapter 4). Furthermore, increases in the 5-HT_{1A} receptor and SERT may also lead to the decreased hippocampal neurogenesis observed by Crandall et al. (97). Lastly, denervation does not necessarily mean loss of the cell body, but loss of the projections to the hippocampal region. Therefore, changes in morphology of serotonergic projections within the hippocampus by 13-*cis*-RA might lead to reductions in neurogenesis.

Surprisingly, studies that have examined the effects of serotonergic denervation on depression-related behaviors have shown that denervation does not lead to increased depression-related behaviors in rats in the forced swim test (61, 62). Serotonergic denervation in these studies lasted for approximately three weeks. These negative results may imply that loss of 5-HT itself is not enough to induce depression. Moreover, the lack of depression-related behavior due to serotonergic denervation might be representative of other phenomena occurring in depression, such as the loss of feedback loops between brain regions, that take longer to occur than the three weeks of induced serotonergic denervation. Unfortunately, we don't know the exact mechanism by which 13-*cis*-RA is able to induce depression-related behaviors, but the mechanism does not appear to involve decreases in 5-HT-labeled neurons or volume changes in the median and dorsal raphe nuclei.

ACKNOWLEDGEMENTS

I would like to thank Dr. Andrea Gore for her help in learning the stereological techniques and for the use of her stereological equipment. I would also like to thank Weiling Yin and Di Wu for technical assistance. This research was supported by a Roaccutane Research Grant (M.L.) and a NIEHS toxicology training grant (T32 ES007247, K.O.).

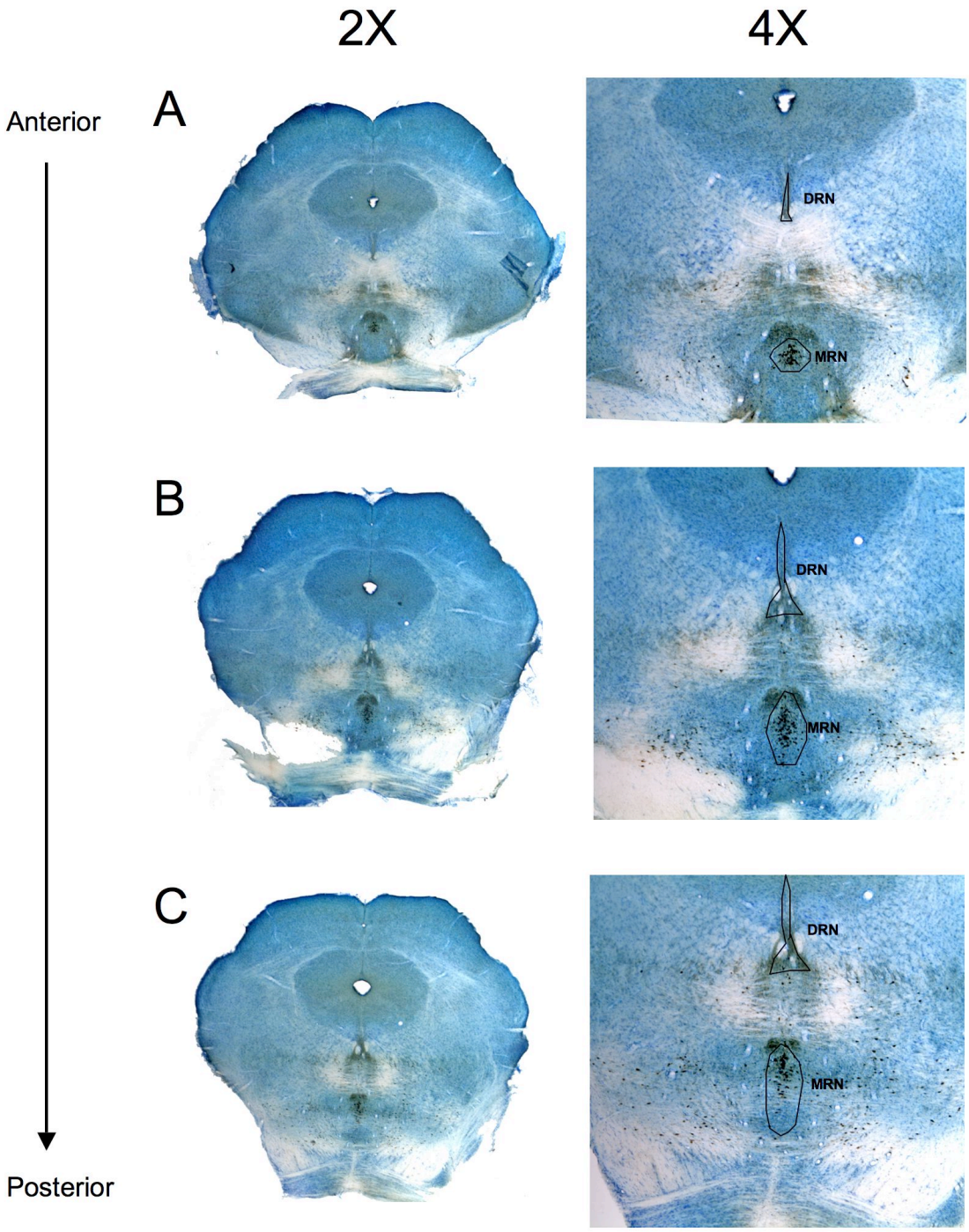
2X
4X
Anterior
A
DRN
MRN
B
DRN
MRN
C
DRN
MRN
Posterior

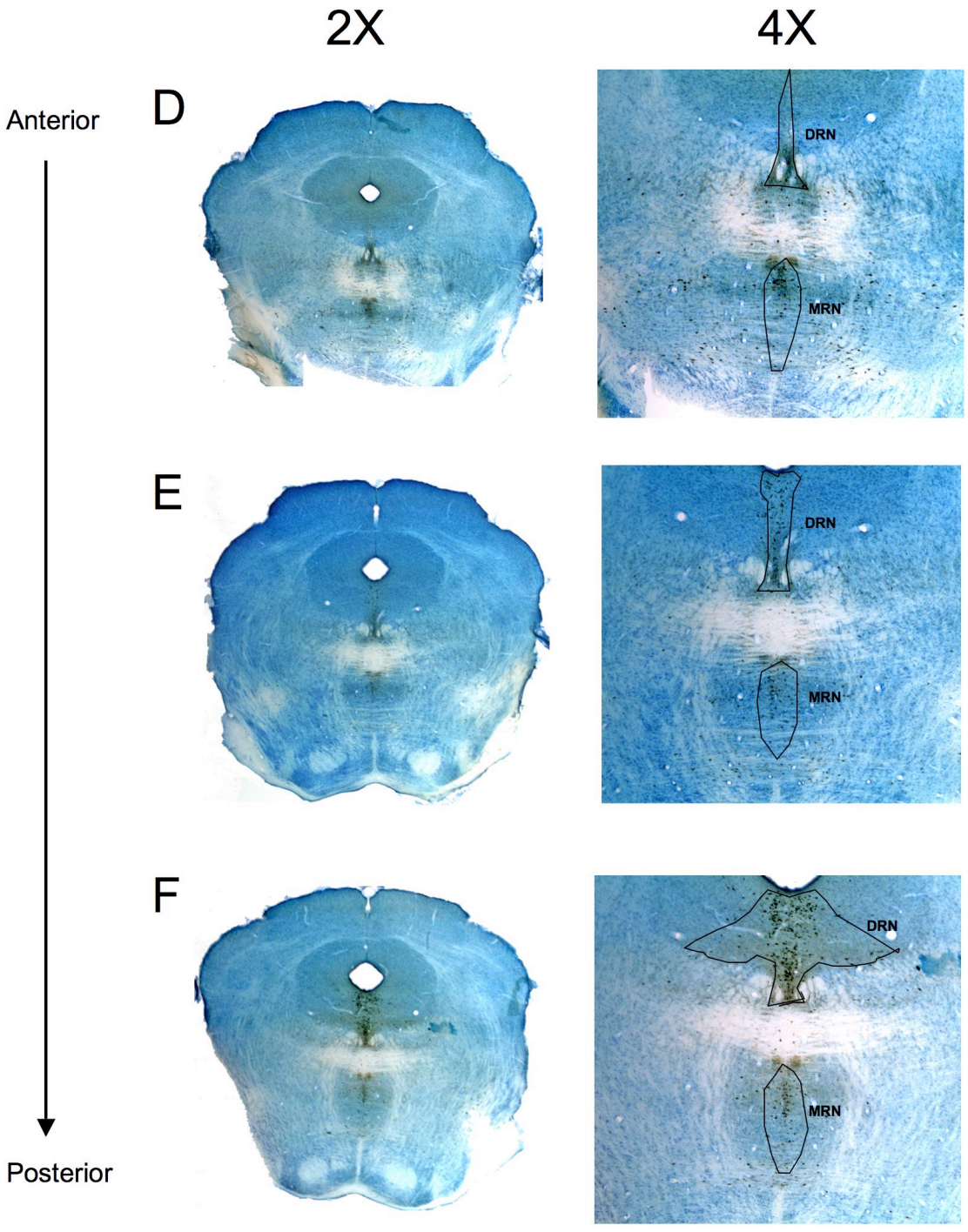
2X
4X
Anterior
D
DRN
MRN
E
DRN
MRN
F
DRN
MRN
Posterior

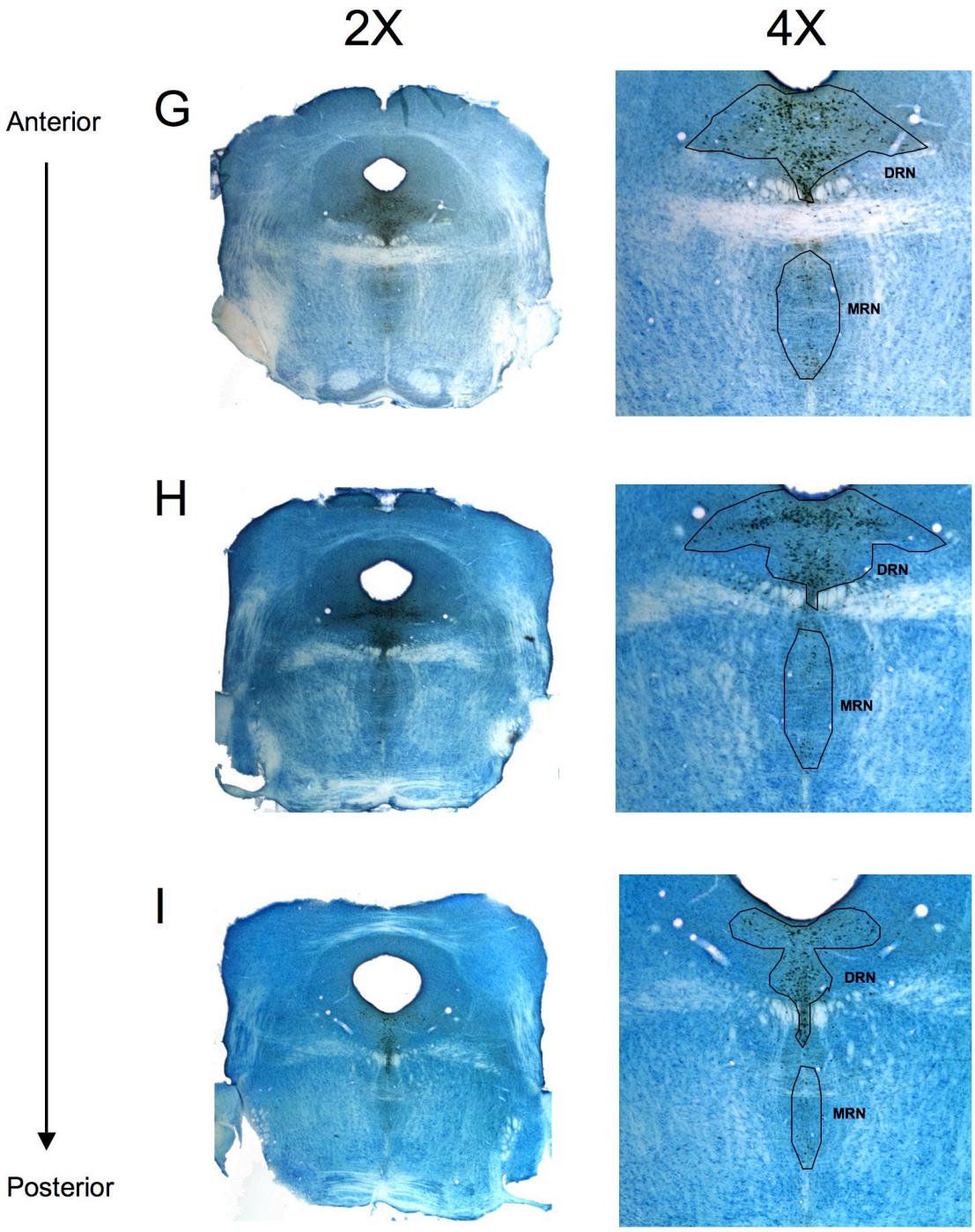
2X
4X
Anterior
G
DRN
MRN
H
DRN
MRN
I
DRN
MRN
Posterior

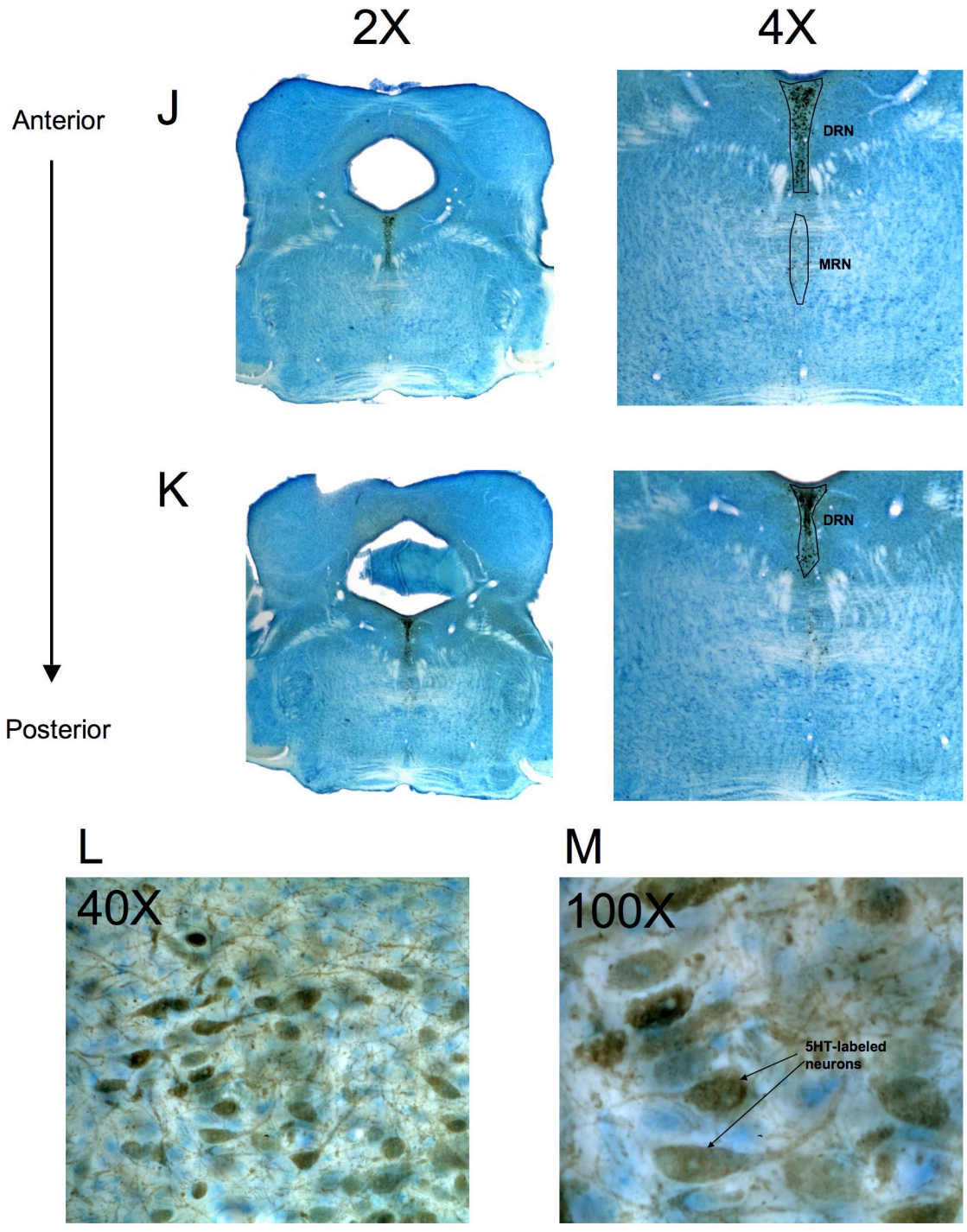
2X
4X
Anterior
J
DRN
MRN
K
DRN
Posterior
L
40X
M
100X
5HT-labeled
neurons

Figure 5.1: Photomicrographs of 5-HT-labeled/Nissl stained tissue sections used for stereology for the dorsal raphe nuclei and the median raphe nuclei.

A-K Serial sections from the mouse brain taken for stereology. Sections were from a 1:3 series and are immunoreactive for 5-HT. They were Nissl stained to help identify the median and dorsal raphe nuclei. The 4X photomicrographs have representative contour plots drawn on them to show the boundaries of the regions examined. MRN = median raphe nuclei. DRN = dorsal raphe nuclei. **L-M** Higher power magnification (40X and 100X respectively) of 5-HT-labeled dorsal raphe nuclei tissue to show a representative density and ability to identify 5-HT-labeled neurons.

A

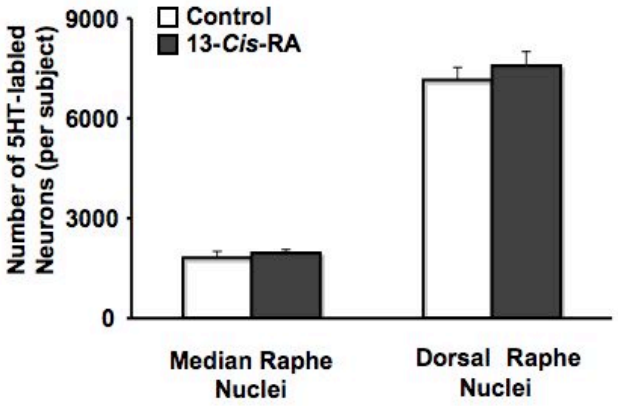
Control
13-Cis-RA
Number of 5HT-labled Neurons (per subject)
9000
6000
3000
0
Median Raphe Nuclei
Dorsal Raphe Nuclei

B

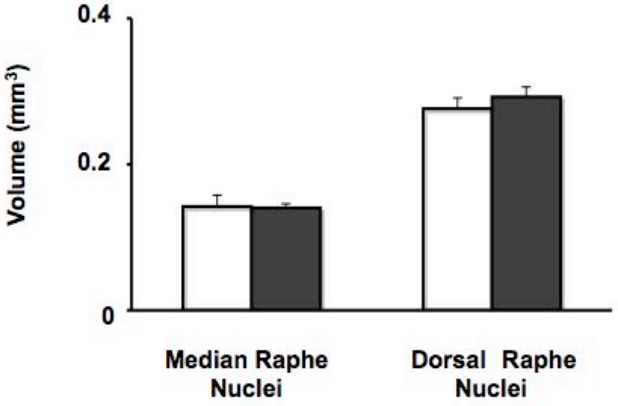
Volume (mm3)
0.4
0.2
0
Median Raphe Nuclei
Dorsal Raphe Nuclei

C

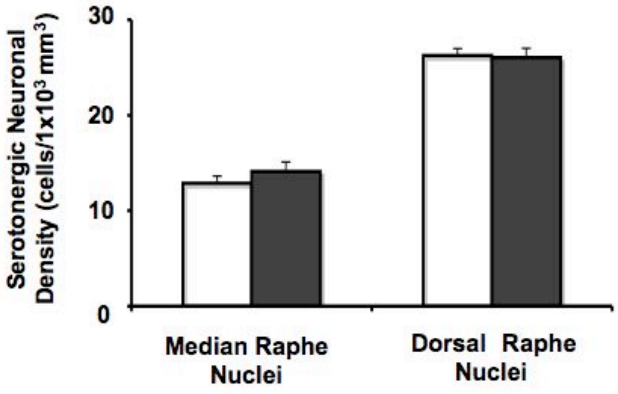
Serotonergic Neuronal Density (cells/1x10³ mm³)
30
20
10
0
Median Raphe Nuclei
Dorsal Raphe Nuclei

Figure 5.2: 13-*Cis*-RA has no effect on the number of serotonergic neurons or the volume of the median or dorsal raphe nuclei.

Stereology was performed on 40 μm slices taken from a 1:3 series over the median and dorsal raphe nuclei to determine **(A)** number of 5-HT-labeled neurons, **(B)** volume, and **(C)** serotonergic neuron density.

Chapter 6: Summary, Future work, and Conclusions

SUMMARY

13-*Cis*-RA is a known teratogen and the role of 13-*cis*-RA, as well as many other retinoids, in development is widely studied. However, there are significantly fewer studies concerning the effects of 13-*cis*-RA and other retinoids on the adult central nervous system. Additionally, although the medical literature suggests that 13-*cis*-RA can cause depression, whether or not 13-*cis*-RA can cause depression has remained controversial. Case studies have reported that onset of depressive symptoms can occur after initiation of 13-*cis*-RA treatment and these symptoms are relieved after cessation of the drug treatment (80). Additionally, some cases have reported that depressive symptoms can reoccur with 13-*cis*-RA rechallenge (81). Perhaps this should be enough evidence that 13-*cis*-RA can cause depression, but only approximately 8% of the population that takes 13-*cis*-RA become depressed (78).

The research discussed within this dissertation has shown, most notably, that 13-*cis*-RA can induce depression-related behaviors. In our behavioral studies, immobility in the tail suspension and forced swim tests was used as a measure of depression-related behaviors (173). Chronic 13-*cis*-RA administration to adolescent male mice increased immobility in both the tail suspension and forced swim tests. Importantly, the increased immobility due to 13-*cis*-RA treatment was not due to decreased motor function or coordination. 13-*Cis*-RA treated animals exhibited the same amount of total mobility in the open field as controls. In addition, 13-*cis*-RA treated animals tended to perform better in the rotarod test at low rotational speeds. Although our method of measuring retinoids did not discriminate between ATRA and 13-*cis*-RA, serum levels of total

retinoids were found to be higher in 13-*cis*-RA treated animals, consistent with human patient data available.

Of the neuronal networks currently thought to be involved in depression, the serotonergic system, which is commonly targeted by antidepressants, appears to be a target of 13-*cis*-RA. *In vitro*, 13-*cis*-RA can increase intracellular levels of 5-HT and 5-HIAA, the metabolite of 5-HT, and can increase protein levels of the 5-HT_{1A} autoinhibitory receptor and SERT (197). The 5-HT_{1A} autoreceptor located on the raphe nuclei acts as an inhibitory receptor that, when activated by 5-HT, leads to inhibition of raphe nuclei firing. SERT transports 5-HT from the synaptic cleft back into the raphe nuclei, therefore terminating 5-HT signaling once the neuron has fired. Ultimately, increases in the 5-HT_{1A} and SERT proteins, if they occurred *in vivo*, would reduce serotonergic neuronal firing.

Chapter 4 shows that, *in vivo*, 13-*cis*-RA treatment tends to decrease CO activity, a measure of neuronal firing, in the median raphe nuclei. We do not know if the tendency for 13-*cis*-RA to decrease median raphe nuclei activity is due to increases in 5-HT_{1A} receptor or SERT levels. Increased 5-HT_{1A} and SERT proteins *in vivo* might have greater impact at the terminal sites of serotonergic neurotransmission rather than on the cell bodies themselves. Thus, should increases in 5-HT_{1A} receptors and SERT occur *in vivo*, activity of 5-HT_{1A} and SERT at the terminals of serotonergic dendrites may be responsible for the uncoupling of functional connectivity between the dorsal raphe nuclei and the hippocampal regions.

Not only does the dorsal raphe nuclei become uncoupled from the hippocampus, but it also loses some connectivity to the lateral habenula, a major regulator of monoamine function. Although there are no direct connections between the lateral habenula and the hippocampus, there are indirect connections between the lateral

habenula and the hippocampus through the dorsal raphe nuclei. In fact, one pathway by which the lateral habenula may control the hippocampus is through inhibitory effects on the dorsal raphe nuclei. 13-*Cis*-RA treatment disrupts this pathway, perhaps forcing another pathway of habenula → hippocampal control to compensate.

The uncoupling of functional connectivity between the dorsal raphe nuclei and the hippocampus due to 13-*cis*-RA treatment may also be reflective of decreased hippocampal neurogenesis due to 13-*cis*-RA, such as was observed in young adult mice by Crandall et al. (97). Only in the 13-*cis*-RA treated animals, where neurogenesis is expected to be decreased, did a lower CO activity in the dentate gyrus strongly predict increased total immobility in the tail suspension and forced swim tests. Thus, the more the dentate gyrus CO activity is decreased by 13-*cis*-RA, the greater the immobility the animal will exhibit.

Because retinoids have the ability to induce apoptosis, we hypothesized that decreased CO activity in the median raphe nuclei could simply be due to neuron loss. Furthermore, because 5-HT has a role in maintaining neurogenesis, removal of 5-HT could contribute to the decreased neurogenesis by 13-*cis*-RA treatment and removal of 5-HT from the hippocampus would also be accomplished by cell loss. However, this was not the case as 13-*cis*-RA had no effect on total number of 5-HT-labeled neurons in either the median or dorsal raphe nuclei; nor did 13-*cis*-RA affect the volume of the median or dorsal raphe nuclei. The stereological study performed here does not discount the fact that 13-*cis*-RA may have an effect on number of serotonergic inputs into the hippocampus. Decreased dendritic input into the hippocampus could also decrease serotonergic signaling and therefore reduce neurogenesis. Dendritic loss may also account for decreased functional connectivity between the dorsal raphe nucleus and the hippocampus. However, in reality, the effects of 13-*cis*-RA on the serotonergic system

and the hippocampus are probably a combination of morphological changes and increases in 5-HT_{1A} receptor and SERT levels as well as other mechanisms leading to decreased hippocampal neurogenesis.

Although the work in this dissertation focused on the serotonergic system, other monoaminergic systems are known to be involved in depression and it is possible for these other monoaminergic systems to be targeted by 13-*cis*-RA, as mentioned in chapter 1. Table 6.1 summarizes all the effects of retinoids on behavior and the monoaminergic systems. However, other studies have pointed toward the disruption of the serotonergic system by retinoids as well. Ferguson et al. (39) showed there was an apparent increase in 5-HT and 5-HIAA levels in the striatum of adult male rats administered 13-*cis*-RA. Additionally, mice fed a vitamin A deficient diet for 4 weeks tended to have lower levels of 5-HT in striatal tissue homogenate (40). Given all this information, it appears as though 13-*cis*-RA may be targeting the serotonergic and hippocampal systems. Disruptions of the serotonergic system by 13-*cis*-RA may lead to, or even result from, decreased hippocampal neurogenesis. Furthermore, decreases in serotonergic signaling and hippocampal neurogenesis, and the uncoupling of these two systems, by 13-*cis*-RA administration may cause depression-related behavior. Surprisingly, the increases in 5-HT_{1A} and SERT by 13-*cis*-RA *in vitro* were not due to increased transcription, and therefore, the effects of 13-*cis*-RA on the mature brain may not be occurring via the traditional RAR-mediated manner. Figure 6.1 summarizes the effects of 13-*cis*-RA on the adolescent brain as observed here and by others, proposing a mechanism by which retinoids could induce depression.

FUTURE WORK

Of the many future directions that this study could take, the first study that comes to mind is to define the timeline for which 13-*cis*-RA administration induces depression-related behaviors. Additionally, because it is currently unknown if decreased hippocampal neurogenesis is a cause or a result of depression, insight could be gained by determining if depression-related behaviors are induced prior to, or after hippocampal neurogenesis is decreased. Furthermore, the timing at which the dorsal raphe nuclei becomes uncoupled from the hippocampal structures should be examined. Examining the uncoupling of these two regions, via CO activity and correlations, may advance understanding concerning the underlying structures and functions of each region of the hippocampus in relation to the serotonergic systems. For instance, if decreased serotonergic signaling is leading to a reduction in neurogenesis in the dentate gyrus, the dentate gyrus may become functionally uncoupled from the dorsal raphe nuclei before the CA1 and CA3 regions do.

Due to the fact that 13-*cis*-RA leads to an increase in 5-HT_{1A} and SERT proteins *in vitro*, it is relevant to investigate the effect of 13-*cis*-RA on these two proteins *in vivo*. Fluorescent co-labeling of tissues with antibodies directed toward the 5-HT_{1A} and SERT would be useful in identifying the autoinhibitory 5-HT_{1A} receptors on the raphe nuclei themselves. Since SERT is primarily located on serotonergic neurons, SERT would be used to identify presynaptic 5-HT_{1A} receptors on co-labeled synapses. It is expected that there would be increased 5-HT_{1A} receptors and SERT in the median and dorsal raphe nuclei as well as on the raphe nuclei terminals in the raphe nuclei projection sites such as the prefrontal cortex and in the hippocampus.

Additionally, electrophysiology recordings could be used to validate the disruption of the lateral habenula → dorsal raphe nuclei → hippocampus pathway by 13-

cis-RA. Electrophysiology could also verify that the median raphe nuclei has reduced firing activity due to 13-*cis*-RA treatment. However, the electrophysiology techniques would be very difficult to perform in a mouse and validation of the findings in this dissertation would need to be performed in a rat in order to do these recordings. Validation in a rat model would also yield interesting information and insight. Given that the adult rats in the studies conducted by Ferguson et al. (98) did not have induced depression-related behaviors, if adolescent rats administered 1 mg/kg/day of 13-*cis*-RA via i.p. injection displayed induced depression-related behaviors, it may be because the method of drug administration or the age is important to the induction of depression-related behaviors. To determine the influence of age on the ability of 13-*cis*-RA to cause depression-related behaviors, both adolescent and adult rats would need to be tested. In fact, our collaborator, Dr. Sarah J Bailey at Bath University, Bath, UK, is conducting these studies. Understanding the influence of 13-*cis*-RA on the components of the serotonergic system as well as the uncoupling of the serotonergic system from the hippocampus, and the age at which an animal is susceptible to these events would offer great insight into the etiology of depression.

CONCLUSIONS

Perhaps the predominant remaining question of this study is, if 13-*cis*-RA can induce depression, why do only 8% of the patients that are treated with Accutane have depressive symptoms, become depressed, or have thoughts of suicide? This question is probably answered by susceptibility to depression in the general population or a genetic background predisposing a person to depression. Tryptophan depletion studies have shown that depleting tryptophan in a normal human does not cause depression (60). However, depleting tryptophan in the diet of remitted depressed patients can lead to the

recurrence of depressive symptoms in these patients (59). Furthermore, tryptophan depletion has mood lowering effects in people who have a family history of depression, even if the person has not been depressed himself (56) and in people with the short allele SERT polymorphism, even if they have not experienced depression (227). It seems, then, that if 13-*cis*-RA is indeed affecting the serotonergic system, there may exist a human subpopulation, such as people with polymorphisms in the 5-HT_{1A} receptor or SERT gene, that is susceptible to becoming depressed while taking Accutane.

Although these experiments, to the general public, may seem like an investigation into the potential side-effects of a drug, examining the mechanisms by which 13-*cis*-RA induces depression-related behaviors may yield greater understanding into the underlying etiology and potential treatments of depression. Since depression is a serious, debilitating disease, the use of pharmacological drugs that could induce depression should be carefully administered and patients taking them should be monitored closely. This study also brings to light the need to perform behavioral assessments on drugs prior to clinical trials, especially if the drug is intended to treat non-life threatening conditions.

Table 6.1. Effect of retinoid deficiency and excess on behavior, cellular, and monoaminergic systems

System	Retinoid Deficiency	Retinoid Excess
Behavioral	↓ Depression (28)	↑ Depression (110, 173)
	↓ Anxiety (28)	↑ Anxiety (107, 110)
		↑ Irritability (107, 110)
	↓ Spatial learning (121, 147)	↓ Spatial learning (97)
Cellular		
Energy Metabolism	N/D	↓ Orbitofrontal cortical glucose metabolism (94)
		↓Coupling of the dorsal raphe nuclei from the hippocampus
Neurogenesis	N/D	↓ Hippocampal neurogenesis (97)
Monoamine Systems		
Norepinephrinergic	↑ Limbic NE (28)	N/D
Serotonergic	↓Striatal 5-HT and 5-HIAA (40)	↑ Striatal 5-HT and 5-HIAA (39)
		↑ Intracellular 5-HT, 5-HT1A, and SERT (197)
Dopaminergic	↓Striatal DA and DOPAC (40)	↑ Tyrosine hydroxylase (37)
		↑ Monoamine oxidase B (38)
		↑ Striatal homovanillic acid (39)

N/D = Not Determined
Yellow highlights indicate findings that were contributed by the work in this dissertation.

A. **Control**

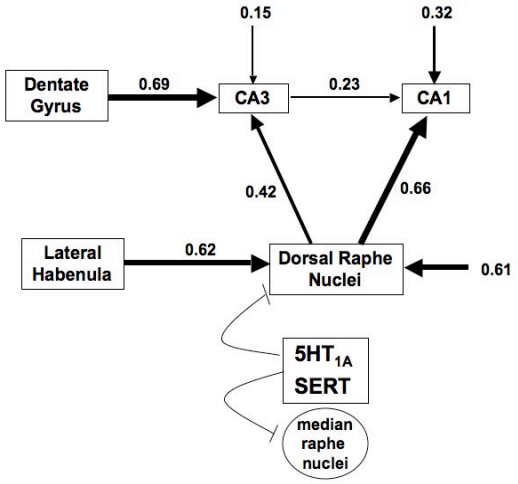

B. **13-*Cis*-RA**

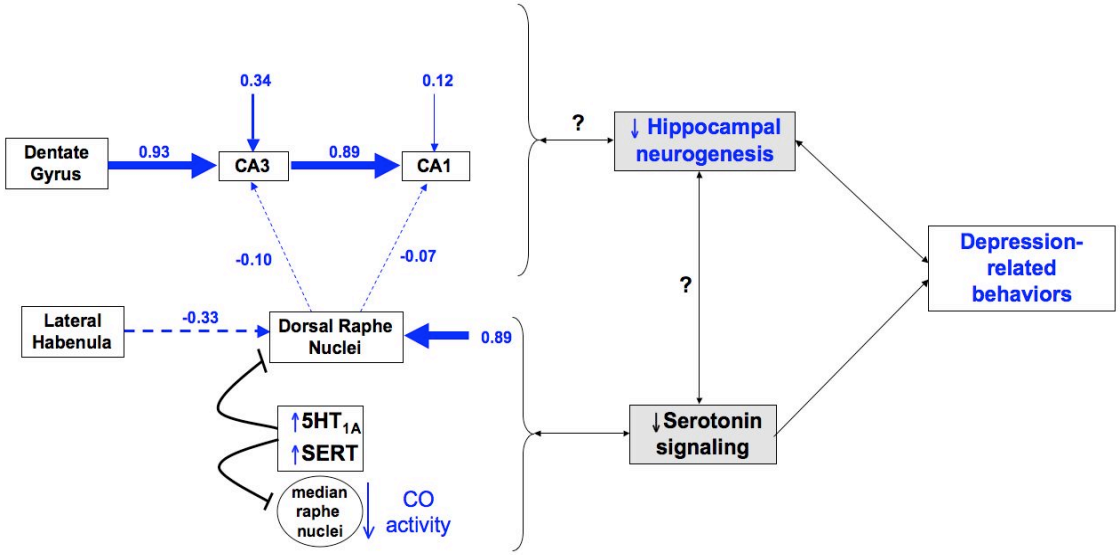

Figure 6.1: Summary of the effects of retinoids leading to depression-related behavior.

Solid lines between brain regions represent positive correlations or path coefficients while dashed lines represent negative correlations or path coefficients. **(A)** In control animals, the serotonergic system is coupled to the hippocampal regions and the lateral habenula is connected to the hippocampus via the dorsal raphe nuclei. **(B)** Known changes due to retinoids measured either *in vivo* or *in vitro* are represented in blue. Yellow highlights indicate changes that were discovered through the work discussed in this dissertation. Although the 5-HT_{1A} receptor and SERT are present in untreated animals to maintain appropriate control of the raphe nuclei, 13-*cis*-RA might increase the 5-HT1A receptor and SERT levels *in vivo*, as it does *in vitro*, causing increased suppression of the serotonergic system. Furthermore, decreased raphe nuclei activity may be uncoupling the dorsal raphe nuclei from the hippocampal regions. Ultimately, 13-*cis*-RA may be decreasing serotonergic function and hippocampal neurogenesis. Decreased hippocampal neurogenesis may, in part, result from decreased serotonergic signaling. Decreased serotonergic signaling and/or decreased neurogenesis due to 13-*cis*-RA may induce depression-related behaviors.

References

1. Vogel S, Gamble MV, Blaner WS. Biosynthesis, absorption, metabolism and transport of retinoids. In: Nau H, Blaner WS, Eds. Retinoids: the biochemical and molecular basis of vitamin A and retinoid action. Berlin Heidelberg: Springer-Verlag, p31-95, 1999.

2. White JA, Beckett-Jones B, Guo YD, Dilworth FJ, Bonasoro J, Jones G, Petkovich M. cDNA cloning of human retinoic acid-metabolizing enzyme (hP450RAI) identifies a novel family of cytochromes P450. The Journal of biological chemistry 272:18538-18541, 1997.

3. Noy N, Slosberg E, Scarlata S. Interactions of retinol with binding proteins: studies with retinol-binding protein and with transthyretin. Biochemistry 31:11118-11124, 1992.

4. Moise AR, Noy N, Palczewski K, Blaner WS. Delivery of retinoid-based therapies to target tissues. Biochemistry 46:4449-4458, 2007.

5. Kurlandsky SB, Gamble MV, Ramakrishnan R, Blaner WS. Plasma delivery of retinoic acid to tissues in the rat. The Journal of biological chemistry 270:17850-17857, 1995.

6. Roche. Accutane (isotretinoin) capsules: complete product information, 2005.

7. O'Donnell J. Overview of existing research and information linking isotretinoin (accutane), depression, psychosis, and suicide. American journal of therapeutics 10:148-159, 2003.

8. Kerr IG, Lippman ME, Jenkins J, Myers CE. Pharmacology of 13-cis-retinoic acid in humans. Cancer research 42:2069-2073, 1982.

9. Tsukada M, Schroder M, Roos TC, Chandraratna RA, Reichert U, Merk HF, Orfanos CE, Zouboulis CC. 13-cis retinoic acid exerts its specific activity on human sebocytes through selective intracellular isomerization to all-trans retinoic acid and binding to retinoid acid receptors. The Journal of investigative dermatology 115:321-327, 2000.

10. Idres N, Marill J, Flexor MA, Chabot GG. Activation of retinoic acid receptor-dependent transcription by all-trans-retinoic acid metabolites and isomers. The Journal of biological chemistry 277:31491-31498, 2002.

11. Landthaler M, Kummermehr J, Wagner A, Plewig G. Inhibitory effects of 13-cis-retinoic acid on human sebaceous glands. Archives of dermatological research 269:297-309, 1980.

12. Strauss JS, Stranieri AM, Farrell LN, Downing DT. The effect of marked inhibition of sebum production with 13cis-retinoic acid on skin surface lipid composition. The Journal of investigative dermatology 74:66-67, 1980.

13. Nelson AM, Gilliland KL, Cong Z, Thiboutot DM. 13-cis Retinoic acid induces apoptosis and cell cycle arrest in human SEB-1 sebocytes. The Journal of investigative dermatology 126:2178-2189, 2006.

14. Motomura K, Mitsuru O, Satre M, Tsukamoto H. Destabilization of TNF-alpha mRNA by retinoic acid in hepatic macrophages: implications for alcoholic liver disease. Am J Physiol Endocrinol Metab 281:E420-E429, 2001.

15. Crowe D. Retinoic acid mediates post-transcriptional regulation of keratin 19 mRNA levels. J Cell Sci 106:183-188, 1993.

16. Qin P, Haberbusch J, Soprano D, Soprano K. Retinoic acid regulates the expression of PBX1, PBX2, and PBX3 in P19 cells both transcriptionally and post-translationally. J Cell Biochem 92:147-163, 2004.

17. Werner EA, Deluca HF. Retinoic acid is detected at relatively high levels in the CNS of adult rats. American journal of physiology 282:E672-678, 2002.

18. Connor MJ, Sidell N. Retinoic acid synthesis in normal and Alzheimer diseased brain and human neural cells. Molecular and chemical neuropathology / sponsored by the International Society for Neurochemistry and the World Federation of Neurology and research groups on neurochemistry and cerebrospinal fluid 30:239-252, 1997.

19. McCaffery P, Drager UC. High levels of a retinoic acid-generating dehydrogenase in the meso-telencephalic dopamine system. Proc Natl Acad Sci U S A 91:7772-7776, 1994.

20. Dev S, Adler AJ, Edwards RB. Adult rabbit brain synthesizes retinoic acid. Brain research 632:325-328, 1993.

21. Zetterstrom RH, Lindqvist E, Mata de Urquiza A, Tomac A, Eriksson U, Perlmann T, Olson L. Role of retinoids in the CNS: differential expression of retinoid binding proteins and receptors and evidence for presence of retinoic acid. The European journal of neuroscience 11:407-416, 1999.

22. Krezel W, Kastner P, Chambon P. Differential expression of retinoid receptors in the adult mouse central nervous system. Neuroscience 89:1291-1300, 1999.

23. White JA, Ramshaw H, Taimi M, Stangle W, Zhang A, Everingham S, Creighton S, Tam SP, Jones G, Petkovich M. Identification of the human cytochrome P450, P450RAI-2, which is predominantly expressed in the adult cerebellum and is responsible for all-trans-retinoic acid metabolism. Proc Natl Acad Sci U S A 97:6403-6408, 2000.

24. Samad TA, Krezel W, Chambon P, Borrelli E. Regulation of dopaminergic pathways by retinoids: activation of the D2 receptor promoter by members of the retinoic acid receptor-retinoid X receptor family. Proceedings of the National Academy of Sciences of the United States of America 94:14349-14354, 1997.

25. Zigova T, Barroso LF, Willing AE, Saporta S, McGrogan MP, Freeman TB, Sanberg PR. Dopaminergic phenotype of hNT cells in vitro. Brain Res Dev Brain Res 122:87-90, 2000.

26. Cervini R, Berrard S, Bejanin S, Mallet J. Regulation by CDF/LIF and retinoic acid of multiple ChAT mRNAs produced from distinct promoters. Neuroreport 5:1346-1348, 1994.

27. Maas JW, Fawcett JA, Dekirmenjian H. Catecholamine metabolism, depressive illness, and drug response. Archives of general psychiatry 26:252-262, 1972.

28. Sousa JC, Grandela C, Fernandez-Ruiz J, de Miguel R, de Sousa L, Magalhaes AI, Saraiva MJ, Sousa N, Palha JA. Transthyretin is involved in depression-like behaviour and exploratory activity. J Neurochem 88:1052-1058, 2004.

29. Naranjo CA, Tremblay LK, Busto UE. The role of the brain reward system in depression. Progress in neuro-psychopharmacology & biological psychiatry 25:781-823, 2001.

30. Nestler EJ, Carlezon WA, Jr. The mesolimbic dopamine reward circuit in depression. Biol Psychiatry 59:1151-1159, 2006.

31. Maj J, Dziedzicka-Wasylewska M, Rogoz R, Rogoz A. Antidepressant drugs given repeatedly change the binding of the dopamine D2 receptors agonist [3H]N-0437, to dopamine D2 receptors in the rat brain. Eur J Pharmacol 304:49-54, 1996.

32. Valdenaire O, Maus-Moatti M, Vincent JD, Mallet J, Vernier P. Retinoic acid regulates the developmental expression of dopamine D2 receptor in rat striatal primary cultures. J Neurochem 71:929-936, 1998.

33. Dziedzicka-Wasylewska M, Solich J. Neuronal cell lines transfected with the dopamine D2 receptor gene promoter as a model for studying the effects of antidepressant drugs. Brain Res Mol Brain Res 128:75-82, 2004.

34. Krezel W, Ghyselinck N, Samad TA, Dupe V, Kastner P, Borrelli E, Chambon P. Impaired locomotion and dopamine signaling in retinoid receptor mutant mice. Science 279:863-867, 1998.

35. Kobayashi M, Matsuoka I, Kurihara K. Cholinergic differentiation of cultured sympathetic neurons induced by retinoic acid. Induction of choline acetyltransferase-mRNA and suppression of tyrosine hydroxylase-mRNA levels. FEBS letters 337:259-264, 1994.

36. Berrard S, Faucon Biguet N, Houhou L, Lamouroux A, Mallet J. Retinoic acid induces cholinergic differentiation of cultured newborn rat sympathetic neurons. J Neurosci Res 35:382-389, 1993.

37. Jeong H, Kim MS, Kim SW, Kim KS, Seol W. Regulation of tyrosine hydroxylase gene expression by retinoic acid receptor. J Neurochem 98:386-394, 2006.

38. Nicotra A, Falasca L, Senatori O, Conti Devirgiliis L. Monoamine oxidase A and B activities in embryonic chick hepatocytes: differential regulation by retinoic acid. Cell Biochem Funct 20:87-94, 2002.

39. Ferguson SA, Cisneros FJ, Gough BJ, Ali SF. Four weeks of oral isotretinoin treatment causes few signs of general toxicity in male and female Sprague-Dawley rats. Food Chem Toxicol 43:1289-1296, 2005.

40. Kitaoka K, Hattori A, Chikahisa S, Miyamoto KI, Nakaya Y, Sei H. Vitamin A deficiency induces a decrease in EEG delta power during sleep in mice. Brain Res 1150C:121-130, 2007.

41. Kessler RC, Chiu WT, Demler O, Merikangas KR, Walters EE. Prevalence, severity, and comorbidity of 12-month DSM-IV disorders in the National Comorbidity Survey Replication. Archives of general psychiatry 62:617-627, 2005.

42. Benmansour S, Cecchi M, Morilak DA, Gerhardt GA, Javors MA, Gould GG, Frazer A. Effects of chronic antidepressant treatments on serotonin transporter function, density, and mRNA level. J Neurosci 19:10494-10501, 1999.

43. Cryan JF, Mombereau C, Vassout A. The tail suspension test as a model for assessing antidepressant activity: review of pharmacological and genetic studies in mice. Neuroscience and biobehavioral reviews 29:571-625, 2005.

44. Cryan JF, Markou A, Lucki I. Assessing antidepressant activity in rodents: recent developments and future needs. Trends in pharmacological sciences 23:238-245, 2002.

45. Dalla C, Antoniou K, Papadopoulou-Daifoti Z, Balthazart J, Bakker J. Oestrogen-deficient female aromatase knockout (ArKO) mice exhibit depressive-like symptomatology. The European journal of neuroscience 20:217-228, 2004.

46. Alcaro A, Cabib S, Ventura R, Puglisi-Allegra S. Genotype- and experience-dependent susceptibility to depressive-like responses in the forced-swimming test. Psychopharmacology 164:138-143, 2002.

47. Singewald N, Sinner C, Hetzenauer A, Sartori SB, Murck H. Magnesium-deficient diet alters depression- and anxiety-related behavior in mice--influence of desipramine and Hypericum perforatum extract. Neuropharmacology 47:1189-1197, 2004.

48. Carlezon WA, Pliakas AM, Parow AM, Detke MJ, Cohen BM, Renshaw PF. Antidepressant-like effects of cytidine in the forced swim test in rats. Biol Psychiatry 51:882-889, 2002.

49. Cryan JF, Hoyer D, Markou A. Withdrawal from chronic amphetamine induces depressive-like behavioral effects in rodents. Biol Psychiatry 54:49-58, 2003.

50. Do-Rego JC, Chatenet D, Orta MH, Naudin B, Le Cudennec C, Leprince J, Scalbert E, Vaudry H, Costentin J. Behavioral effects of urotensin-II centrally administered in mice. Psychopharmacology 183:103-117, 2005.

51. Dunn AJ, Swiergiel AH. Effects of interleukin-1 and endotoxin in the forced swim and tail suspension tests in mice. Pharmacology, biochemistry, and behavior 81:688-693, 2005.

52. Azmitia EC, Segal M. An autoradiographic analysis of the differential ascending projections of the dorsal and median raphe nuclei in the rat. The Journal of comparative neurology 179:641-667, 1978.

53. Molliver ME. Serotonergic neuronal systems: what their anatomic organization tells us about function. Journal of clinical psychopharmacology 7:3S-23S, 1987.

54. Benkelfat C, Ellenbogen MA, Dean P, Palmour RM, Young SN. Mood-lowering effect of tryptophan depletion. Enhanced susceptibility in young men at genetic risk for major affective disorders. Archives of general psychiatry 51:687-697, 1994.

55. Klaassen T, Riedel WJ, van Someren A, Deutz NE, Honig A, van Praag HM. Mood effects of 24-hour tryptophan depletion in healthy first-degree relatives of patients with affective disorders. Biological psychiatry 46:489-497, 1999.

56. van der Veen FM, Evers EA, Deutz NE, Schmitt JA. Effects of acute tryptophan depletion on mood and facial emotion perception related brain activation and performance in healthy women with and without a family history of depression. Neuropsychopharmacology 32:216-224, 2007.

57. Smith KA, Fairburn CG, Cowen PJ. Relapse of depression after rapid depletion of tryptophan. Lancet 349:915-919, 1997.

58. Moreno FA, Gelenberg AJ, Heninger GR, Potter RL, McKnight KM, Allen J, Phillips AP, Delgado PL. Tryptophan depletion and depressive vulnerability. Biological psychiatry 46:498-505, 1999.

59. Neumeister A, Nugent AC, Waldeck T, Geraci M, Schwarz M, Bonne O, Bain EE, Luckenbaugh DA, Herscovitch P, Charney DS, Drevets WC. Neural and behavioral responses to tryptophan depletion in unmedicated patients with remitted major depressive disorder and controls. Archives of general psychiatry 61:765-773, 2004.

60. Schmitt JA, Jorissen BL, Sobczak S, van Boxtel MP, Hogervorst E, Deutz NE, Riedel WJ. Tryptophan depletion impairs memory consolidation but improves focussed attention in healthy young volunteers. Journal of psychopharmacology (Oxford, England) 14:21-29, 2000.

61. Haidkind R, Eller M, Kask A, Harro M, Rinken A, Oreland L, Harro J. Increased behavioural activity of rats in forced swimming test after partial denervation of serotonergic system by parachloroamphetamine treatment. Neurochemistry international 45:721-732, 2004.

62. Rosenbrock H, Bloching A, Weiss C, Borsini F. Partial serotonergic denervation decreases progenitor cell proliferation in the adult rat hippocampus, but has no effect on rat behavior in the forced swimming test. Pharmacology, biochemistry, and behavior 80:549-556, 2005.

63. Sheline YI, Wang PW, Gado MH, Csernansky JG, Vannier MW. Hippocampal atrophy in recurrent major depression. Proc Natl Acad Sci U S A 93:3908-3913, 1996.

64. Bremner JD, Narayan M, Anderson ER, Staib LH, Miller HL, Charney DS. Hippocampal volume reduction in major depression. Am J Psychiatry 157:115-118, 2000.

65. Shah PJ, Ebmeier KP, Glabus MF, Goodwin GM. Cortical grey matter reductions associated with treatment-resistant chronic unipolar depression. Controlled magnetic resonance imaging study. Br J Psychiatry 172:527-532, 1998.

66. Sapolsky RM. Glucocorticoids and hippocampal atrophy in neuropsychiatric disorders. Archives of general psychiatry 57:925-935, 2000.

67. Malberg JE, Eisch AJ, Nestler EJ, Duman RS. Chronic antidepressant treatment increases neurogenesis in adult rat hippocampus. J Neurosci 20:9104-9110, 2000.

68. Castren E, Voikar V, Rantamaki T. Role of neurotrophic factors in depression. Current opinion in pharmacology 7:18-21, 2007.

69. Duman RS, Monteggia LM. A neurotrophic model for stress-related mood disorders. Biol Psychiatry 59:1116-1127, 2006.

70. Peyron C, Petit JM, Rampon C, Jouvet M, Luppi PH. Forebrain afferents to the rat dorsal raphe nucleus demonstrated by retrograde and anterograde tracing methods. Neuroscience 82:443-468, 1998.

71. Herkenham M, Nauta WJ. Efferent connections of the habenular nuclei in the rat. The Journal of comparative neurology 187:19-47, 1979.

72. Ferraro G, Montalbano ME, Sardo P, La Grutta V. Lateral habenular influence on dorsal raphe neurons. Brain research bulletin 41:47-52, 1996.

73. Yang LM, Hu B, Xia YH, Zhang BL, Zhao H. Lateral habenula lesions improve the behavioral response in depressed rats via increasing the serotonin level in dorsal raphe nucleus. Behavioural brain research, 2007.

74. Shumake J, Edwards E, Gonzalez-Lima F. Opposite metabolic changes in the habenula and ventral tegmental area of a genetic model of helpless behavior. Brain research 963:274-281, 2003.

75. Drevets WC. Orbitofrontal cortex function and structure in depression. Annals of the New York Academy of Sciences 1121:499-527, 2007.

76. Rajkowska G, Miguel-Hidalgo JJ, Wei J, Dilley G, Pittman SD, Meltzer HY, Overholser JC, Roth BL, Stockmeier CA. Morphometric evidence for neuronal and glial prefrontal cell pathology in major depression. Biological psychiatry 45:1085-1098, 1999.

77. Manji HK, Moore GJ, Rajkowska G, Chen G. Neuroplasticity and cellular resilience in mood disorders. Molecular psychiatry 5:578-593, 2000.

78. Goulden V, Layton AM, Cunliffe WJ. Current indications for isotretinoin as a treatment for acne vulgaris. Dermatology (Basel, Switzerland) 190:284-287, 1995.

79. Wysowski D, Pitts M, Beitz J. Depression and suicide in patients treated with isotretinoin. New Engl J Med 334:460-461, 2001.

80. Hull PR, D'Arcy C. Isotretinoin use and subsequent depression and suicide. American Journal of Clinical Dermatology 4:493-505, 2003.

81. Charakida A, Mouser PE, Chu AC. Safety and side effects of the acne drug, oral isotretinoin. Expert opinion on drug safety 3:119-129, 2004.

82. Hazen PG, Carney JF, Walker AE, Stewart JJ. Depression--a side effect of 13-cis-retinoic acid therapy. J Am Acad Dermatol 9:278-279, 1983.

83. Bigby M, Stern RS. Adverse reactions to isotretinoin. A report from the Adverse Drug Reaction Reporting System. J Am Acad Dermatol 18:543-552, 1988.

84. Scheinman PL, Peck GL, Rubinow DR, DiGiovanna JJ, Abangan DL, Ravin PD. Acute depression from isotretinoin. J Am Acad Dermatol 22:1112-1114, 1990.

85. Byrne A, Hnatko G. Depression associated with isotretinoin therapy. Canadian journal of psychiatry 40:567, 1995.

86. Ng CH, Schweitzer I. The association between depression and isotretinoin use in acne. The Australian and New Zealand journal of psychiatry 37:78-84, 2003.

87. O'Connell KA, Wilkin JK, Pitts M. Isotretinoin (Accutane) and serious psychiatric adverse events. J Am Acad Dermatol 48:306-308; author reply 308, 2003.

88. Barak Y, Wohl Y, Greenberg Y, Bar Dayan Y, Friedman T, Shoval G, Knobler HY. Affective psychosis following Accutane (isotretinoin) treatment. International clinical psychopharmacology 20:39-41, 2005.

89. Jick SS, Kremers HM, Vasilakis-Scaramozza C. Isotretinoic use and risk of depression, psychotic symptoms, suicide, and attempted suicide. Arch Dermatol 136:1231-1236, 2000.

90. Jacobs DG, Deutsch NL, Brewer M. Suicide, depression, and isotretinoin: is there a causal link? J Am Acad Dermatol 45:S168-175, 2001.

91. Ferahbas A, Turan MT, Esel E, Utas S, Kutlugun C, Kilic CG. A pilot study evaluating anxiety and depressive scores in acne patients treated with isotretinoin. The Journal of dermatological treatment 15:153-157, 2004.

92. Chia CY, Lane W, Chibnall J, Allen A, Siegfried E. Isotretinoin therapy and mood changes in adolescents with moderate to severe acne: a cohort study. Arch Dermatol 141:557-560, 2005.

93. Hersom K, Neary MP, Levaux HP, Klaskala W, Strauss JS. Isotretinoin and antidepressant pharmacotherapy: a prescription sequence symmetry analysis. J Am Acad Dermatol 49:424-432, 2003.

94. Bremner JD, Fani N, Ashraf A, Votaw JR, Brummer ME, Cummins T, Vaccarino V, Goodman MM, Reed L, Siddiq S, Nemeroff CB. Functional brain imaging alterations in acne patients treated with isotretinoin. Am J Psychiatry 162:983-991, 2005.

95. Kempermann G, Jessberger S, Steiner B, Kronenberg G. Milestones of neuronal development in the adult hippocampus. Trends in neurosciences 27:447-452, 2004.

96. Kempermann G, Wiskott L, Gage FH. Functional significance of adult neurogenesis. Curr Opin Neurobiol 14:186-191, 2004.

97. Crandall J, Sakai Y, Zhang J, Koul O, Mineur Y, Crusio WE, McCaffery PJ. 13-*Cis*-retinoic acid suppresses hippocampal cell division and hippocampal-dependent learning in mice. Proc Natl Acad Sci U S A 101:5111-5116, 2004.

98. Ferguson S, Cisneros F, Gough B, Hanig J, Berry K. Chronic oral treatment with *13-cis*-retinoic acid (isotretinoin) or *all-trans*-retinoic acid does not alter depression-like behaviors in rats. Toxicol Sci 87:451-459, 2005.

99. Ferguson SA, Cisneros FJ, Hanig JP, Berry KJ. Oral treatment with ACCUTANE does not increase measures of anhedonia or depression in rats. Neurotoxicology and teratology 29:642-651, 2007.

100. Stipanuk M. Biochemical and physiological aspects of human nutrition. Philadelphia: W.B. Saunders Company, 2000.

101. Koo J. The psychosocial impact of acne: patients' perceptions. J Am Acad Dermatol 32:S26-30, 1995.

102. White GM. Recent findings in the epidemiologic evidence, classification, and subtypes of acne vulgaris. Journal of the American Academy of Dermatology 39:S34-37, 1998.

103. Spear LP. The adolescent brain and age-related behavioral manifestations. Neuroscience and biobehavioral reviews 24:417-463, 2000.

104. JaxNotesTM. New physiological data summaries available for many popular JAX(R) mice strains. 507:body weight information, 2007.

105. Mey J, McCaffery P. Retinoic acid signaling in the nervous system of adult vertebrates. Neuroscientist 10:409-421, 2004.

106. Lane MA, Bailey SJ. Role of retinoid signalling in the adult brain. Progress in neurobiology 75:275-293, 2005.

107. Wallace A. Mental Illness, biology, and culture. In: Hsu F, Ed. Psychological anthropology. Cambridge, MA: Shenkman, p363-402, 1972.

108. Restak RM. Pseudotumor cerebri, psychosis, and hypervitaminosis A. The Journal of nervous and mental disease 155:72-75, 1972.

109. Wieland RG, Hendricks FH, Amat y Leon F, Gutierrez L, Jones JC. Hypervitaminosis A with hypercalcaemia. Lancet 1:698, 1971.

110. Muenter MD, Perry HO, Ludwig J. Chronic vitamin A intoxication in adults. Hepatic, neurologic and dermatologic complications. The American journal of medicine 50:129-136, 1971.

111. Dillard AC, Lane MA. Retinol decreases beta-catenin protein levels in retinoic acid-resistant colon cancer cell lines. Molecular carcinogenesis 46:315-329, 2007.

112. Park EY, Dillard A, Williams EA, Wilder ET, Pepper MR, Lane MA. Retinol inhibits the growth of all-trans-retinoic acid-sensitive and all-trans-retinoic acid-resistant colon cancer cells through a retinoic acid receptor-independent mechanism. Cancer research 65:9923-9933, 2005.

113. Park EY, Wilder ET, Lane MA. Retinol inhibits the invasion of retinoic acid-resistant colon cancer cells in vitro and decreases matrix metalloproteinase mRNA, protein, and activity levels. Nutrition and cancer 57:66-77, 2007.

114. Valdenaire O, Vernier P, Maus M, Dumas Milne Edwards JB, Mallet J. Transcription of the rat dopamine-D2-receptor gene from two promoters. European journal of biochemistry / FEBS 220:577-584, 1994.

115. Iniguez MA, Morte B, Rodriguez-Pena A, Munoz A, Gerendasy D, Sutcliffe JG, Bernal J. Characterization of the promoter region and flanking sequences of the neuron-specific gene RC3 (neurogranin). Brain Res Mol Brain Res 27:205-214, 1994.

116. Husson M, Enderlin V, Alfos S, Boucheron C, Pallet V, Higueret P. Expression of neurogranin and neuromodulin is affected in the striatum of vitamin A-deprived rats. Brain Res Mol Brain Res 123:7-17, 2004.

117. Cho S, Chung J, Han J, Ju Lee B, Han Kim D, Rhee K, Kim K. 9-cis-Retinoic acid represses transcription of the gonadotropin-releasing hormone (GnRH) gene via proximal promoter region that is distinct from all-trans-retinoic acid response element. Brain Res Mol Brain Res 87:214-222, 2001.

118. Cho S, Chung JJ, Choe Y, Choi HS, Han Kim D, Rhee K, Kim K. A functional retinoic acid response element (RARE) is present within the distal promoter of the rat gonadotropin-releasing hormone (GnRH) gene. Brain Res Mol Brain Res 87:204-213, 2001.

119. Richard S, Zingg HH. Identification of a retinoic acid response element in the human oxytocin promoter. The Journal of biological chemistry 266:21428-21433, 1991.

120. Chiang MY, Misner D, Kempermann G, Schikorski T, Giguere V, Sucov HM, Gage FH, Stevens CF, Evans RM. An essential role for retinoid receptors RARbeta and RXRgamma in long-term potentiation and depression. Neuron 21:1353-1361, 1998.

121. Etchamendy N, Enderlin V, Marighetto A, Pallet V, Higueret P, Jaffard R. Vitamin A deficiency and relational memory deficit in adult mice: relationships with changes in brain retinoid signalling. Behavioural brain research 145:37-49, 2003.

122. Jacobs BL, Praag H, Gage FH. Adult brain neurogenesis and psychiatry: a novel theory of depression. Molecular psychiatry 5:262-269, 2000.

123. Malberg JE, Schechter LE. Increasing hippocampal neurogenesis: a novel mechanism for antidepressant drugs. Current pharmaceutical design 11:145-155, 2005.

124. Lane MA, Chen AC, Roman SD, Derguini F, Gudas LJ. Removal of LIF (leukemia inhibitory factor) results in increased vitamin A (retinol) metabolism to 4-oxoretinol in embryonic stem cells. Proceedings of the National Academy of Sciences of the United States of America 96:13524-13529, 1999.

125. Lucki I, Dalvi A, Mayorga AJ. Sensitivity to the effects of pharmacologically selective antidepressants in different strains of mice. Psychopharmacology 155:315-322, 2001.

126. Mathis C, Paul SM, Crawley JN. Characterization of benzodiazepine-sensitive behaviors in the A/J and C57BL/6J inbred strains of mice. Behavior genetics 24:171-180, 1994.

127. Prut L, Belzung C. The open field as a paradigm to measure the effects of drugs on anxiety-like behaviors: a review. European journal of pharmacology 463:3-33, 2003.

128. Brooks SP, Pask T, Jones L, Dunnett SB. Behavioural profiles of inbred mouse strains used as transgenic backgrounds. I: motor tests. Genes, brain, and behavior 3:206-215, 2004.

129. Shumake J, Barrett D, Gonzalez-Lima F. Behavioral characteristics of rats predisposed to learned helplessness: reduced reward sensitivity, increased novelty seeking, and persistent fear memories. Behavioural brain research 164:222-230, 2005.

130. Lucki I. The forced swimming test as a model for core and component behavioral effects of antidepressant drugs. Behavioural pharmacology 8:523-532, 1997.

131. Axelson DA, Birmaher B. Relation between anxiety and depressive disorders in childhood and adolescence. Depression and anxiety 14:67-78, 2001.

132. Ducottet C, Belzung C. Correlations between behaviours in the elevated plus-maze and sensitivity to unpredictable subchronic mild stress: evidence from inbred strains of mice. Behavioural brain research 156:153-162, 2005.

133. Eichele G. Retinoids: from hindbrain patterning to Parkinson disease. Trends Genet 13:343-345, 1997.

134. Luthi-Carter R, Strand A, Peters NL, Solano SM, Hollingsworth ZR, Menon AS, Frey AS, Spektor BS, Penney EB, Schilling G, Ross CA, Borchelt DR, Tapscott SJ, Young AB, Cha JH, Olson JM. Decreased expression of striatal signaling genes in a mouse model of Huntington's disease. Human molecular genetics 9:1259-1271, 2000.

135. Detke MJ, Rickels M, Lucki I. Active behaviors in the rat forced swimming test differentially produced by serotonergic and noradrenergic antidepressants. Psychopharmacology 121:66-72, 1995.

136. Bhatnagar S, Nowak N, Babich L, Bok L. Deletion of the 5-HT3 receptor differentially affects behavior of males and females in the Porsolt forced swim and defensive withdrawal tests. Behavioural brain research 153:527-535, 2004.

137. Shumake J, Gonzalez-Lima F. Brain systems underlying susceptibility to helplessness and depression. Behavioral and cognitive neuroscience reviews 2:198-221, 2003.

138. Klimek V, Schenck JE, Han H, Stockmeier CA, Ordway GA. Dopaminergic abnormalities in amygdaloid nuclei in major depression: a postmortem study. Biological psychiatry 52:740-748, 2002.

139. Strobel A, Gutknecht L, Rothe C, Reif A, Mossner R, Zeng Y, Brocke B, Lesch KP. Allelic variation in 5-HT1A receptor expression is associated with anxiety- and depression-related personality traits. J Neural Transm 110:1445-1453, 2003.

140. Charest A, Wainer BH, Albert PR. Cloning and differentiation-induced expression of a murine serotonin1A receptor in a septal cell line. J Neurosci 13:5164-5171, 1993.

141. Malberg JE, Duman RS. Cell proliferation in adult hippocampus is decreased by inescapable stress: reversal by fluoxetine treatment. Neuropsychopharmacology 28:1562-1571, 2003.

142. Maden M. Retinoid signalling in the development of the central nervous system. Nature reviews 3:843-853, 2002.

143. Takahashi J, Palmer TD, Gage FH. Retinoic acid and neurotrophins collaborate to regulate neurogenesis in adult-derived neural stem cell cultures. Journal of neurobiology 38:65-81, 1999.

144. Thompson Haskell G, Maynard TM, Shatzmiller RA, Lamantia AS. Retinoic acid signaling at sites of plasticity in the mature central nervous system. The Journal of comparative neurology 452:228-241, 2002.

145. Lane MA, Bailey SJ. Role of retinoid signaling in the adult brain. Prog Neurobiol 72:275-293, 2005.

146. Chaing M, Misner D, Kempermann G, Schikorski T, Giguere V, Sucov H, Gage F, Stevens C, Evans R. An essentail role for retinoid receptors RARbeta and RXRgamma in long-term potentiation and depression. Neuron 21:1353-1361, 1998.

147. Cocco S, Diaz G, Stancampiano R, Diana A, Carta M, Curreli R, Sarais L, Fadda F. Vitamin A deficiency produces spatial learning and memory impairment in rats. Neuroscience 115:475-482, 2003.

148. Brezun JM, Daszuta A. Depletion in serotonin decreases neurogenesis in the dentate gyrus and the subventricular zone of adult rats. Neuroscience 89:999-1002, 1999.

149. Santarelli L, Saxe M, Gross C, Surget A, Battaglia F, Dulawa S, Weisstaub N, Lee J, Duman R, Arancio O, Belzung C, Hen R. Requirement of hippocampal neurogenesis for the behavioral effects of antidepressants. Science 301:805-809, 2003.

150. Shalita AR, Armstrong RB, Leyden JJ, Pochi PE, Strauss JS. Isotretinoin revisited. Cutis; cutaneous medicine for the practitioner 42:1-19, 1988.

151. Kellett SC, Gawkrodger DJ. The psychological and emotional impact of acne and the effect of treatment with isotretinoin. The British journal of dermatology 140:273-282, 1999.

152. Gerard JM, Buehler C. Cumulative environmental risk and youth maladjustment: the role of youth attributes. Child development 75:1832-1849, 2004.

153. Blier P, Pineyro G, el Mansari M, Bergeron R, de Montigny C. Role of somatodendritic 5-HT autoreceptors in modulating 5-HT neurotransmission. Annals of the New York Academy of Sciences 861:204-216, 1998.

154. Vertes RP. A PHA-L analysis of ascending projections of the dorsal raphe nucleus in the rat. The Journal of comparative neurology 313:643-668, 1991.

155. Vertes RP, Fortin WJ, Crane AM. Projections of the median raphe nucleus in the rat. The Journal of comparative neurology 407:555-582, 1999.

156. Elhwuegi AS. Central monoamines and their role in major depression. Progress in neuro-psychopharmacology & biological psychiatry 28:435-451, 2004.

157. Graeff FG, Guimaraes FS, De Andrade TG, Deakin JF. Role of 5-HT in stress, anxiety, and depression. Pharmacology, biochemistry, and behavior 54:129-141, 1996.

158. Barnes NM, Sharp T. A review of central 5-HT receptors and their function. Neuropharmacology 38:1083-1152, 1999.

159. Inoue T, Kusumi I, Yoshioka M. Serotonin transporters. Current drug targets 1:519-529, 2002.

160. Blier P, de Montigny C. Current advances and trends in the treatment of depression. Trends in pharmacological sciences 15:220-226, 1994.

161. Blier P, de Montigny C. Serotonin and drug-induced therapeutic responses in major depression, obsessive-compulsive and panic disorders. Neuropsychopharmacology 21:91S-98S, 1999.

162. Mann JJ. Role of the serotonergic system in the pathogenesis of major depression and suicidal behavior. Neuropsychopharmacology 21:99S-105S, 1999.

163. Lemonde S, Turecki G, Bakish D, Du L, Hrdina PD, Bown CD, Sequeira A, Kushwaha N, Morris SJ, Basak A, Ou XM, Albert PR. Impaired repression at a 5-hydroxytryptamine 1A receptor gene polymorphism associated with major depression and suicide. J Neurosci 23:8788-8799, 2003.

164. Lesch KP, Bengel D, Heils A, Sabol SZ, Greenberg BD, Petri S, Benjamin J, Muller CR, Hamer DH, Murphy DL. Association of anxiety-related traits with a polymorphism in the serotonin transporter gene regulatory region. Science 274:1527-1531, 1996.

165. Caspi A, Sugden K, Moffitt TE, Taylor A, Craig IW, Harrington H, McClay J, Mill J, Martin J, Braithwaite A, Poulton R. Influence of life stress on depression: moderation by a polymorphism in the 5-HTT gene. Science 301:386-389, 2003.

166. Neumeister A, Young T, Stastny J. Implications of genetic research on the role of the serotonin in depression: emphasis on the serotonin type 1A receptor and the serotonin transporter. Psychopharmacology 174:512-524, 2004.

167. Blier P, de Montigny C, Chaput Y. A role for the serotonin system in the mechanism of action of antidepressant treatments: preclinical evidence. The Journal of clinical psychiatry 51 Suppl:14-20; discussion 21, 1990.

168. Heils A, Teufel A, Petri S, Stober G, Riederer P, Bengel D, Lesch KP. Allelic variation of human serotonin transporter gene expression. Journal of neurochemistry 66:2621-2624, 1996.

169. Heisler LK, Chu HM, Brennan TJ, Danao JA, Bajwa P, Parsons LH, Tecott LH. Elevated anxiety and antidepressant-like responses in serotonin 5-HT1A receptor mutant mice. Proc Natl Acad Sci U S A 95:15049-15054, 1998.

170. Lira A, Zhou M, Castanon N, Ansorge M, Gordon J, Francis J, Bradley-Moore M, Lira J, Underwood M, Arango V, Kung H, Hofer M, Hen R, Gingrich J. Altered depression-related behaviors and functional changes in the dorsal raphe nucleus of serotonin transporter deficient mice. Biol Psychiatry 54:960-971, 2003.

171. Ansorge M, Zhou M, Lira A, Hen R, Gingrich J. Early-life blockage of the 5-HT transporter alters emotional behavior in adult mice. Science 306:879-881, 2004.

172. Soprano DR, Qin P, Soprano KJ. Retinoic acid receptors and cancers. Annual review of nutrition 24:201-221, 2004.

173. O'Reilly KC, Shumake J, Gonzalez-Lima F, Lane MA, Bailey SJ. Chronic administration of 13-cis-retinoic acid increases depression-related behavior in mice. Neuropsychopharmacology 31:1919-1927, 2006.

174. Eaton MJ, Whittemore SR. Autocrine BDNF secretion enhances the survival and serotonergic differentiation of raphe neuronal precursor cells grafted into the adult rat CNS. Experimental neurology 140:105-114, 1996.

175. Eaton MJ, Staley JK, Globus MY, Whittemore SR. Developmental regulation of early serotonergic neuronal differentiation: the role of brain-derived neurotrophic factor and membrane depolarization. Developmental biology 170:169-182, 1995.

176. White LA, Eaton MJ, Castro MC, Klose KJ, Globus MY, Shaw G, Whittemore SR. Distinct regulatory pathways control neurofilament expression and neurotransmitter synthesis in immortalized serotonergic neurons. J Neurosci 14:6744-6753, 1994.

177. Bai F, Lau SS, Monks TJ. Glutathione and N-acetylcysteine conjugates of alpha-methyldopamine produce serotonergic neurotoxicity: possible role in methylenedioxyamphetamine-mediated neurotoxicity. Chemical research in toxicology 12:1150-1157, 1999.

178. Pierce PA, Xie GX, Meuser T, Peroutka SJ. 5-Hydroxytryptamine receptor subtype messenger RNAs in human dorsal root ganglia: a polymerase chain reaction study. Neuroscience 81:813-819, 1997.

179. Strausberg RL, Feingold EA, Grouse LH, Derge JG, Klausner RD, Collins FS, Wagner L, Shenmen CM, Schuler GD, Altschul SF, Zeeberg B, Buetow KH, Schaefer CF, Bhat NK, Hopkins RF, Jordan H, Moore T, Max SI, Wang J, Hsieh F, Diatchenko L, Marusina K, Farmer AA, Rubin GM, Hong L, Stapleton M, Soares MB, Bonaldo MF, Casavant TL, Scheetz TE, Brownstein MJ, Usdin TB, Toshiyuki S, Carninci P, Prange C, Raha SS, Loquellano NA, Peters GJ, Abramson RD, Mullahy SJ, Bosak SA, McEwan PJ, McKernan KJ, Malek JA, Gunaratne PH, Richards S, Worley KC, Hale S, Garcia AM, Gay LJ, Hulyk SW, Villalon DK, Muzny DM, Sodergren EJ, Lu X, Gibbs RA, Fahey J, Helton E, Ketteman M, Madan A, Rodrigues S, Sanchez A, Whiting M, Madan A, Young AC, Shevchenko Y, Bouffard GG, Blakesley RW, Touchman JW, Green ED, Dickson MC, Rodriguez AC, Grimwood J, Schmutz J, Myers RM, Butterfield YS, Krzywinski MI, Skalska U, Smailus DE, Schnerch A, Schein JE, Jones SJ, Marra MA. Generation and initial analysis of more than 15,000 full-length human

and mouse cDNA sequences. Proceedings of the National Academy of Sciences of the United States of America 99:16899-16903, 2002.

180. Ozsarac N, Santha E, Hoffman BJ. Alternative non-coding exons support serotonin transporter mRNA expression in the brain and gut. Journal of neurochemistry 82:336-344, 2002.

181. Bry K, Lappalainen U. Pathogenesis of bronchopulmonary dysplasia: the role of interleukin 1beta in the regulation of inflammation-mediated pulmonary retinoic acid pathways in transgenic mice. Seminars in perinatology 30:121-128, 2006.

182. Nishizawa H, Manabe N, Morita M, Sugimoto M, Imanishi S, Miyamoto H. Effects of in utero exposure to bisphenol A on expression of RARalpha and RXRalpha mRNAs in murine embryos. The Journal of reproduction and development 49:539-545, 2003.

183. Husson M, Enderlin V, Alfos S, Feart C, Higueret P, Pallet V. Triiodothyronine administration reverses vitamin A deficiency-related hypo-expression of retinoic acid and triiodothyronine nuclear receptors and of neurogranin in rat brain. The British journal of nutrition 90:191-198, 2003.

184. Arias B, Arranz MJ, Gasto C, Catalan R, Pintor L, Gutierrez B, Kerwin RW, Fananas L. Analysis of structural polymorphisms and C-1018G promoter variant of the 5-HT(1A) receptor gene as putative risk factors in major depression. Molecular psychiatry 7:930-932, 2002.

185. Olivier B, Pattij T, Wood SJ, Oosting R, Sarnyai Z, Toth M. The 5-HT(1A) receptor knockout mouse and anxiety. Behavioural pharmacology 12:439-450, 2001.

186. Richer M, Hen R, Blier P. Modification of serotonin neuron properties in mice lacking 5-HT1A receptors. European journal of pharmacology 435:195-203, 2002.

187. Parsons LH, Kerr TM, Tecott LH. 5-HT(1A) receptor mutant mice exhibit enhanced tonic, stress-induced and fluoxetine-induced serotonergic neurotransmission. Journal of neurochemistry 77:607-617, 2001.

188. He M, Sibille E, Benjamin D, Toth M, Shippenberg T. Differential effects of 5-HT1A receptor deletion upon basal and fluoxetine-evoked 5-HT concentrations as revealed by in vivo microdialysis. Brain research 902:11-17, 2001.

189. Serretti A, Benedetti F, Zanardi R, Smeraldi E. The influence of Serotonin Transporter Promoter Polymorphism (SERTPR) and other polymorphisms of the

serotonin pathway on the efficacy of antidepressant treatments. Progress in neuro-psychopharmacology & biological psychiatry 29:1074-1084, 2005.

190. Greenberg BD, Tolliver TJ, Huang SJ, Li Q, Bengel D, Murphy DL. Genetic variation in the serotonin transporter promoter region affects serotonin uptake in human blood platelets. American journal of medical genetics 88:83-87, 1999.

191. Little KY, McLaughlin DP, Zhang L, Livermore CS, Dalack GW, McFinton PR, DelProposto ZS, Hill E, Cassin BJ, Watson SJ, Cook EH. Cocaine, ethanol, and genotype effects on human midbrain serotonin transporter binding sites and mRNA levels. Am J Psychiatry 155:207-213, 1998.

192. Collier DA, Stober G, Li T, Heils A, Catalano M, Di Bella D, Arranz MJ, Murray RM, Vallada HP, Bengel D, Muller CR, Roberts GW, Smeraldi E, Kirov G, Sham P, Lesch KP. A novel functional polymorphism within the promoter of the serotonin transporter gene: possible role in susceptibility to affective disorders. Molecular psychiatry 1:453-460, 1996.

193. Thakker DR, Natt F, Husken D, van der Putten H, Maier R, Hoyer D, Cryan JF. siRNA-mediated knockdown of the serotonin transporter in the adult mouse brain. Molecular psychiatry 10:782-789, 714, 2005.

194. Bengel D, Murphy DL, Andrews AM, Wichems CH, Feltner D, Heils A, Mossner R, Westphal H, Lesch KP. Altered brain serotonin homeostasis and locomotor insensitivity to 3, 4-methylenedioxymethamphetamine ("Ecstasy") in serotonin transporter-deficient mice. Molecular pharmacology 53:649-655, 1998.

195. Montanez S, Owens WA, Gould GG, Murphy DL, Daws LC. Exaggerated effect of fluvoxamine in heterozygote serotonin transporter knockout mice. Journal of neurochemistry 86:210-219, 2003.

196. Mathews TA, Fedele DE, Coppelli FM, Avila AM, Murphy DL, Andrews AM. Gene dose-dependent alterations in extraneuronal serotonin but not dopamine in mice with reduced serotonin transporter expression. Journal of neuroscience methods 140:169-181, 2004.

197. O'Reilly K C, Trent S, Bailey SJ, Lane MA. 13-cis-Retinoic Acid Alters Intracellular Serotonin, Increases 5-HT1A Receptor, and Serotonin Reuptake Transporter Levels In Vitro. Experimental biology and medicine (Maywood, NJ 232:1195-1203, 2007.

198. Drevets WC, Price JL, Simpson JR, Jr., Todd RD, Reich T, Vannier M, Raichle ME. Subgenual prefrontal cortex abnormalities in mood disorders. Nature 386:824-827, 1997.

199. Mayberg HS, Brannan SK, Mahurin RK, Jerabek PA, Brickman JS, Tekell JL, Silva JA, McGinnis S, Glass TG, Martin CC, Fox PT. Cingulate function in depression: a potential predictor of treatment response. Neuroreport 8:1057-1061, 1997.

200. Caldecott-Hazard S, Mazziotta J, Phelps M. Cerebral correlates of depressed behavior in rats, visualized using 14C-2-deoxyglucose autoradiography. J Neurosci 8:1951-1961, 1988.

201. Wong-Riley MT. Cytochrome oxidase: an endogenous metabolic marker for neuronal activity. Trends in neurosciences 12:94-101, 1989.

202. Shumake J, Poremba A, Edwards E, Gonzalez-Lima F. Congenital helpless rats as a genetic model for cortex metabolism in depression. Neuroreport 11:3793-3798, 2000.

203. Gozalez-Lima F, Cada A. Quantitative histochemistry of cytochrome oxidase activity. In: Gonzalez-Lima F, Ed. Cytochrome oxidase in neuronal metabolism and Alzheimer's disease. New York: Plenum Press, p55-90, 1998.

204. Gonzalez-Lima F, Berndt JD, Valla JE, Games D, Reiman EM. Reduced corpus callosum, fornix and hippocampus in PDAPP transgenic mouse model of Alzheimer's disease. Neuroreport 12:2375-2379, 2001.

205. Paxinos G, Franklin K. The mouse brain in stereotaxic coordinates. San Diego: Academic, 2001.

206. Gundersen HJ, Bendtsen TF, Korbo L, Marcussen N, Moller A, Nielsen K, Nyengaard JR, Pakkenberg B, Sorensen FB, Vesterby A, et al. Some new, simple and efficient stereological methods and their use in pathological research and diagnosis. Apmis 96:379-394, 1988.

207. Puga F, Barrett DW, Bastida CC, Gonzalez-Lima F. Functional networks underlying latent inhibition learning in the mouse brain. NeuroImage 38:171-183, 2007.

208. Vertes RP, Kocsis B. Projections of the dorsal raphe nucleus to the brainstem: PHA-L analysis in the rat. The Journal of comparative neurology 340:11-26, 1994.

209. Del-Fava F, Hasue RH, Ferreira JG, Shammah-Lagnado SJ. Efferent connections of the rostral linear nucleus of the ventral tegmental area in the rat. Neuroscience 145:1059-1076, 2007.

210. Flores JA, Galan-Rodriguez B, Ramiro-Fuentes S, Fernandez-Espejo E. Role for dopamine neurons of the rostral linear nucleus and periaqueductal gray in the

rewarding and sensitizing properties of heroin. Neuropsychopharmacology 31:1475-1488, 2006.

211. Oades RD, Halliday GM. Ventral tegmental (A10) system: neurobiology. 1. Anatomy and connectivity. Brain research 434:117-165, 1987.

212. Ferraro G, Montalbano ME, Sardo P, La Grutta V. Lateral habenula and hippocampus: a complex interaction raphe cells-mediated. J Neural Transm 104:615-631, 1997.

213. Paxinos G, Watson C. The rat brain in stereotaxic coordinates. San Diego: Academic Press, 1997.

214. Shumake J, Edwards E, Gonzalez-Lima F. Dissociation of septo-hippocampal metabolism in the congenitally helpless rat. Neuroscience 114:373-377, 2002.

215. Aihara M, Ida I, Yuuki N, Oshima A, Kumano H, Takahashi K, Fukuda M, Oriuchi N, Endo K, Matsuda H, Mikuni M. HPA axis dysfunction in unmedicated major depressive disorder and its normalization by pharmacotherapy correlates with alteration of neural activity in prefrontal cortex and limbic/paralimbic regions. Psychiatry research 155:245-256, 2007.

216. Mayberg HS, Brannan SK, Tekell JL, Silva JA, Mahurin RK, McGinnis S, Jerabek PA. Regional metabolic effects of fluoxetine in major depression: serial changes and relationship to clinical response. Biol Psychiatry 48:830-843, 2000.

217. Brezun JM, Daszuta A. Serotonergic reinnervation reverses lesion-induced decreases in PSA-NCAM labeling and proliferation of hippocampal cells in adult rats. Hippocampus 10:37-46, 2000.

218. Brezun JM, Daszuta A. Serotonin may stimulate granule cell proliferation in the adult hippocampus, as observed in rats grafted with foetal raphe neurons. The European journal of neuroscience 12:391-396, 2000.

219. Kanarik M, Matrov D, Koiv K, Eller M, Tonissaar M, Harro J. Changes in regional long-term oxidative metabolism induced by partial serotonergic denervation and chronic variable stress in rat brain. Neurochemistry international 52:432-437, 2008.

220. Sun SY, Hail N, Jr., Lotan R. Apoptosis as a novel target for cancer chemoprevention. Journal of the National Cancer Institute 96:662-672, 2004.

221. Ongur D, Drevets WC, Price JL. Glial reduction in the subgenual prefrontal cortex in mood disorders. Proceedings of the National Academy of Sciences of the United States of America 95:13290-13295, 1998.

222. Rajkowska G. Postmortem studies in mood disorders indicate altered numbers of neurons and glial cells. Biol Psychiatry 48:766-777, 2000.

223. Underwood MD, Khaibulina AA, Ellis SP, Moran A, Rice PM, Mann JJ, Arango V. Morphometry of the dorsal raphe nucleus serotonergic neurons in suicide victims. Biol Psychiatry 46:473-483, 1999.

224. Daftary SS, Gore AC. Developmental changes in hypothalamic insulin-like growth factor-1: relationship to gonadotropin-releasing hormone neurons. Endocrinology 144:2034-2045, 2003.

225. Chakraborty TR, Ng L, Gore AC. Age-related changes in estrogen receptor beta in rat hypothalamus: a quantitative analysis. Endocrinology 144:4164-4171, 2003.

226. Sheline YI, Sanghavi M, Mintun MA, Gado MH. Depression duration but not age predicts hippocampal volume loss in medically healthy women with recurrent major depression. J Neurosci 19:5034-5043, 1999.

227. Neumeister A, Konstantinidis A, Stastny J, Schwarz MJ, Vitouch O, Willeit M, Praschak-Rieder N, Zach J, de Zwaan M, Bondy B, Ackenheil M, Kasper S. Association between serotonin transporter gene promoter polymorphism (5HTTLPR) and behavioral responses to tryptophan depletion in healthy women with and without family history of depression. Archives of general psychiatry 59:613-620, 2002.

Vita

Kally Corissa O'Reilly was born in Tucson, Arizona to Duane and Darlene Bowers. She has one older sister, Alexia. Kally's family moved to northern New Mexico when she was 5 and eventually settled in Waterflow, New Mexico where she lived until graduating as from Kirtland Central High School in 1995. In the fall of 1995, Kally attended New Mexico State University where she pursued her Bachelor of Science in Chemical Engineering. After graduating from New Mexico State University with her BS in 2000, Kally worked for 2 years at Dow Chemical in process and run-plant engineering. She decided to pursue her graduate degree in 2002 at the University of Texas at Austin, where she became acquainted and fell in love with Cellular and Molecular Biology. In May of 2003, Kally married her other love, Colm O'Reilly. In addition to her graduate studies, Kally was a member of the alternative/rock band, **incompatible sleep patterns**, as vocalist, lyricist, and rhythm guitarist. Kally currently resides in Austin, Texas.

This dissertation was typed by Kally Corissa O'Reilly